

**Development of self-adjusting cytokine neutralizer cells as a closed-loop
delivery system of anti-inflammatory biologicals**

**Entwicklung von selbstregulierenden Zytokin-Neutralisierer-Zellen
als Closed-Loop Abgabesystem von anit-inflammatorischen Biologikals**

Dissertation zur Erlangung des
naturwissenschaftlichen Doktorgrades
der Julius-Maximilians-Universität Würzburg

vorgelegt von

Dennis Hell

Geb. 07.07.1987 Rottweil

Würzburg, 2018

Eingereicht am:

Mitglieder der Promotionskommission:

Vorsitzender:

Gutachter: Prof. Dr. Harald Wajant

Gutachter: PD Dr. Robert Hock

Tag des Promotionskolloquiums:

Doktorurkunde ausgehändigt am:

Zusammenfassung

Die derzeit üblichen Behandlungsstrategien von Krankheiten werden auf Basis diagnostizierter phänotypischer Veränderungen erhoben, die auf eine Ansammlung asymptomatischer Ereignisse in physiologischen Vorgängen zurückzuführen sind. Da die Feststellung einer Diagnose bislang erst in fortgeschrittenen Krankheitsstadien, vor allem aufgrund unzureichender Früherkennungsmöglichkeiten von physiologischen Störungen, erfolgen kann, sehen sich Ärzte gezwungen, Krankheiten vornehmlich zu behandeln anstatt ihnen vorzubeugen. Daher ist es erstrebenswert, wenn zukünftige therapeutische Interventionen bereits an die Früherkennung von physiologischen Veränderungen gekoppelt werden könnten. Sogenannte Sensor-Effektor Systeme sollen krankheitsspezifische Biomarker erkennen und die Produktion und Bereitstellung von therapeutischen Faktoren in einer selbstständigen und automatisierten Art und Weise koordinieren. Solche Ansätze und deren Entwicklung werden unter anderem durch die Disziplin der synthetischen Biologie erforscht und vorangetrieben.

Die vorliegende Arbeit konzentriert sich vor diesem Hintergrund auf das *in vitro* Design von Zytokin-neutralisierenden Sensor-Effektor Zellen, die für die potentielle Behandlung wiederkehrender Autoimmunerkrankungen, insbesondere der rheumatoiden Arthritis, konstruiert wurden.

Die gezielte Ansteuerung zur induzierbaren Genexpression konnte in humanen Zellen erfolgreich generiert werden. In der vorliegenden Arbeit wurde zunächst ein NF- κ B abhängiger Promoter zur induzierbaren Genexpression auf der Grundlage von HIV-1 ableitenden DNA-Bindemotiven entwickelt. Die Aktivierbarkeit dieses Promoters wurde durch verschiedene Induktoren, insbesondere auch durch die physiologisch wichtigen NF- κ B Aktivatoren Tumornekrosefaktor alpha (TNF α) und Interleukin 1 beta (IL-1 β) überprüft. Die Aktivierungsstärke des NF- κ B abhängigen Promoters wurde durch die Integration einer nicht-kodierenden RNA verdoppelt. Diese RNA kombiniert Strukturelemente, die im RNA-Doppelstrang DNA-Strukturen imitieren, und für die in Vorarbeiten die Bindung an p50 oder p65 nachgewiesen werden konnten. Für TNF α und IL-1 β lagen das Detektionslimit und die EC50 Werte der NF- κ B getriggerten Genexpression im unteren pikomolaren Bereich. Neben der Sensitivität wurde das induzierbare System bezüglich seiner Reversibilität und Dynamik charakterisiert. Dabei konnte eine enge Korrelation zwischen Pulszeiten und Expressionsmustern aufgezeigt werden.

Ferner wurde der NF- κ B abhängige Promoter an etablierte TNF α - und IL-1-blockierende Biologicals gekoppelt, um Sensor-Effektor Systeme mit anti-entzündlicher Aktivität zu erhalten, die potentiell zur Behandlung von Autoimmunerkrankungen, wie beispielsweise der rheumatoiden Arthritis, eingesetzt werden könnten. Bei den Biologicals wurde zwischen Ligand-

blockierenden und Rezeptor-blockierenden Biologicals differenziert und unterschiedliche Varianten ausgewählt: Adalimumab, Etanercept und Anakinra. Erneut verbesserte die zusätzliche Integration der nicht-kodierenden RNA die Aktivierungsstärke der NF- κ B abhängig exprimierten Biologicals, das die universelle Nutzbarkeit des hier entwickelten optimierten NF- κ B-Promoters unterstreicht. Ferner wurde gezeigt, dass die TNF α -induzierte Expression von NF- κ B-regulierten TNF α -blockierenden Biologika zu einem extrazellulären negativen Feedback Loop führte. Interessanterweise hat die Integration der nicht-kodierender RNA und dieser negative Feedback Loop die Dynamik und Reversibilität der NF- κ B-regulierten Genexpression erhöht. Die Kontrollierbarkeit der Wirkstoffabgabe kann zudem durch den Einsatz von Inhibitoren der klassischen NF- κ B-Signalisierung wie z.B. TPCA-1 erweitert werden. Die Wirksamkeit der exprimierten Biologicals wurde durch Neutralisation der Zytokine in verschiedenen Experimenten nachgewiesen. Für zukünftige *in vivo* Versuche konnten erste Alginat-Verkapselungen der Zellen durchgeführt werden. Die Aktivierbarkeit des NF- κ B abhängigen Promoters wurde ferner durch Ko-Kultivierung mit humanen Plasmaproben und Synovialflüssigkeiten nachgewiesen.

Mit diesem generierten Sensor-Effektor-System haben wir selbstregulierende Zytokin-Neutralisierer-Zellen als Closed-Loop Abgabesystem von anti-inflammatorischen Biologikals entwickelt.

Summary

The current treatment strategies for diseases are assessed on the basis of diagnosed phenotypic changes due to an accumulation of asymptomatic events in physiological processes. Since a diagnosis can only be established at advanced stages of the disease, mainly due to insufficient early detection possibilities of physiological disorders, doctors are forced to treat diseases rather than prevent them. Therefore, it is desirable to link future therapeutic interventions to the early detection of physiological changes. So-called sensor-effector systems are designed to recognise disease-specific biomarkers and coordinate the production and delivery of therapeutic factors in an autonomous and automated manner. Such approaches and their development are being researched and promoted by the discipline of synthetic biology, among others.

Against this background, this paper focuses on the *in vitro* design of cytokine-neutralizing sensor-effector cells designed for the potential treatment of recurrent autoimmune diseases, especially rheumatoid arthritis.

The precise control of inducible gene expression was successfully generated in human cells. At first, a NF- κ B-dependent promoter was developed, based on HIV-1 derived DNA-binding motives. The activation of this triggerable promoter was investigated using several inducers including the physiologically important NF- κ B inducers tumor necrosis factor alpha (TNF α) and interleukin 1 beta (IL-1 β). The activation strength of the NF- κ B-triggered promoter was doubled by integrating a non-coding RNA. The latter combined expressed RNA structures, which mimic DNA by double stranded RNAs and have been demonstrated to bind to p50 or p65 by previous publications. The sensitivity was investigated for TNF α and IL-1 β . The detection limit and the EC50 values were in the lower picomolar range. Besides the sensitivity, the reversibility and dynamic of the inducible system were characterized. Hereby a close correlation between pulse times and expression profile was shown.

The optimized NF- κ B-dependent promoter was then coupled to established TNF α - and IL-1-blocking biologicals to develop sensor-effector systems with anti-inflammatory activity, and thus potential use against autoimmune diseases such as rheumatoid arthritis. The biologicals were differentiated between ligand-blocking and receptor-blocking biologicals and different variants were selected: Adalimumab, etanercept and anakinra. The non-coding RNA improved again the activation strength of NF- κ B-dependent expressed biologicals, indicating its universal benefit. Furthermore, it was shown that the TNF α -induced expression of NF- κ B-regulated TNF α -blocking biologics led to an extracellular negative feedback loop. Interestingly, the integration of the non-coding RNA and this negative feedback loop has increased the dynamics and reversibility of the NF- κ B-regulated gene expression. The controllability of drug release can also be extended by

the use of inhibitors of classical NF- κ B signalling such as TPCA-1. The efficacy of the expressed biologicals was detected through neutralization of the cytokines using different experiments. For future *in vivo* trials, first alginate encapsulations of the cells were performed. Furthermore, the activation of NF- κ B-dependent promoter was demonstrated using co-cultures with human plasma samples or using synovial liquids.

With this generated sensor-effector system we have developed self-adjusting cytokine neutralizer cells as a closed-loop delivery system for anit-inflammatory biologics.

Table of contents

I. Introduction	
Synthetic biology-based cell and gene therapies	1
Sensor-effector cells	1
TNF α and IL-1 β -triggered NF- κ B signaling and autoimmune diseases	2
Rheumatoid arthritis and its therapy	3
The signaling and self-regulation of NF- κ Bs as starting point for sensor-effector cells	4
General influencing factors of NF- κ B signaling and NF- κ B-regulated gene expression	7
Ligand blocking biologicals	8
Receptor blocking biologicals	11
Aim of this work	13
II. Material and Methods	
2.1 Materials	
Biochemical kits	14
Biochemical reagents and enzymes	14
Buffers, solution and media	14
Primary cell, cell lines and bacterial strains	15
Chemicals and reagents	15
Computational software	16
Equipment	16
Plasmids	17
Primer	21
2.2 Methods	
Molecular biology	21
DNA synthesis and vector design	21
Polymerase chain reaction	22
Agarose gel electrophoresis and DNA purification	23
Restriction digest	23
Ligation	23
Chemical competent cells	23
Chemical transformation	24
Isolation and purification of plasmid DNA	24
DNA quantification and purity	24
Glycerol stock	25
Mammalian cell culture	25
Cultivation and general handling of eukaryotic cell lines	25
Cryoconservation and reactivation	25
Transient transfection	25
Protein expression and determination of protein concentrations	26
Western Blot	26
NF- κ B-triggered gene expression	27
Reporter assays	27
SEAP assay	28

	GPL assay	27
	ELISA	28
	Detection of fluorescence proteins	28
	Flow cytometry and fluorescence detection	28
	Alginate encapsulation	28
III.	Design and Results	
	3.1 Design and validation of NF-κB-triggered gene expression	29
	Design and construction of NF- κ B-dependent promoters	29
	Validation of NF- κ B-triggered gene expression	30
	Design and construction of p65 dependent activation of Gal4/UAS chimeric promoters	33
	Results of p65-dependent activation of chimeric Gal4/UAS promoter	38
	Analysis and optimization of the NF- κ B-triggered gene expression	41
	3.2 Development of cytokine neutralizer cells	46
	NF- κ B-regulated expression of biologicals and <i>in vitro</i> validation	46
	Controllability of the cytokine neutralizer cells	51
	Dynamic and reversibility of NF- κ B-triggered gene expression	53
	3.3 Outlook for <i>in vivo</i> implantations	58
	Validation of NF- κ B-regulated gene expression of alginate encapsulated cells	58
	The NF- κ B-regulated promoter works in blood plasma and synovial liquids	61
	NF- κ B-regulated gene expression induced by murine TNF α	62
IV.	Discussion	
	Characteristics of NF- κ B-regulated gene expression	63
	NF- κ B-dependent activation of chimeric Gal4/UAS promoter	64
	Optimization of NF- κ B-triggered gene expression	65
	Characteristics and <i>in vitro</i> validation of the cytokine neutralizer cells	65
	Challenge and problems	67
	Outlook for <i>in vivo</i> trials	67
	Rheumatoid arthritis disease models	68
	Outlook of RA patients - TNF α or IL-1 β are suitable <i>in vivo</i> biomarkers?	69
	Closing words: Vision of intelligent and self-regulated medicine for recurring autoimmune diseases	71
V.	References	72
VI.	DNA sequences	81
VII.	Abbreviations	108
VIII.	Appendix	110

I. Introduction

Synthetic biology-based cell and gene therapies

Synthetic biology is a promising new field of research, encompassing all fields of engineering for the design and construction of effective biological devices and systems. Employing *de novo* engineering of genetic circuits, biological modules and synthetic pathways, synthetic biology makes new applications possible. An ambitious subclass of synthetic biology aims to create synthetic cells for prospective therapies. So-called sensor-effector cells with controllable genetic switches hold great hopes for the generation of novel cell-based therapies. Such cellular circuits allow for regulated inhibition of pathological signals by sensing and responding to disease markers (Ausländer *et al.*, 2012, 2017).

To create possible cell therapies for autoimmune diseases, especially for RA, we harness the contiguity of TNF α , IL-1 β , NF- κ B signaling and TNF α and IL-1 β -blocking biologicals. The aim of this thesis is to bring these actors together in a cooperating and interacting circuit, creating controllable genetic switches to generate sensor-effector cells. The sensor-effector cells generated in this work, expressing neutralizing biologicals under the control of the NF- κ B-dependent promoter, are highlighted as “cytokine neutralizer cells”.

Sensor-effector cells

The basic design of sensor-effector cells is illustrated in Figure 1. Such cells can be structured in two basic modules: Sensitive elements for recognizing and binding analytes, and transducer modules for signal transmission by reporting, transducing and generating outputs (Ruder *et al.*, 2011). Modern methods of molecular biology have simplified the engineering of cells – for example, synthetic DNA sequences can be computationally designed and synthesized *in vitro*.

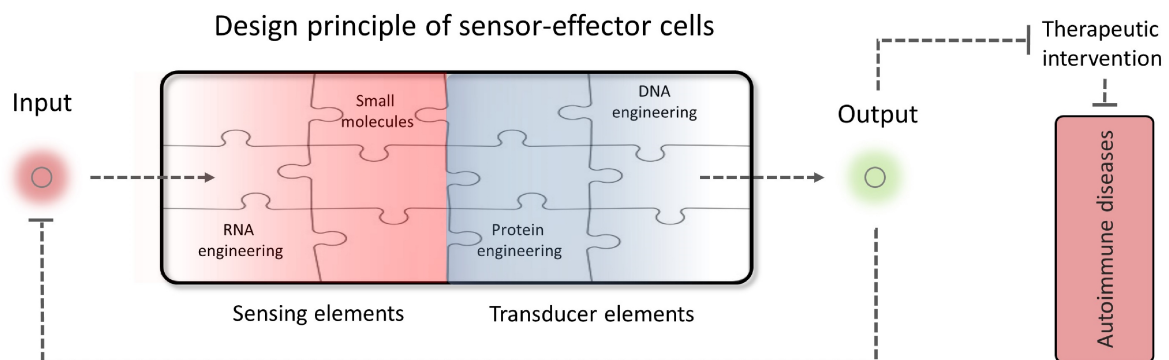


Figure 1. Design principles of sensor-effector cells. Cell-based sensor-effectors consist of two basic modules: Sensitive elements for recognizing and binding analytes, and transducer modules for transmitting, reporting and regulating signals. Such biosensors are predestined for therapeutic interventions, especially for recurrent autoimmune diseases.

Tumor necrosis factor alpha (TNF α) and interleukin 1 beta (IL-1 β) triggered nuclear factor kappa B (NF- κ B) signaling and autoimmune diseases

Nuclear factor of kappa-light-chain-enhancer of activated B cells (NF- κ B) refers to a group of dimeric transcription factors involved in many cell biology processes. The role of gene expression by NF- κ B transcription factors in immune regulation is undisputed (Hayden *et al.*, 2006). There are five different NF- κ B proteins (p65 or RelA, RelB, c-Rel, p50 or NF- κ B1 and NF- κ B2) in mammals, which all build variants of homodimers and heterodimers, with p50/p65 heterodimers occurring most frequently. The molecular structure of several NF- κ Bs is largely elucidated by X-ray structures and protein engineering. Active p50/p65 forms a heterodimer, and the dimer binds to specific DNA motives. NF- κ Bs belongs to the family of eukaryotic transcription factors with a Rel homology domain (RHD) for DNA binding. The transactivation domain contains the C-terminal domain of p65, which is necessary for enhancing gene expression (O'Shea *et al.*, 2008; Wan *et al.*, 2009). By contrast, the corresponding p50 dimer domain is described for gene repression (Plaksin *et al.*, 1993). The classical NF- κ B signaling is described and illustrated in more detail on page 6.

Tumor necrosis factor alpha (TNF α) induces NF- κ B signaling and is one of the best investigated proinflammatory cytokines (Wajant *et al.*, 2003). TNF α and several structurally related cytokines constitute the TNF super family and are major immune regulators (Marks *et al.*, 2008). The fact, that TNF α and NF- κ Bs are conserved in all vertebrates, substantiates their enormous evolutionary impact (Roca *et al.*, 2008, Friedman *et al.*, 2002). Interleukin 1 (IL-1) was the first interleukin to be discovered and has served as a groundbreaking molecule with implications extending far beyond its family (Garlanda *et al.*, 2013).

This thesis will mainly focus on TNF α 's and IL-1's interactions in autoimmune diseases. The cytokines TNF α and IL-1 β are both strong NF- κ B activators and some of the first cytokines to be released in an inflammatory process (Hellweg *et al.*, 2006). In contrast to many other cytokines, TNF α and IL-1 operate systemically in the body – in an autocrine, paracrine and endocrine fashion – among others as acute-phase reactants (Bode *et al.*, 2012). They play a crucial role in many autoimmune diseases, such as rheumatoid arthritis (RA), psoriasis, and diabetes mellitus (Kollias *et al.*, 2002, Feldmann *et al.*, 1996, Yost *et al.*, 2009, Lee *et al.*, 2005). Within the RA-inflamed joint, TNF α is a dominant pro-inflammatory cytokine and is able to induce the production of IL-1 (Butler *et al.*, 1995). Interestingly, TNF α neutralizing antibodies inhibited *in vitro* the synovial culture synthesis of other important pro-inflammatory cytokines - IL-1 (Brennan *et al.*, 1989), IL-6 and GM-CSF (Haworth *et al.*, 1991). This led to the concept that TNF α was at the

apex of a pro-inflammatory cytokine cascade. This unexpected finding could explain why blocking a single cytokine (TNF α) clinically impact a complex inflammatory process (RA) with over-expression of a host of pro-inflammatory cytokines (IL-1, IL-6, TNF, GM-CSF, IFN- γ , etc.) which had overlapping biological effects (Monaco *et al.*, 2014).

Both cytokines and intermediates of NF- κ B pathways became attractive, molecular targets for rationally designed therapies for autoimmune diseases. In fact, TNF α - and IL-1 β -blocking therapies have been applied for many years, and are established as broadly accepted and powerful treatments (Rosman *et al.*, 2013). Especially for recurring chronic inflammations like autoimmune diseases, implanted long-term treatment and monitoring are desirable for future therapies. The biggest motivation for cell-based therapies (e.g. Tregs amplification) are still the fact that patients relapse after conventional therapy stop or patients lose the response to the drug (Wildner *et al.*, 2013). Hence, we aim to develop novel cell therapies, which harness and assemble the described interactions. IL-1 β , TNF α and NF- κ B signaling are an ideal match for synthetic biology-based circuits in human cells to rewire the transmission to TNF α - or IL-1 β -blocking biologicals.

Rheumatoid arthritis and its therapy

RA is a serious and widespread autoimmune disease. In 2015, there were 24.5 million persons worldwide suffering from RA, and the mortality rate of 28 000 deaths in 1990, had increased to 38 000 deaths by 2013 (Vos *et al.*, 2015, Naghavi *et al.*, 2013). The pathogenesis manifests as inflamed and degraded joints as a result of abnormal immune responses to normal body parts, and thus RA patients may suffer severe pain and be confined to bed. The causes of autoimmune diseases are mostly unknown: Heredity, infections, environmental factors, or combinations of these may trigger such inflammation imbalances (McInnes *et al.*, 2011). Likewise, the progression of RA has still not been fully elucidated. However the influence of the following, selected immune factors is undisputed (for recent review: McInnes *et al.*, 2011):

- Autoreactive T cells (Wang *et al.*, 2015)
- Regulatory T cells (Esensten *et al.*, 2009)
- TNF α and IL-1 β (Feldmann *et al.*, 1996)
- Rheumatoid factors (autoreactive antibodies) (van Leeuwen *et al.*, 1995)
- Osteoclasts (IL-1 β -based differentiation of macrophages to osteoclasts) (Kim *et al.*, 2009)
- Th17 cells bringing the cytokine balance in imbalance (Leipe *et al.*, 2010)

First-line medications reduce symptoms and pain. Depending on the type and severity of the RA, typical treatments concern the inflammation progress: Immunosuppressive small molecule drugs, targeting lymphocytes (methotrexate or cyclosporine), and nonsteroidal anti-inflammatory drugs (NSAIDs) such as ibuprofen and diclofenac are widely used (Emery *et al.*, 2006). However, the base therapy is disease-modifying anti-rheumatic drugs (DMARDs). For non-responsive patients the strongest feasible medicine today are biologicals. Figure 2 indicates the building blocks of therapy, with a focus on DMARDs, or rather biologicals (Tony *et al.*, 2010).

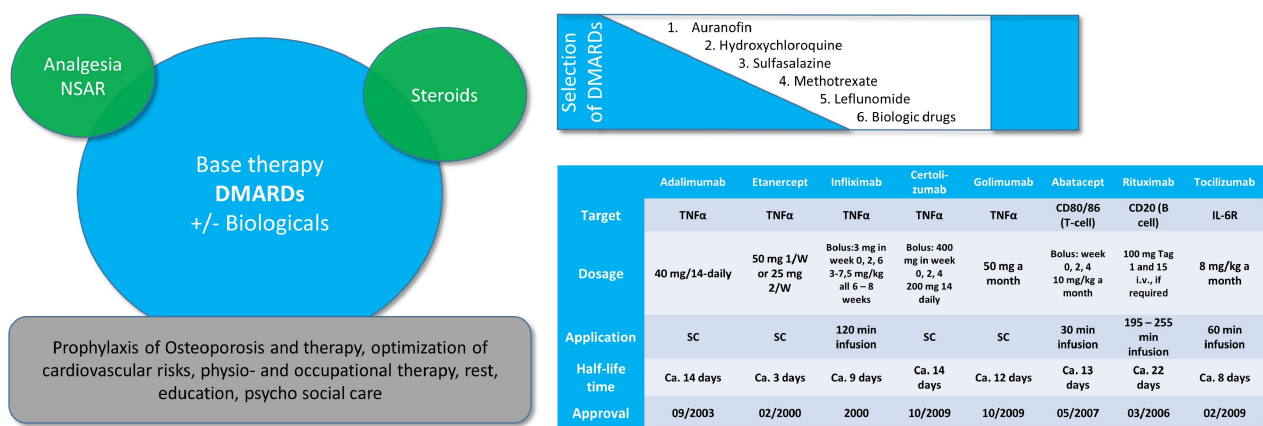


Figure 2. The building blocks of RA therapy. DMARDs constitute the base therapy. On the right side common DMARDs are listed, while to date biologicals have the highest efficiency. The biologicals used most frequently in the treatment of RA and their clinical characteristics are listed.

Like many other autoimmune diseases, RA has a latent form with minimal or no symptoms and periodic relapse. Even after treatment patients suffer setbacks (Wildner *et al.*, 2013).

The signaling and self-regulation of NF- κ Bs as starting point for sensor-effector cells

NF- κ B signaling is predestined for creating controllable genetic switches to generate novel cell therapies. The NF- κ B transcription factors possess a strong gene expression and a strong, self-regulation. The two prototypical NF- κ B pathways (classical and alternative pathway) can be activated by many inducers, depending on receptor expression and cell type. Hundreds of inducers are listed and described on the internet platform of Boston University (<http://www.bu.edu/nf-kb/physiological-mediators/inducers>). However, independent of the inducers, all activations of the classical NF- κ B pathway have the intersection point I κ B kinase (IKK) complex combine (Hayden *et al.*, 2004). The serine-specific IKK complex phosphorylate I κ Bs. An exceptional case is the IKK independent, alternative NF- κ B pathway, which however is not discussed in this work. Figure 3 illustrates the classical NF- κ B pathway triggered by different inducers.

Self-regulation of NF- κ B transcriptions factors

I κ Bs are a protein family, which contain multiple copies of a sequence called ankyrin repeat. The I κ Bs typically masks the nuclear localization signal (NLS) of NF- κ B dimers. For example, I κ B α binds the p50/p65 heterodimer (Jacobs *et al.*, 1998). Hence, the p50/p65 dimer does not translocate into the nucleus and remains inactive. The phosphorylated I κ B α (serines 32 and 36) undergoes a conformational switch, gets ubiquitinated and finally degraded by proteasomes (Boisson *et al.*, 2017). As a consequence the released p50/p65 heterodimer can be transferred into the nucleus, binds to consensus DNA sequences and enhances the expression of different genes (Hayden *et al.*, 2004). One gene expressed by p50/p65 dimers is its own repressor, I κ B α . Newly synthesized I κ B α binds to and masks again p50/p65, resulting in oscillating levels of activity (Hoffmann *et al.*, 2002). This natural negative feedback regulation is predestined for controllable genetic switches to generate sensor-effector cells. Furthermore p50/p65 dimer is a strong transcription factor through the transactivation domain of p65: p50/p65 regulates the expression of acute-phase proteins, which circulate in high concentrations (O'Shea *et al.*, 2008, Bode *et al.*, 2012).

The aims to be achieved with sensor-effector cells are: (i) High sensitivity and specificity and (ii) strong and reversible gene expression. Classical NF- κ B signaling as an auto-regulated molecular switch for strong gene expression is one fundamental, biologic module of this work. However, synthetic biology aims to advance natural genetic circuits and pathways to create new features. Modern molecular methods may enable such efforts by the insertion of synthetic and interfering elements (Ruder *et al.*, 2011). In Figure 3 possible interventions are red-marked and exemplary described (interfering, rewiring, or enhancing natural NF- κ B signaling by synthetic interlocking modules).

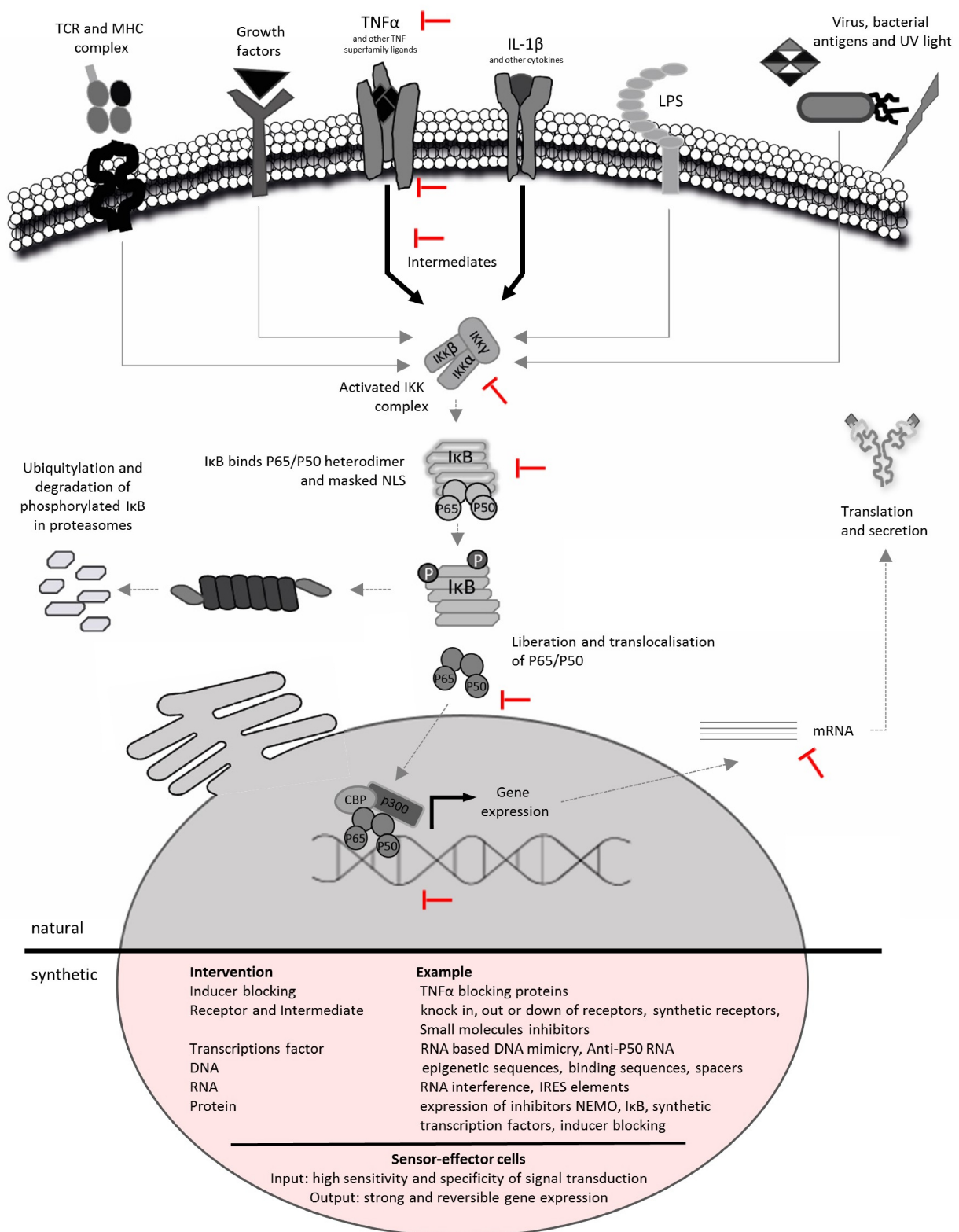


Figure 3. Natural NF-κB signaling and synthetic biology-based interventions. The aim with synthetic biology-based sensor-effector cells is the sensitive recognition of analytes with tightly regulated transmission, resulting in a strongly expressed and therapeutic output. Regardless of different ligand-receptor interactions, the intersection of classical NF-κB signaling is the activation of the IKK complex (Hayden *et al.*, 2004). The red marks demonstrate interesting and synthetic regulating interventions in the classical NF-κB signaling which can be addressed by help of modern molecular methods of cell engineering.

General influencing factors of NF- κ B signaling and NF- κ B-regulated gene expression

NF- κ B transcription factors show different activity patterns depending on (i) the exposure time of inducers, which influences the NF- κ B-dependent expression profile, (ii) different inducer stimuli with different strengths and (iii) the cell type or the cellular differentiation (Hoffmann *et al.*, 2002, Hellweg *et al.*, 2006). In the most cell types, NF- κ Bs activate hundreds of genes including a variety of immune-stimulating factors (Hayden *et al.*, 2006). In some immune cells, NF- κ Bs also activate immunosuppressing genes or influence cell differentiation (Cao *et al.*, 2006).

The following example is intended to illustrate this: In the development of regulatory T cells (Tregs). C-Rel directly regulate Foxp3 expression by binding to the methylated Foxp3 enhancer region. Thus, the ability of c-Rel to bind to the methylated Foxp3 enhancer region in T cells developed beyond double positive stage (during thymic Treg cell development) makes it a candidate for being the pioneer transcription factor, which initiates chromatin remodeling that is characteristic of natural Treg cells. (Long *et al.*, 2009). Thus, NF- κ B-dependent expression profiles vary depending on inducer type, pulse time and cellular differentiation or cell type.

Another aim to be achieved with therapeutic sensor-effector cells is therefore to inhibit or reduce the NF- κ B-activated endogenous genes and to potentially influence the cell type specific secretome. As a side project, we attempted to capture and rewire p50/p65 to a non-mammalian inducible promoter, to consider the secretome of p50/p65 activated genes (see Page 33). By another step the endogenous p50/p65 binding sites must be inhibited using for example repressors or dynamic genome engineering by single RNA strands (Ausländer *et al.*, 2014).

Ligand-blocking biologicals

Before their discovery, antibodies were first described as magic bullets. As early as 1896 they made passive immunization against diphtheria possible after transferring the blood serum of diseased animals (Tan *et al.*, 2010). Today it is understood that antibodies are one fundamental backbone of the adaptive immune system. Furthermore, through the opsonization of pathogens, antibodies become adapters to the innate immune system (Murphy *et al.*, 2009). The repertoire of one human consist more than 10^{12} different antibodies, each antibody created by strict regulation and clonal selection of B-cells (Albert *et al.*, 2002).

From a clinical point of view, antibody-based treatments have revolutionized modern medicine today and research on antibodies is still continuing (Liu *et al.*, 2014). In comparison to other biologicals, antibodies have certain fundamental advantages: (i) Their big size enables longer half-life times by reducing kidney filtration; (ii) there are two antigen binding arms in one molecule; (iii) the Fc-tail enables Fc-receptor binding (Charmes *et al.*, 2009); and (iv) the constant regions (CL, CH1, CH2 and CH3) provide a steric fundament for the variable domains with their CDR loops (antigen-binding). Those features are challenging antibody mimetics such as: scFvs, DARPins, anticalins, avimers and affibodies (Janda *et al.*, 2016, Sedláč *et al.*, 2015, Torres *et al.*, 2008). The 2D and 3D structures of antibodies are illustrated in Figure 4. As mentioned previously, TNF α -blocking therapies are widespread and powerful medicines and have been approved for various diseases. The success of TNF α -blocking therapies, especially in treatment of autoimmune diseases, reflects the crucial role of TNF α in these diseases (Rosman *et al.*, 2013). For more than 20 years now, the TNF α -blocking biologicals adalimumab and etanercept have been clinically applied and are the gold standard in RA treatment (Haraoui *et al.*, 2007, Mease *et al.*, 2007). In addition, the therapeutic application of these biologicals is permanently being expanded to other related diseases.

Adalimumab and etanercept

In respect of adalimumab, its clinical application is being extended to psoriatic arthritis, ankylosing spondylitis, Crohn's disease, ulcerative colitis, plaque psoriasis (Scheinfeld *et al.*, 2003, Maxwell *et al.*, 2015, Baumgart, 2009, Sandborn *et al.*, 2012, Croom *et al.*, 2009). Adalimumab is a complete humanized, synthetic immunoglobulin G1 (IgG1) antibody, developed by modern molecular methods and rational design. Adalimumab was the first humanized antibody-based therapy approved by the United States Food and Drug Administration (FDA) (Mease *et al.*, 2007).

In comparison to other TNF α blocking biologicals, adalimumab has the following competitive features:

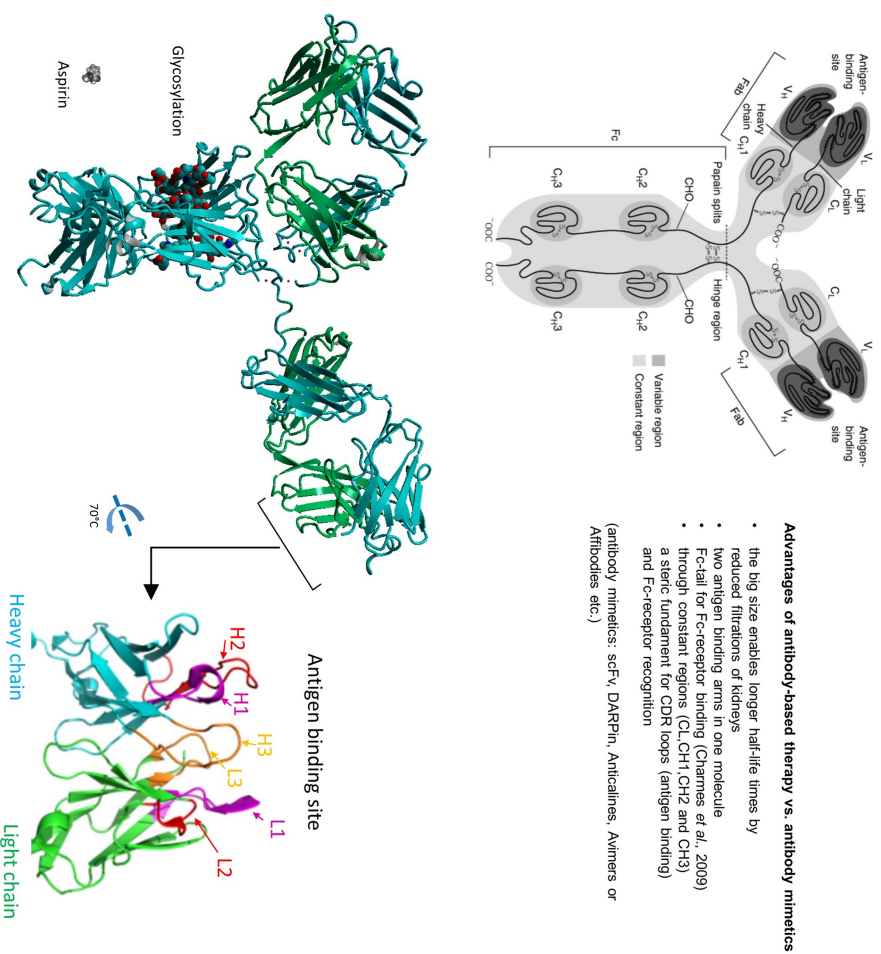
- Completely humanized
- Longer half-life times (Figure 2)
 - Infliximab, etanercept, golimumab
 - Similar half-life times of certolizumab, but higher concentrations
- Binds only active TNF α (binding pattern on two monomers; Figure 4)
- Higher affinity of molecular epitope-paratope interactions (bigger contact area, stronger electronegativity-based non-covalent forces of side chains interaction; Figure 4)

Etanercept is a synthetic soluble decoy receptor, which contains the TNFR2 ectodomain followed by the IgG1 Fc domain (Haraoui *et al.*, 2007). Soluble etanercept mimics the native TNFR2 binding patterns to TNF α (Haraoui *et al.*, 2007). In comparison to natural TNF α -TNFR2 complexes, the TNF α -etanercept complexes miss one site-specific contact: Etanercept proteins bind to TNF α twice as homodimers and natural TNF α -TNFR2 complexes are formed by three receptors binding to one TNF α trimer (Figure 5).

Furthermore, etanercept has a broader contact area to TNF compared to infliximab. Similar to human antibodies, the C-terminal fused Fc-tail enables Fc-receptor binding. However, in comparison to antibodies, the etanercept-TNF α complex develops no cross-linking, which is shown to enhance phagocytosis by macrophages (Murphy *et al.*, 2009). One to two etanercept molecules bind to one TNF α trimer, resulting in a complex of 180 kDa to 300 kDa, while adalimumab or infliximab can bind several times to one TNF α trimer, getting a cross-linking complex of 4000 kDa to 14000 kDa (Kohno *et al.*, 2007). Also, shorter half-life times are detected for etanercept.

Both biologicals, etanercept and adalimumab, showed inhibition of ligand activity of transmembrane TNF- α , while etanercept showed less activity. Accumulating evidence suggests that also transmembrane TNF- α is involved in the inflammatory response (Horiuchi *et al.*, 2010). Nevertheless, like adalimumab, etanercept has now been applied for two decades and has gained clinical experiences (Rosman *et al.*, 2002). Adalimumab and etanercept are highly predestined for their interaction with TNF α -triggered NF- κ B signaling and for therapeutic output.

Human IgG1 antibody



Molecular view of Anti-TNF α therapy

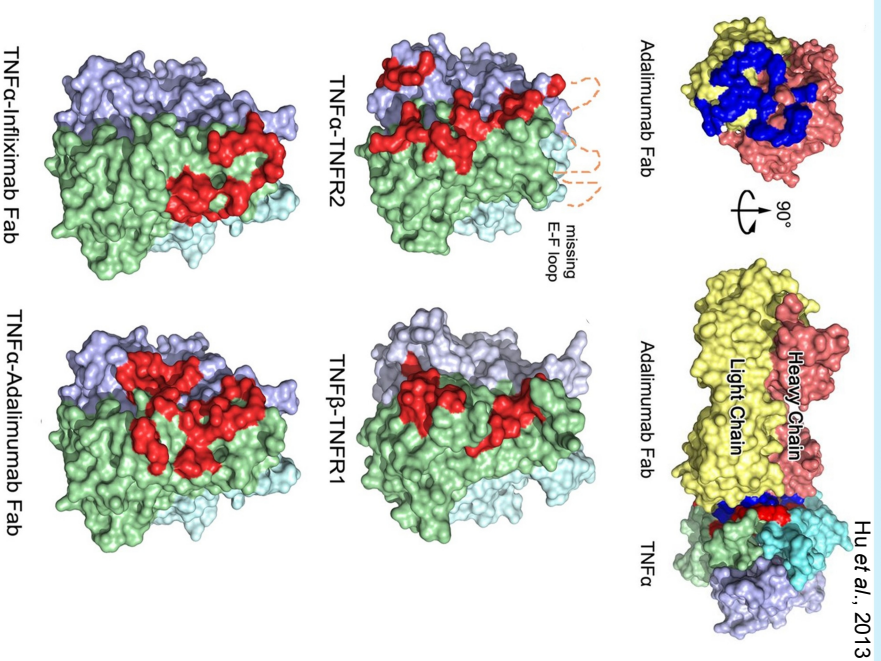


Figure 4. The human IgG1 antibody and adalimumab. Top left: 2D schematic illustration of the human IgG1 antibody and description of important features (Skerra, 2013). Antibodies have high variable sequences on their N-terminal ends, so-called CDRs. Bottom left: In the 3D structure of IgG1 antibodies, one can see the variable CDR formed by six loops (Harris *et al.*, 1998, PDB 1IGY). These loops and their high variants enable binding with almost unlimited different molecules. The aspirin placed next to the 3D structure serves to illustrate its size. On the right side: Adalimumab is the first approved complete humanized antibody therapy and one of the most successful. Here, the epitope surface of TNF α is emphasized in comparison of other TNF α -binding biologicals. Adalimumab binds more than one TNF α monomer with strong affinity (Hu *et al.*, 2013).

Receptor-blocking biologicals

Receptor-ligand interactions are the first step and initiator of signal transductions. Without the corresponding receptors, cells do not respond to the ligand. Most receptors are membrane proteins. Approximately 20 % to 30 % of all genes in most genomes encode membrane proteins, which are the targets of over 50 % of all modern medicinal drugs (Krogh *et al.*, 2001, Overington *et al.*, 2006). It is therefore a common strategy of biologicals to interfere here.

The following therapeutic biologicals act in a receptor blocking way and interfere with the cross-talking of the immune system:

- Antibodies-based:
 - Avelumab human PD-L1 (Apolo *et al.*, 2017)
 - Ipilimumab CTLA-4 (Della Vittoria Scarpati *et al.*, 2014)
 - Basiliximab CD25-antigen (interleukin 2 receptor) (Chapman *et al.*, 2003)
 - Brodalumab interleukin 17 receptor (Farahnik *et al.*, 2016)
- Non-antibodies:
 - Abatacept (CD80 or CD86 on T cells) (Keating *et al.*, 2013)
 - Alefacept (CD2 on T cells) (Jenneck *et al.*, 2007)
 - Anakinra interleukin 1 receptor antagonist (Fleischmann *et al.*, 2003)

Anakinra

Anakinra is a recombinant interleukin 1 receptor antagonist and approved for the treatment of RA (Schiff *et al.*, 2004). Anakinra mimics native IL-1 β binding, but does not activate IL-1 receptors. One major advantage of anakinra is that it also inhibits IL-1 α . A second advantage is its small size, which allows for better tissue penetration (Dinarello *et al.*, 2012).

Humans and other vertebrates also express interleukin 1 receptor antagonist for immune regulation by itself. IL-1 receptor antagonist deficient mice develop autoimmune diseases, which emphasize its importance in immune regulation (Akitsu *et al.*, 2015). Anakinra acts in a different way compared to antibody-based treatments. To extend the therapeutic spectrum and for comparison, we used interleukin 1 receptor antagonist as an effector molecule of sensor-effector cells. All three biologicals used in this thesis are illustrated in Figure 5, with their corresponding effect mechanisms.

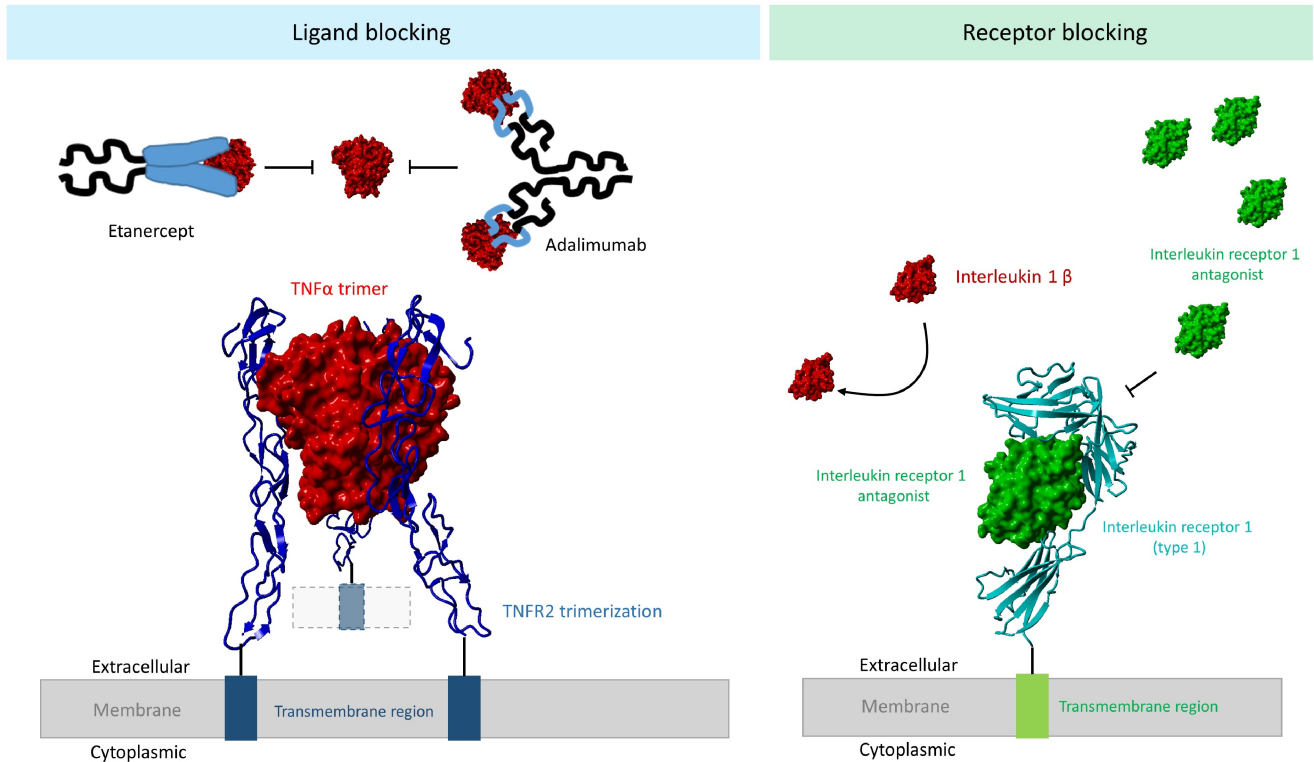


Figure 5. Ligand-blocking vs. receptor-blocking. Left side: Etanercept and adalimumab bind to the ligand TNF α . Bound TNF α trimers are not anymore able to bind to and activate TNF receptors (TNFR1 and TNFR2). Furthermore, etanercept and adalimumab showed an inhibition of ligand activity of transmembrane bound TNF α (Horiuchi *et al.*, 2010). Right side: Anakinra, the interleukin receptor 1 antagonist, mimics the structure of IL-1 β and binds directly to the interleukin 1 receptor without triggering a signal transduction (x-ray structure of TNFR2: PDB 3ALQ; IL-1RA: PDB 1IRA).

Aim of this work

The aim of this thesis is to develop synthetic biology-based sensor-effector cells for prospective therapies against autoimmune diseases such as RA. We inserted controllable genetic switches in human cells, which are capable to sense RA-related cytokines and respond with the production of RA suppressing biologicals. By merging of the following three interacting modules, it was strived to establish a tight self-controlled sensor-effector circuit in human cells: (i) Sensing of TNF α or IL-1 β by endogenously expressed receptors (ii) an optimized artificial NF- κ B-regulated promoter and (iii) neutralizing those inputs by TNF α or IL-1 β -blocking biologicals. With this established sensor-effector system, we developed self-adjusting neutralizer cells as a closed-loop delivery system of anti-inflammatory biologicals (Figure 6).

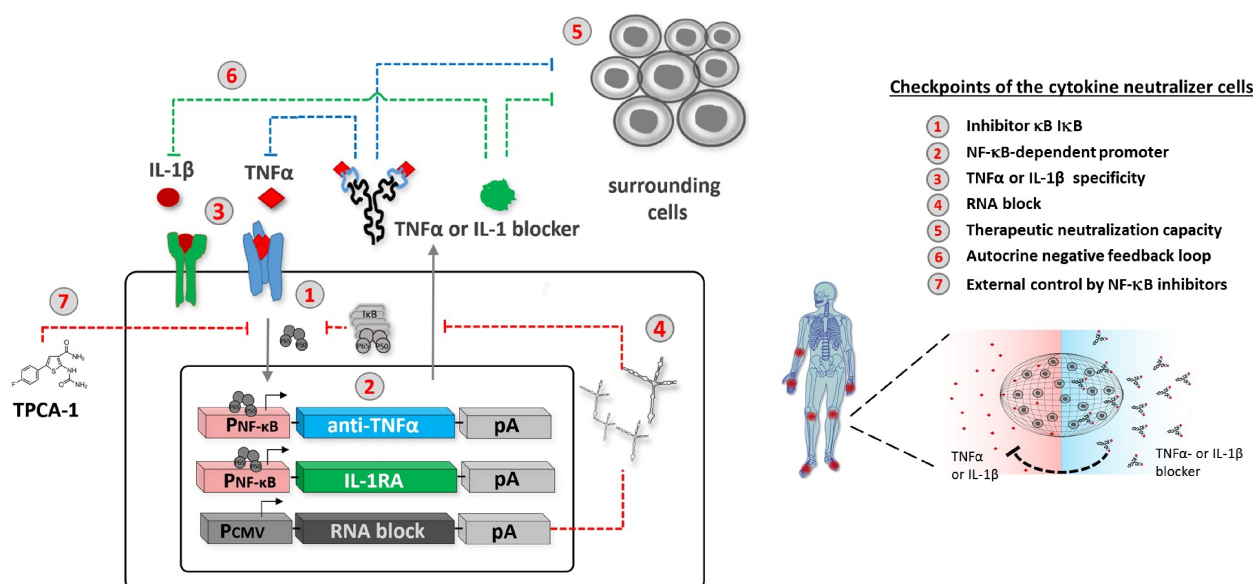


Figure 6. Design and construction of the cytokine neutralizer. Overview of the natural and synthetic interacting molecular components, resulting in a tight controlled sensor-effector system. Non-active NF- κ Bs are naturally captured by endogenously expressed I κ Bs, which are induced by NF- κ Bs themselves, demonstrating a natural self-controlled negative feedback system. TNF α and IL-1 β triggers NF- κ B signaling in human HEK293T cells and produce dose-dependent and self-regulated TNF α or IL-1 β blocking biologicals. The NF- κ B translocalisation into nucleus, triggered by TNF α or IL-1 β , activate a synthetic NF- κ B-dependent promoter. NF- κ B-driven expression is furthermore influenced by an RNA block, improving the activation strength. The therapeutic output, expressing biologicals, neutralize the incoming signal. This autonomous self-regulated drug delivery can be further and specifically controlled by the NF- κ B inhibitor TPCA-1. The interactions of natural and synthetic cellular regulations (checkpoints) optimized the cellular dynamic of the neutralizer cells. These designer cells, encapsulated and implanted *in vivo* as a local molecular sensor-effector system, may perhaps enable a monitoring real and longtime treatment by rebalancing autonomously cytokine levels in chronic disease, such as RA.

II. Material and Methods

2.1 Material

Biochemical kits

Table 1: Biochemical kits

Name	Manufacturer
DC Protein Assay	Bio-Rad Laboratories GmbH, München, Germany
JETSTAR 2.0 Plasmid Midiprep Kit	ZYMO Research, Freiburg im Breisgau, Germany
Zymoclean™ Gel DNA Recovery Kit	ZYMO Research, Freiburg im Breisgau, Germany
Zyppy™ Plasmid Miniprep Kit	ZYMO Research, Freiburg im Breisgau, Germany

Biochemical reagents and enzymes

Table 2: Biochemical reagents and enzymes

Name	Manufacturer
Adalimumab	InvivoGen, Toulouse, France; cat. no. htnfa-mab1
Antarctic Phosphatase	New England Biolabs Inc., Ipswich, MA, U.S.A.
Goat anti-Human IgG Secondary antibody HRP conjugated (62-8420)	Thermo Fischer Scientific GmbH, Dreieich, Germany
Mouse anti-Human IgG Fc Secondary antibody (MA1-10378)	Thermo Fischer Scientific GmbH, Dreieich, Germany
Rabbit IgG Isotype Control (02-6102)	Thermo Fischer Scientific GmbH, Dreieich, Germany
Phusion © High-fidelity DNA Polymerase	New England Biolabs Inc., Ipswich, MA, U.S.A.
Protease Inhibitor, complete, EDTA-free	Roche Diagnostics AG, Rotkreuz, Switzerland
Restriction Enzymes	New England Biolabs Inc., Ipswich, MA, U.S.A.
T4 DNA Ligase	New England Biolabs Inc., Ipswich, MA, U.S.A.
Taq Polymerase	New England Biolabs Inc., Ipswich, MA, U.S.A.
Trypsin-EDTA	Sigma, Deisenhofen, Germany

Buffers, solutions and media

Table 3: Buffers, solutions and media

Name	Manufacturer or composition
Antarctic Phosphatase Reaction Buffer	New England Biolabs Inc., Ipswich, MA, U.S.A.
DMEM low glucose	Thermo Fischer Scientific GmbH, Dreieich, Germany
DMEM Complete Medium	Thermo Fischer Scientific GmbH, Dreieich, Germany
GeneRuler™ DNA Ladder Mix	Fermentas GmbH, St. Leon-Rot, Germany
LB media	10 g/l tryptone, 5 g/l yeast extract, 2.5 g/l NaCl
Loading Buffer, 6X	60% (v/v) Glycerol, 0.03 % (w/v) Bromphenolblue, 0.03 % (w/v) Xylene cyanid FF, Tris-HCL (pH 7.4) 10 mM, EDTA 60 mM
PBS Buffer, 10x	Sigma, Deisenhofen, Germany
PCR Buffers HF/GC, 5x	New England Biolabs Inc., Ipswich, MA, U.S.A.
PEI Transfection Solution	1 mg/mL in MQ H ₂ O, pH = 7.2
pNPP Substrate (P5994-25TAB)	Sigma, Deisenhofen, Germany
PageRuler™ Plus Protein Ladder	Thermo Fischer Scientific GmbH, Dreieich, Germany
RPMI 1640 medium	Thermo Fischer Scientific GmbH, Dreieich, Germany
Restriction Enzyme NEB Buffer 1-4	New England Biolabs Inc., Ipswich, MA, U.S.A.
SDS-PAGE Running Buffer, 10x	25mM Tris, 192 mM Glycine, 0.1% SDS

Lämmli buffer (1x)	62.5 mM Tris, 10% Glycerol (v/v), 2% β -mercaptoethanol (v/v), 1.5 % SDS (w/v), 0.003 % Bromphenol blue (w/v)
SEAP Assay Buffer, 2x	20 mM Homoarginine, 1 mM $MgCl_2$, 21% (v/v) Diethanolamine, pH = 9.8
T4 DNA Ligase Buffer	Fermentas GmbH, St. Leon-Rot, Germany
TAE Buffer, 50x	2 M Tris, 10 mM Glacial acetic acid, 50 mM EDTA
Transfer Buffer, 10x	25 mM Tris, 200 mM glycine, 10% Methanol (v/v)

Primary cells, cell lines and bacterial strains

Table 4: Primary cells, cell lines and bacterial strains

Name	Specification or manufacturer
NEB 5-alpha Competent <i>E. coli</i>	New England Biolabs Inc., Ipswich, MA, U.S.A.
Jurkat	Jurkat (suspension cells) Institute own stock (Prof. Wajant, Division of Molecular Internal Medicine) human T cell lymphoma
HEK-293-T	Human embryonic kidney cells, transgenic for the simian vacuolating virus 40 (SV40) large T antigen American Type Culture Collection: CRL-11268
Hela	Institute own stock (Prof. Walles, Department Tissue engineering and regenerative medicine) human epithelial cervix cells
CHO-K1	Chinese hamster ovary, American Type Culture Collection: CCL-61

Chemicals and reagents

For all solutions, mixtures and other purposes where ultra pure water was necessary. Millipore water, previously purified and deionized by EMD Millipore Milli-Q™ Advantage A10, was used.

Table 5: Chemicals and reagents

Name	Manufacturer
Acrylamide	Sigma, Deisenhofen, Germany
Agar	Sigma, Deisenhofen, Germany
Agarose	Biozym, Hessisch Oldendorf, Germany
Ampicillin	Sigma, Deisenhofen, Germany
BSA	New England Biolabs Inc., Ipswich, MA, USA
DMSO	Sigma, Deisenhofen, Germany
dNTPs	New England Biolabs Inc., Ipswich, MA, USA
EDTA	Sigma, Deisenhofen, Germany
Ethanol	Sigma, Deisenhofen, Germany
FCS (FCS.ADD.050)	Bio & SELL GmbH (D), Nürnberg, Germany
Glycerol	Sigma, Deisenhofen, Germany
LPS (cat. no. L2654)	Sigma, Deisenhofen, Germany
Milk, non-fat powder	Carl Roth, Karlsruhe, Germany
Isopropanol	Sigma, Deisenhofen, Germany
SDS	Carl Roth, Karlsruhe, Germany
GelRed™	Genaxxon bioscience GmbH
WesternBright Chemiluminescence substrat Quantum (Western Blot)	Biozym, Hessisch Oldendorf, Germany

Tween-20	Sigma, Deisenhofen, Germany
Trypanblau (0,4 %)	Sigma, Deisenhofen, Germany
Polyethylenimin (PEI)	Polysciences Europe GmbH, Hirschberg an der Bergstrasse, Germany
Poly(I:C) (cat. no. P9582)	Sigma, Deisenhofen, Germany
p-Nitrophenyl Phosphate (pNPP)	New England Biolabs Inc., Ipswich, MA, USA
Trizma Base	Sigma, Deisenhofen, Germany
Tryptone	Sigma, Deisenhofen, Germany
Thioglycollate	Sigma, Deisenhofen, Germany

Computational software

Table 6: Computational software

Software	Developer
Adobe Creative Suite	Adobe Systems Corp., San Jose, CA, U.S.A.
Clone Manager Basic 8.0	Scientific & Educational Software, Cary, NC, U.S.A.
EndNote X4.0.2	Thomson Reuters Corp., New York City, NY, U.S.A.
FlowJo	FlowJo (USA)
Fluor-Chem Q	CellBioscience, California, USA
Finch TV 1.4	Geospiza Inc., Seattle, WA, U.S.A.
GraphPad Prism 6.0	GraphPad Software Inc., La Jolla, CA, U.S.A.
Keyence BZ II Analyze	Keyence, Neu-Isenburg, Germany
Keyence BZ II Viewe	Keyence, Neu-Isenburg, Germany
Microsoft Office Professional Plus 2010	Microsoft Corp., Redmond, WA, U.S.A.
Tecan iconcontrol	Tecan Deutschland GmbH
YASARA (protein structure)	YASARA Biosciences GmbH, Elmar Krieger, Vienna, Austria

Equipment

Table 7: Equipment

Equipment	Manufacturer
Autoclave	Systec GmbH, Linden, Germany
Biometra (Blotting Semi-Dry)	Analytik Jena AG, Jena, Germany
Vacusafer	NTEGRA Biosciences Deutschland GmbH
Cell culture laminar flow workbench S2	Thermo Fischer Scientific GmbH, Dreieich, Germany
Cell culture incubator CO ₂ hera cell 240	Heraeus Holding GmbH, Hanau, Germany
Centrifuge 5424	Eppendorf AG, Hamburg, Germany
Centrifuge 5417R	Eppendorf AG, Hamburg, Germany
Centrifuge Avanti J-HC	BeckmannCoulter Inc., Brea, CA, USA
Durchflussszytometer (BD FACS Calibur)	BD Biosciences, Heidelberg, Germany
Electrophoresis chamber	Bio-Rad Laboratories Inc., Hercules, CA, USA
Mini-PROTEAN Tetra System	Bio-Rad Laboratories Inc., Hercules, CA, USA
Freezer -20 °C Premium	Liebherr-International AG, Bulle, Switzerland
Freezer -80 °C hera freeze	Heraeus Holding GmbH, Hanau, Germany
Mikroskop BZ-9000 BIOREVO System	Keyence, Neu-Isenburg, Germany
Laser-Scanning-Mikroskop TCS-SP	Leica Microsystems GmbH, Wetzlar, Germany

Nitrogen cryo tank MV 815 P-190 (–180°C)	Jutta Ohst german-cryo GmbH, Jüchen, Germany
Multichannel pipettes Research plus PCR Thermocycler, SensQuest	Eppendorf AG, Hamburg, Germany Bio-Rad Laboratories Inc., Hercules, CA, USA
pH meter 632	Metrohm GmbH % Co. KG, Filderstadt, Germany
Pipetboy Easypet	Eppendorf AG, Hamburg, Germany
Pipettes Pipetman	Gilson Inc., Middleton, WI, USA
Magnet stirrer	VWR, Ismaning, Germany
Mikroscope Axiovert	Carl Zeiss AG, Oberkochen, Germany
UV Transilluminator	Vilber Lourmat Deutschland GmbH
Tecan infinite M200	Tecan Austria GmbH, Grödig, Austria
EMD Millipore Milli-Q™ Advantage A10	Merck Millipore, Darmstadt, Germany
Fluor-Chem Q Imaging-device	CellBioscience, California, USA
Vortex Genie 2	Bender und Hobein AG, Zürich, Switzerland
Waterbath EO	LAUDA DR. R. WOBSE GMBH & CO. KG, Lauda-Königshofen, Germany
Fine balance	KERN & SOHN GmbH, Balingen, Germany

Plasmids

Table 8: Comprehensive list and description of all cloning and expression vectors used in this study

Plasmid	Description and cloning strategy	Reference
pcDNA3.1+	Versatile mammalian expression vector containing a CMV-promotor	Life technologies
pDH1	pNFκB-driven SEAP expression vector. First, NF-κB binding sites and CMV _{min} were DNA synthesized and cloned into pcDNA3.1+ by MluI and HindIII. Sequence of NF-κB binding sites were previously published (28). Second, SEAP open reading frame was PCR amplified from SEAP2Ctronrol (Clontech) by oDHSEAP_fw and oDHSEAP_rev_NotI and inserted by HindIII and NotI.	This work
pDH2	pDH2-CMVmin-shRNA1-SEAP. A CMV _{min} expressed shRNA against SEAP mRNA. CMVmin Promoter and shRNA1 against SEAP were DNA synthesized and cloned in pcDNA3.1+ by MluI and NotI. SEAP shRNA sequence of pDH2 has been previously proved (Wooddell <i>et al.</i> , 2005): GACATGAAATACGAGATCCACCGAGACCTCGAGGTCTCGGTGGA TCTCGTATTTTCATGTCTTTTTTT	This work
pDH3	pDH3-CMVmin-shRNA2-SEAP. Same cloning like pDH2. SEAP shRNA sequence were blasted: GACAGCTGCCAGGATCCTAAACTCGAGTTTAGGATCCTGGCAGC TGCTTTTTTTT	This work
pDH4	pDH4-CMVmin-shRNA3-SEAP. Same cloning like pDH2. SEAP shRNA sequence were blasted: GAGGCCGAAAGTACATGTTTCCTCGAGGAAACATGTACTTTTCGG CCTCTTTTTTTT	This work
pDH5	pDH5-CMVmin-shRNA4-SEAP. Same cloning like pDH2. SEAP shRNA sequence were blasted: ACGGTCCTCCTATACGGAACCTCGAGGTTTCCGTATAGGAGGA CCGTTTTTTTTT	This work
pDH6-Gal4-SEAP	pGal4-driven SEAP expression vector. First, Gal4/UAS binding sites and CMVmin were DNA synthesized and cloned into pcDNA3.1+ by MluI and HindIII. Sequence were previously published (28). Second, SEAP open reading frame was PCR amplified from SEAP2Ctronrol (Clontech) by oDH1_fw and oDH2_rev and inserted by HindIII and NotI.	This work

pDH7	pDH7.1-CMV-TC1 CMV expressed non-coding RNA, containing P50 binding and P65 binding sites (based on previously published; Wurster <i>et al.</i> , 2009), Rev binding sites and nuclear localization sites. Secondary structure were calculated by web tool: http://rna.urmc.rochester.edu/RNAstructureWeb/Servers/Predict1/Predict1.html . Sequence see supplementary DNA sequences and Figure 11. DNA synthesized and cloned into pcDNA3.1+ by NheI and NotI.	This work
pDH8	pDH7.2-CMV-TC4 description see pDH7	This work
pDH9	pDH7.3-CMV-TC5 description see pDH7	This work
pDH10	pDH7.4-CMV-TC6 description see pDH7	This work
pDH11	pDH7.5-CMV-TC7 description see pDH7	This work
pDH12	pDH7.6-CMV-TC8 description see pDH7	This work
pDH13	pDH7.7-CMV-TC11 description see pDH7	This work
pDH14	pDH7.8-CMV-TC12 description see pDH7	This work
pDH15	pDH7.9-CMV-TC17 description see pDH7	This work
pDH16	pDH7.10-CMV-TC18 description see pDH7	This work
pDH17	pDH7.11-CMV-TC21 description see pDH7	This work
pDH18	pDH7.12-CMV-TC22 description see pDH7	This work
pDH19	pDH7.13-CMV-TC23 description see pDH7	This work
pDH20	pDH7.14-CMV-TC24 description see pDH7	This work
pDH21	pDH7.15-CMV-TC25 description see pDH7	This work
pDH22	pDH7.16-CMV-TC26 description see pDH7	This work
pDH23	pDH7.17-CMV-TC27 description see pDH7	This work
pDH24	pDH24-CMV-RevM10-Gal4BD_Zürich_Linkers CMV driven synthetic fusion protein, containing Gal4DBD (De Bosscher <i>et al.</i> , 2000, Seipel <i>et al.</i> , 1992), RevM10 and a protein linker (Seipel <i>et al.</i> , 1992). DNA was synthesized and cloned into pcDNA3.1+ by HindIII and NotI. Sequence see supplementary and Figure 11.	This work
pDH25	pDH25-CMV-Gal4DBD-RevM10-C-term_revers_Zürich_Linkers CMV driven synthetic fusion protein, containing Gal4DBD (De Bosscher <i>et al.</i> , 2000, Seipel <i>et al.</i> , 1992), RevM10 (Guzik <i>et al.</i> , 2001) in reversed sequence and a protein linker (Seipel <i>et al.</i> , 1992). DNA was synthesized and cloned into pcDNA3.1+ by HindIII and NotI. Sequence see supplementary and Figure 11.	This work
pDH26	pDH26-CMV-RevM10-Gal4BD_GS_Linkers CMV driven synthetic fusion protein, containing Gal4DBD (De Bosscher <i>et al.</i> , 2000, Seipel <i>et al.</i> , 1992), RevM10 (Guzik <i>et al.</i> , 2001) and a protein GS-linker (Reddy Chichili <i>et al.</i> , 2013). DNA was synthesized and cloned into pcDNA3.1+ by HindIII and NotI. Sequence see supplementary and Figure 11.	This work

pDH27	pDH27-CMV-Gal4DBD--RevM10-C-term__revers_GS_Linkers CMV driven synthetic fusion protein, containing Gal4DBD (De Bosscher <i>et al.</i> , 2000, Seipel <i>et al.</i> , 1992), RevM10 (Guzik <i>et al.</i> , 2001) in reversed sequence and a protein GS-linker (Reddy Chichili <i>et al.</i> , 2013). DNA was synthesized and cloned into pcDNA3.1+ by HindIII and NotI. Sequence see supplementary and Figure 11.	This work
pDH28	pDH28-CMV-RevM10-Gal4BD_Helix_Linkers CMV driven synthetic fusion protein, containing Gal4DBD (De Bosscher <i>et al.</i> , 2000, Seipel <i>et al.</i> , 1992), RevM10 (Guzik <i>et al.</i> , 2001) in and a protein linker (Arai <i>et al.</i> , 2001). DNA was synthesized and cloned into pcDNA3.1+ by HindIII and NotI. Sequence see supplementary and Figure 11.	This work
pDH29	pDH29-CMV-Gal4DBD--RevM10-C-term__revers_Helix_Linkers CMV driven synthetic fusion protein, containing Gal4DBD (De Bosscher <i>et al.</i> , 2000, Seipel <i>et al.</i> , 1992), RevM10 (Guzik <i>et al.</i> , 2001) in reversed sequence and a protein linker (Arai <i>et al.</i> , 2001). DNA was synthesized and cloned into pcDNA3.1+ by HindIII and NotI. Sequence see supplementary and Figure 11.	This work
pDH30	pDH30-CMV--Gal4DBD-c-term p50_Zürich_Linkers CMV driven synthetic fusion protein, containing Gal4DBD (De Bosscher <i>et al.</i> , 2000, Seipel <i>et al.</i> , 1992), P50 dimer domain (Figure 10) and a protein linker (Seipel <i>et al.</i> , 1992). DNA was synthesized and cloned into pcDNA3.1+ by HindIII and NotI. Sequence see supplementary and Figure 10.	This work
pDH31	pDH31-CMV-Gal4DBD-reversedseq-c-term p50_revers_Zürich_Linkers CMV driven synthetic fusion protein, containing Gal4DBD (De Bosscher <i>et al.</i> , 2000, Seipel <i>et al.</i> , 1992), P50 dimer domain (Figure 10) and a protein linker (Seipel <i>et al.</i> , 1992). DNA was synthesized and cloned into pcDNA3.1+ by HindIII and NotI. Sequence see supplementary and Figure 10.	This work
pDH32	pDH32-CMV-Gal4DBD-c-term p50-helix-linker_Helix_Linkers CMV driven synthetic fusion protein, containing Gal4DBD (De Bosscher <i>et al.</i> , 2000, Seipel <i>et al.</i> , 1992), P50 dimer domain (Figure 10) and a protein linker (Arai <i>et al.</i> , 2001). DNA was synthesized and cloned into pcDNA3.1+ by HindIII and NotI. Sequence see supplementary and Figure 10.	This work
pDH33	pDH33-CMV-Gal4DBD-reversedseq-c-term p50_revers_Helix_Linkers CMV driven synthetic fusion protein, containing Gal4DBD (De Bosscher <i>et al.</i> , 2000, Seipel <i>et al.</i> , 1992), P50 dimer domain in reversed sequence (Figure 10) and a protein linker (Arai <i>et al.</i> , 2001). DNA was synthesized and cloned into pcDNA3.1+ by HindIII and NotI. Sequence see supplementary and Figure 10.	This work
pDH38	pNFkB driven tGFP with PEST degradation tag (Dest1). DNA sequence was used from evrogen.com and synthesized and cloned into pcDNA3.1+ by HindIII and NotI.	This work
pDH39	CMV driven tGFP with PEST degradation tag (Dest1). DNA sequence was used from evrogen.com and synthesized and cloned into pcDNA3.1+ by HindIII and NotI. Sequence see supplementary.	This work
pDH40	pNFkB-TNFR2-Fc-GPL. NF-kB driven expression of soluble TNFR2-Fc-GPL. Sequence of TNFR2-Fc-GPL were previously published (40) and PCR amplified by oDHTNFR2-Fc-GPL_fw_HindIII and oDHTNFR2-Fc-GPL_rev_NotI and inserted into pDH1 by HindIII and NotI.	This work
pDH41	hCMV-TNFR2-Fc-GPL. hCMV driven expression of soluble TNFR2-Fc-GPL. Same like pDH40, and inserted into pcDNA3.1+ by HindIII and NotI.	This work
pDH64	pNFkB-sIL1RA. NF-kB driven expression of Interleukin 1receptor antagonist. Aminoacid sequence were taken from drugbank (DB00026). Aminoacid sequence were calculated in DNA sequence,	This work

	codon-optimized and DNA synthesized and cloned into pDH1 by HindIII and NotI.	
pDH67	pNFκB-anti-TNFα. NF-κB driven expression of anti-TNFα (Adalimumab). Aminoacid sequence were taken from drugbank (DB00051). Aminoacid sequence were calculated in DNA sequence, codon-optimized and DNA synthesized and cloned into pDH1 by HindIII and NotI. The light Chain were co-expressed with the heavy chain, in one open reading frame by using internal ribosomal entry site (IRES) from encephalomyocarditis virus (EMCV), procedure based on (Ho <i>et al.</i> , 2012, Komar <i>et al.</i> , 2011).	This work
pDH68	pNFκB-TNFR2-Fc. NF-κB driven expression of Entanercept. Aminoacid sequence were taken from drugbank (DB00005). Aminoacid sequence were calculated in DNA sequence, codon-optimized and DNA synthesized and cloned into pDH1 by HindIII and NotI.	This work
pDH71	pDH71-CMV-shRNA2-SEAP. SEAP shRNA sequence is the same like pDH3. DNA were synthesized and cloned into pcDNA3.1+ by HindIII and NotI.	This work
pDH72	pDH72-CMV-shRNA2-SEAP. SEAP shRNA sequence is the same like pDH4. DNA were synthesized and cloned into pcDNA3.1+ by HindIII and NotI.	This work
pDH73	pDH73-CMV-shRNA2-SEAP. SEAP shRNA sequence is the same like pDH5. DNA were synthesized and cloned into pcDNA3.1+ by HindIII and NotI.	This work
pDH79	pDH79-SV40-mRFP. SV40 promoter driven expression of red fluorescent protein. Fluorescent protein were DNA synthesized. Sequence Uniprot Number: X5DSL3_ANAMA. Cloned into SEAP2Control (Clontech) by HindIII and XbaI.	This work
pp65-pEYFP-C1	hCMV-p65-eYFP, C-terminal fused with eYFP	Institute Prof. Wajant
pbabe-hTERT+p53DD	addgene: 11128	(Kendall <i>et al.</i>, 2005)
pbabe-cyclinD1+CDK4R24C	addgene: 11129	(Kendall <i>et al.</i>, 2005)
pbabe-c-mycT58A+HRasG12V	addgene: 11130	(Kendall <i>et al.</i>, 2005)
pBABE-neo-hTERT	addgene: 1774	(Counter <i>et al.</i>, 1998)
pRV.GFP FOXP3	addgene: 13250	(Wu <i>et al.</i>, 2006)
pSEAP2-Control	SV40-Promoter driven SEAP expression.	Clontech, CA

Primer

All primers were synthesized by Eurofins Genomics, Ebersberg, Germany

Table 9: Primer

Name	Sequence (5' - 3')
oDH1_fw_MluI	GGGCCAGATATACGCTTG
oDH1_rev_HindIII	GGTGGGCAAGCTTCTTTACC
oDH2_fw_MluI	TTGACGCGTGATCAAGC
oDH2_rev_NotI	GCCCTCTAGACTCGAGC
oDHSEAP_fw	AGTCAAGCTTAAAGTATTGCCCCACCATGCTGCTGCTG
oDHSEAP_rev_NotI	AGTCGCGGCCGCATGTATCTTATCATGTCTGCTCGAAG
oDHSEAP_rev_NotI_XhoI	AGTCCTCGAGGCGGCCGCATGTATCTTATCATGTCTGCTCGAAG
oDHSEAP_rev_seq	ATGCCCAGGGAGAGCTGTAG
oDH7_TC_fw_NheI	TTGACGGCTAGCAAACAC
oDH7_TC_rev_NotI	GCCCTCTAGACTCGAGC
oDH9_fw_HindIII	GGCAATGGTACTGTTGG
oDH9_rev_NotI	CCCTCTAGACTCGAGC
oDH2_shRNA2_fw	AGTCAAGCTTCCGGTGACATGAAATACGAG
oDH2_shRNA2_rev	AAACGGGGCCCTCTAGACTCG
oDH2_shRNA3_rev	AGTCAAGCTTCCGGTGACAGCTGCCAGGATCC
oDHSEAP_seq_rev	CTGGAAGTTGCCCTTGACC
oDH1_seq_fw	GATATACGCGTGATCTTGGG
oDHtGFP_fw_HindIII	TTCGCCCACCAAGCTTTAAGCCACCATGGAG
oDHtGFP_rev_NotI	ATACGCGGCCGCGTAAGACTAGTAGTCGCGGCCGATCCTACAC
oDHTNFR2-Fc-GPL_fw_HindIII	AGAAGCTTGCCACCATGGCGCCCGTCGCCGTCTG
oDHTNFR2-Fc-GPL_rev_NotI	AGCGCGGCCGCTCATTAGTCTCCTCCAGCGCCTTTG

2.2 Methods

Molecular biology

DNA Synthesis and vector design

The design and construction details for all expression vectors are provided in Table 8. DNA synthesis were provided by Geneart Regensburg, Germany, General Biosystems, Inc., Morrisville, USA and Eurofins, Hamburg, Germany. The cloning vector pcDNA3.1+, and plasmids encoding TNFR2-Fc-GPL or p65-pEYFP-C1 were kindly provided by Prof. Harald Wajant (Division of Molecular Internal Medicine, UKW Würzburg). Further subclonings were performed by restriction digests and polymerase chain reactions, using the given plasmids and the designed primers (Table 9). Primers consisted of the desired insert sequence at the 5' end and an annealing region of approximately 20 nucleotides. An additional 5' overhang was added for integration of new recognition sites for restriction enzymes.

Some primers for PCRs without any restriction site were ordered with a 5' phosphate group to enable T4 ligation. In general, the primers were designed to provide following conditions: Nucleotide repeats (>4), T_m (55 – 80°C), GC content (50 – 60%), G or C base at both ends and overall stability (> 1.2 kcal). To design primers the cloning program clone manager 8 was used.

Using agarose gel electrophoresis, we analyzed the backbones and inserts after PCR and restriction digests. After gel extraction, the purified fragments were ligated into a cloning vector and reaction mixtures were afterwards transformed into chemical competent *E. coli* (NEB 5-alpha) cells. To indicate the success of transfection correctly transformed strains were enriched using an antibiotic resistance gene, which is provided by the cloning vector and the growth in media, containing the corresponding antibiotic. After verification by commercial sequencing (LGC genomics) and control digests, plasmids were stored as DNA preparations in H₂O and as bacterial glycerol stocks (50 % *E. coli*).

Polymerase chain reaction

PCRs were performed with the Phusion® High-Fidelity DNA polymerase for cloning purposes and with Taq polymerase for analytical PCRs. Hereby sequence specific primers (Table 9) were used.

The PCR reaction mixture composition and the PCR program generally used in this work are listed in Table 10 and Table 11. If required, an annealing temperature gradient (45 - 65 °C) was used. The HF buffer promises a lower error rate, while the GC buffer implies improved results with long, GC rich and complex structured primers.

Table 10: Standard reaction mixture

Reagent	Volume [μL]	Final concentration
MQ H ₂ O	63.8	Ad 100 μL
HF or GC Buffer, 5x	20	1x
DMSO, 100%	4	4%
dNTPs, [2.5 mM]	8	200 μM
Template [10 ng/μL]	2	0.2 ng/μL
Forward Primer, [100 μM]	0.6	600 nM
Reverse Primer, [100μM]	0.6	600 nM
Phusion®, [2 U/μL]	1	0.02 U/μL

Table 11: PCR standard protocol

Step	Temperature [°C]	Time [min:s]
1 Initial Denaturation	98.0	00:30
2 Denaturation	98.0	00:15
3 Annealing	58 (50-72)	00:30
4 Elongation	72	20 / kbp
5 Final extension	72	07:00
25x cycles of steps 2-4		

Agarose gel electrophoresis and DNA purification

To analyze and separate DNA fragments of different lengths, horizontal agarose gel electrophoresis was used. The gel composition was 0.8 – 1 % (w/v) agarose dissolved in boiling 1x TAE buffer. Dissolved agarose was poured into the chamber setup after cooling to RT. For the molecular weight standard, GeneRuler™ DNA Ladder Mix was used and for DNA detection we added GelRed Nucleic Acid Staining Solution (Genaxxon bioscience GmbH). The bands were visualized with UV light transilluminator (250 - 365 nm) after electrophoresis in 1x TAE buffer at 100 V for 30 - 60 min. In the case of preparative agarose gel electrophoresis, DNA fragments of interest were cut out and were purified using the Zymoclean™ Gel DNA Recovery Kit according to manufacturer's protocol.

Restriction digest

In a total volume of 50 µL, DNA solutions were mixed with recommended 10X NEB Buffer and 2 U/µL enzymes in MQ H₂O. For control digestions, 0.5 µg DNA and for cloning digestions, 1.5 µg DNA of plasmid were used. Insert fragments were incubated for 1-2 hours, while vector backbones were digested generally 4-6 hours or overnight. Based on the recommendations of the manufacturer of the enzymes, required reactions temperatures and buffers were selected. Further, we dephosphorylated vector backbones after digestion with 10x Antarctic Phosphatase Reaction Buffer and 1 U/µL Antarctic Phosphatase for 15 min at 37°C to prevent re-ligation and to boost the frequencies of positive clones.

Ligation

Ligations were performed in a total volume of 10 - 15 µL using T4-Ligase and its buffer (NEB) and incubation for 15 - 60 min at room temperature. 50 ng of dephosphorylated vector backbone were mixed with a fourfold molar excess of insert. With long inserts, the ligation calculator (www.nebiocalculator.neb.com) were used to consider insert-backbone ratios by the corresponding molecular weight. To check for unwanted vector relegation, a control ligation without insert was additionally performed.

Chemical competent cells

250 mL LB medium was inoculated with 1:100 of a previous o/n culture of *E. coli* (NEB 5-alpha) and grown at 37 °C, 230 rpm until an OD₆₀₀ = 0.2 - 0.3 was reached. Cells were incubated for 5 min on ice after harvesting through centrifugation (5000 rpm, 15 min, 4 °C) and resuspension with 40 mL ice-cold buffer 1.

After one last centrifugation (5000 rpm, 15 min, 4 °C), cells were resuspended in 4 mL freezing solution of buffer 2. Last, 50 µl aliquots of competent cells were immediately frozen by liquid nitrogen and stored at -80 °C. Compositions of Buffer 1 and 2 are listed in Table 12.

Table 12: Chemical competent *E.coli*. Composition of Buffer 1 and 2.

Buffer 1 (3x40ml for 120 ml)	Buffer 2 (for 12 ml)
RbCl 1450.8 mg (100 mM)	MOPS, pH 7.0 25.2 mg (10 mM)
MnCl ₂ 755.1 mg (50 mM)	CaCl ₂ * 2 H ₂ O 132.2 mg (75 mM)
CaCl ₂ * 2H ₂ O 176.4 mg (10 mM)	NaCl 6.9 mg (10 mM)
KOAc (Kaliumacetat) 353.4 mg (30 mM, pH 6.0)	Glycerin 1.8 ml (15% v/v)
Glycerin 18 ml (15% v/v)	
H ₂ O to 120 ml	H ₂ O to 120 ml

Chemical transformation

Plasmids were transformed into chemical competent *E. coli* (NEB 5-alpha) cells. For this, 10-15 µL of the ligation mixture were added to 50 µL competent cells after thawing the cells on ice. After the mixture was incubated on ice for 20-30 min, it was heat-shocked at 42°C for 45-60 sec. 800 µL of prewarmed, antibiotic free LB medium was then directly added and the mixture was incubated for 1-2 hours at 37 °C on a shaker (230 rpm). 100 µL of the culture was streaked out on LB plates with 100 µg/µL of appropriate antibiotic resistance (Amp, KM) and incubated o/n at 37 °C.

Isolation and purification of plasmid DNA

Plasmids were purified with the Miniprep Kit, Zymo Resaerch, according to the manufacturer's instructions and sequenced by Microsynth AG (Balgach, Switzerland). According to the manufacturer's instructions, plasmids were purified with the Miniprep Kit from Zymo Resaerch. Plasmids and they were sequenced by LGC genomics (Berlin). With the JETSTAR 2.0 Plasmid Midiprep Kit, higher amounts were isolated, also according to manufacturers instructions. The plasmids were eluted in either 30-50 µL or 300-500 µL, respectively, and stored at -20 °C.

DNA quantification and purity

DNA concentrations and contaminations of RNA and proteins were determined using a Tecan infinite M200 spectrophotometer. UV absorption measurements of DNA, RNA (A₂₆₀ nm) and Protein (A₂₈₀ nm) and sample purity (A₂₆₀/A₂₈₀ nm, A₂₆₀/A₂₃₀ nm ratios) were carried out with water or elution buffer as a reference.

Glycerol stock

For long term storage, *E. coli* (NEB 5-alpha) containing plasmids were prepared by mixing 500 μ L of bacterial o/n culture with 500 μ L of glycerol (50 %). The glycerol stocks were stored at -80 °C.

Mammalian cell culture

Cultivation and general handling of eukaryotic cell lines

All mammalian cell lines (Table 4) were incubated in a humidified, 5 % CO₂ atmosphere at 37 °C in a copper incubator. For HEK-293T cells, Dulbecco's modified Eagle medium (DMEM), supplemented with 5 % (v/v) FCS, was used as a cultivation medium. Generally, cells were grown in T75 flasks to 70-80 % confluence until they were split. Cells were detached through short incubation with 4 mL Trypsin-EDTA solution and resuspended in fresh DMEM + 5% FCS. Finally, the cells were centrifuged (discard supernatant), re-suspended in fresh DMEM and plated onto new dishes. Cell number and viability were quantified using a hemocytometer. Cells were regularly checked for confluence, morphology and potential contamination by microscopic evaluations.

Cryoconservation and reactivation

Cells were resuspended in freezing medium, containing 90 % (v/v) FCS and 10 % (v/v) DMSO and aliquots of 1 mL containing 10⁶ cells were filled immediately into cryotubes and transferred into a cryobox at -80 °C. For successful cryopreservation of cells, a cryobox ensure a slow freezing with 1 °C/min cooling rate. For long-term storage the cryotubes were transferred to the liquids nitrogen tank after two days. By thawing immediately a frozen cryotube in a water bath of 37 °C for 5 min and transferring the solution to 37 °C pre-warmed DMEM, the cells were reactivated. After one resuspension by pre-warmed DMEM, to reduce residual DMSO, cells were centrifuged, again resuspended in fresh pre-warmed medium and replaced.

Transient transfection

Cells were transfected using an optimized polyethyleneimine (Polyscience, Inc., Germany, cat. no. 23966-2) transfection method with the following components: A transfection solution for (250 μ L DMEM and app. 2.5*10⁴ cells/well; 48 well plate) consisted of totally 250 ng of plasmid DNA mixture, 100 μ L serum- and antibiotics-free DMEM (no FCS) and 1.25 μ L of PEI transfection solution. The transfection solution was incubated for 20 min at RT after quickly vortexing and finally it was applied to the cells drop-wise. If less DNA had to be introduced, the amount was

filled up with pDH79 (red fluorescent protein), to standardize and ensure comparable condition, respectively. The transfection solution was adapted directly proportionally, if the well contained more or less cell medium. After 24 hours of incubation at 37 °C, the complete medium was replaced with fresh pre-warmed DMEM to prevent cytotoxic effects by PEI.

Protein expression: Preparing samples and protein concentration

Cells were transiently transfected in 6-well plates, mixed with protease inhibitors (Table 2) and incubated for at least 24 - 48 hours. The supernatant was taken to detect secret proteins. If necessary proteins were concentrated by using ultrafiltration spin columns. By the colorimetric Bio-Rad Protein assay, total protein concentrations of the samples were determined.

The 5x Bradford dye reagent was diluted with MQ H₂O and stored at RT in the dark and filtered. At least 5 different dilutions, 0 - 0.5 mg/mL, of reference BSA were prepared. In a 96-well plate, 200 µL of prepared dye reagent was mixed with 10 µL of pre-diluted sample. Absorbance was measured at 595 nm, after an incubation period of at least 5 min at RT. The protein concentrations were determined using the linear regression of the reference BSA results.

Western Blot

Before loading 50 µg protein on a 10 % SDS-Polyacrylamid gel (Table 13), it was mixed with Lämmli Buffer and denatured at 90°C for 5min. As standard the prestained PageRuler was used. After at least 1 hour at 100 Volt, the gel was blotted on a PVDF membrane (at 20 Volt, 15 mA) by a Semi-Dry blotting device. Before blotting, the membrane was activated with methanol for 10 min and after blotting the membrane was blocked with 5 % dry milk in PBS-T for 90 min. The primary antibody was incubated o/n at 4 °C and 1:1000 diluted in 5 % dry milk. After three wash steps with PBS-T the membrane was incubated with the respective horseradish peroxidase (HRP) labeled secondary antibody 1:1000-5000 diluted in 5 % dry milk for 1 hour. Further wash steps with PBS were done, before finally ECL substrate was added for 5 min and the chemiluminescence was recorded in the Fluor-Chem Q Imaging. If another antibody blocking was desired, the membrane was washed twice with PBS-T and PBS.

Table 13: SDS gel mixtures

Reagent	Running gel, 12 %, 15 mL	Stacking gel, 5 %, 6 mL
MQ H ₂ O	4.9 mL	3.4 mL
30 % Acrylamide, 29:1	6 mL	1 mL
1.5 M Tris-HCl, pH = 8.8	3.8 mL	-
0.5 M Tris-HCl, pH = 6.8	-	1.5 mL
10 % (v/v) SDS	150 µL	60 µL
10 % (v/v) APS	150 µL	75 µL

NF-κB-triggered gene expression

After transfection of NF-κB-regulated expression plasmids, cells were exposed to different cytokines levels or inflammatory molecules, previously diluted in cell media 5% FCS.

The following recombinant cytokines were purchased from PeproTech Inc, Hamburg, Germany: hTNFα (cat. no. 300-01A); hIL-1β (cat. no. 200-01B); hIL-6 (cat. no. 200-06); sIL-6R (cat. no. 200-06R); hIL-17a (cat. no. 200-17); hIL-2 (cat. no. 200-02). The following small molecules were purchased from Sigma Aldrich, Munich, Germany: Poly(I:C) (cat. no. P9582); Thioglycollate (70157-100G); LPS (cat. no. L2654), TPCA-1 (T1452-1MG). Recombinant adalimumab were purchased from InvivoGen, Toulouse, France; cat. no. htnfa-mab1.

Reporter assays

SEAP assay

Secreted alkaline phosphatase (SEAP) production was quantified by the colorimetric 96-well plate SEAP assay (Berger *et al.*, 1988). One of the major advantages of SEPA as a reporter was high stability and low toxicity, which allows for reporter accumulation in the supernatant. To inactivate endogenous phosphatases, 100 - 200 μL of supernatant were collected at different time points and heated for 30 min at 65 °C. For the assay, 10 μL sample was added to 70 μL H₂O_{dd} and 100 μL 2x SEAP assay buffer and transferred into a 96-well plate. 20 μL of p-Nitrophenyl Phosphate (pNPP, Sigma Aldrich, Munich, Germany; cat. no. P5994-25TAB 40 mg tablets) substrate was added to each well, right before the measurement. SEAP dephosphorylate pNPP to pNP and 1 U SEAP corresponds to the conversion of 1 μmol pNPP to pNP per minute. The colorimetric measurement was started immediately by reading absorbance values (405 nm for pNP every 60 s in 30 cycles). The increase in absorbance is directly proportional to the SEAP activity, the SEAP concentration [U/L] could be calculated.

$$\text{Enzymatic activity (EA): } EA = \frac{\Delta c}{\min} = \frac{s\vartheta}{\epsilon d}$$

ϑ denotes the dilution factor [total assay volume/supernatant volume]; the molar extinction coefficient of pNPP is given with ε_{pNPP} = 18600 M⁻¹cm⁻¹ and the slope S [min⁻¹] being the increase in absorption per min. The equation derives from the Lambert-Beer's law: A = εcd. As standard 100 ng/ml recombinant SEAP Protein (InvivoGen, Toulouse, France; cat. no. rec-hseap) were additional measured.

GPL Assay

Gaussia princeps Luciferase levels in culture supernatants were profiled using the BioLux® *Gaussia* Luciferase Assay Kit (New England Biolabs GmbH, Frankfurt a.M., Germany; cat. no. E3300L). As standard, 100 ng/ml of GPL were additionally measured.

ELISA IgG1

Antibody IgG1 expression (pDH67; anti-TNF α) levels in culture supernatants were quantified with the Human IgG total ELISA Ready Set Go (Fisher Scientific GmbH, Schwerte, Germany; cat. no. 88-50550-88).

Detection of fluorescent proteins

Expression was observed and visualized by fluorescence microscopy using a BZ-9000E microscope and compatible software (Keyence, Neu-Isenburg, Germany). Several pictures were made from uniform cut-outs and were processed equally afterwards. Exposure times were optimized between 0.5 – 7 ms. For live cell imaging the inverted confocal microscope (Laser-Scanning-Mikroskope TCS-SP, Leica, Wetzlar, Germany) system was used. These techniques were used to observe the localization of p65, captured in cytoplasm by I κ B α or activated in the nucleus.

Flow cytometry and fluorescence detection

Cells were transfected with plasmids encoding NF- κ B-triggered tGFP, GFP variants tagged with a degradation domain (PEST, see also evrogen.com). As control, a plasmid encoding constitutive driven SEAP (SEAP2Ctr.) was used. After stimulation with or without TNF α , the cells were harvested by trypsinization, centrifuged and resuspended with DMEM + 5% FCS. After another centrifugation, the cells were dissolved in PBS and transferred into FACS (Fluorescence Activated Cell Sorter) tubes. The intracellular fluorescence was detected with BD FACS Calibur.

Alginate encapsulation

After transfection, trypsinization, centrifugation and resuspension in fresh DMEM + 5%FCS, HEK23T cells were centrifuged twice and 1×10^6 cells were dissolved in 1 ml of 1,5 % alginate ddH₂O (Na-alginate Sigma Number). The cell suspensions were immediately encapsulated by droplets in CaCl solution (1 %). The Ca²⁺ cation induces polymerization of the Alginate molecules, which encapsulate the cells. The capsules were transferred immediately to fresh pre-warmed DMEM medium. After 24 hours incubation (37° C and 5 % CO₂), the cells were treated with TNF α .

III. Design and Results

3.1 Design and validation of NF- κ B-triggered gene expression

Design and construction of NF- κ B-dependent promoters

The purpose of this work was to harness and rewire NF- κ B signaling to anti-inflammatory biologicals, developing finally cytokine neutralizer cells for potentially treating autoimmune diseases such as RA.

HEK293T cells were preferably used for this work. HEK293T cells showed intact NF- κ B signaling, simple handling and good transfection rates. As a standard reference and to analyze cell viability in all experiments, we simultaneously tested the constitutive expression of SEAP (SEAP2Ctr.). The constitutive expression of a red fluorescent protein (RFP; pDH79) was used as a negative control, to subtract the background noise of SEAP quantification and to count transfection rates. With regard to co-transfections, the required plasmid content was up-filled with pDH79 to ensure comparable transfection conditions.

We started with computational designs for DNA elements: we combined previously published HIV-1 derived NF- κ B-binding motives with a CMV minimal promoter (CMVmin; based on a minimal promoter fragment derived from the CMV immediate early promoter) using spacer sequences and reduced GC islets to minimize methylations (Badr *et al.*, 2009, Gossen *et al.*, 1992). Methylations of promoter elements are mostly responsive for gene silencing, with especially CMV promoters are susceptible for methylations (Mortiz *et al.*, 2015). Figure 7 illustrates the spatial distribution of these elements, resulting in the here used NF- κ B-dependent promoter (pNF κ B).

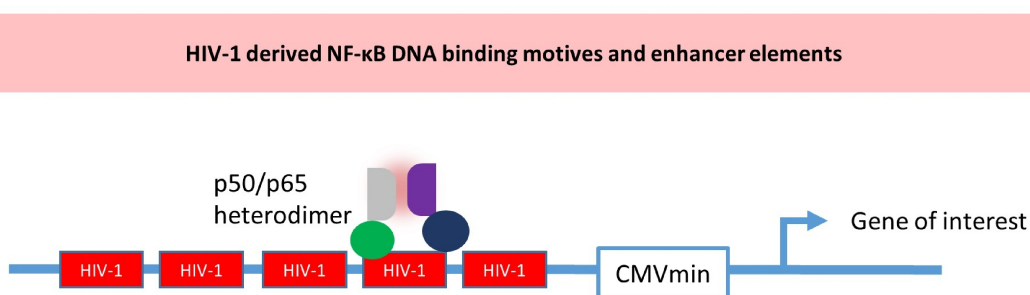


Figure 7. Design and construction of NF- κ B-triggered gene expression. Five repeats of HIV-1 derived bindings sites of p50/p65 were placed upstream of a CMVmin element together with a designed Kozak sequence (Badr *et al.*, 2009, Gossen *et al.*, 1992).

Validation of NF- κ B-triggered gene expression

We first investigated the induction of NF- κ B signaling using pNF κ B-SEAP (pDH1), a plasmid encoding the easily quantifiable SEAP under the control of our NF- κ B-dependent promoter. HEK293T cells were transfected with pNF κ B-SEAP (pDH1) and exposed to various RA relevant pro-inflammatory cytokines: IL17a, IL2, IL6/sIL6R, IL-1 β and TNF α (Figure 8B). We received a strong signal only with IL-1 β and TNF α . These cells were further treated with RA-unrelated inflammatory substances, mimicking bacterial and viral infections by lipopolysaccharide (LPS) or polyinosinic-polycytidylic acid [poly(I:C)], a synthetic double-stranded RNA analog or thioglycollate for unspecific sterile inflammation (Caskey *et al.*, 2011; Lam *et al.*, 2013). None of these molecules enhanced SEAP expression (Figure 8B).

To get an impression of the specificity of our promoter to NF- κ B signaling or to cross-talks between other signal pathways, we tested the impact of various other signaling pathways on our sensor system by ectopic overexpression of corresponding signaling intermediates. Thus, we co-transfected expression plasmids encoding proteins which promote the activity of pathways regulating cell growth, differentiation or apoptosis (Figure 8B). Among others we tested: pbabe-hTERT+p53DD, pbabe-cyclinD1+CDK4R24C, pbabe-c-mycT58A+HRasG12V, pBABE-neo-hTERT, pRV.GFP FOXP3 (Kendall *et al.*, 2005; Caounter *et al.*, 1998; Wu *et al.*, 2006). None of these genetic interventions influenced the NF- κ B-triggered SEAP expression to a remarkable extent, which may verify the interdependence of the promoter to other signaling pathways or genetic interfering sources. The TNF α -based activation of NF- κ Bs remained also stable with the co-transfected expression plasmids (data not shown).

To sum up, SEAP was enhanced expressed only in response to circulating TNF α and IL-1 β , even when influencing elements were co-transfected.

Active NF- κ B transcription factors translocalize into the nucleus, which reflects the last step in activation, before p50/p65 bind to DNA and trigger the gene expression. The kinetics of p65 containing NF- κ B dimers were visualized by transfection of HEK293T cells with plasmid pp65-EYFP-C1 (encoding p65 fused with eYFP) and the nuclear translocation of p65 was studied under real-time conditions (Figure 8C). Even though we synthetically increased the amount of p65 in cells, p65-eYFP was predominantly localized in the cytoplasm, indicating the presence of sufficient inhibitor I κ Ba and thus a strong natural negative feedback loop. After triggering NF- κ B signaling with TNF α , p65-eYFP translocalized into the nucleus in 20 minutes.

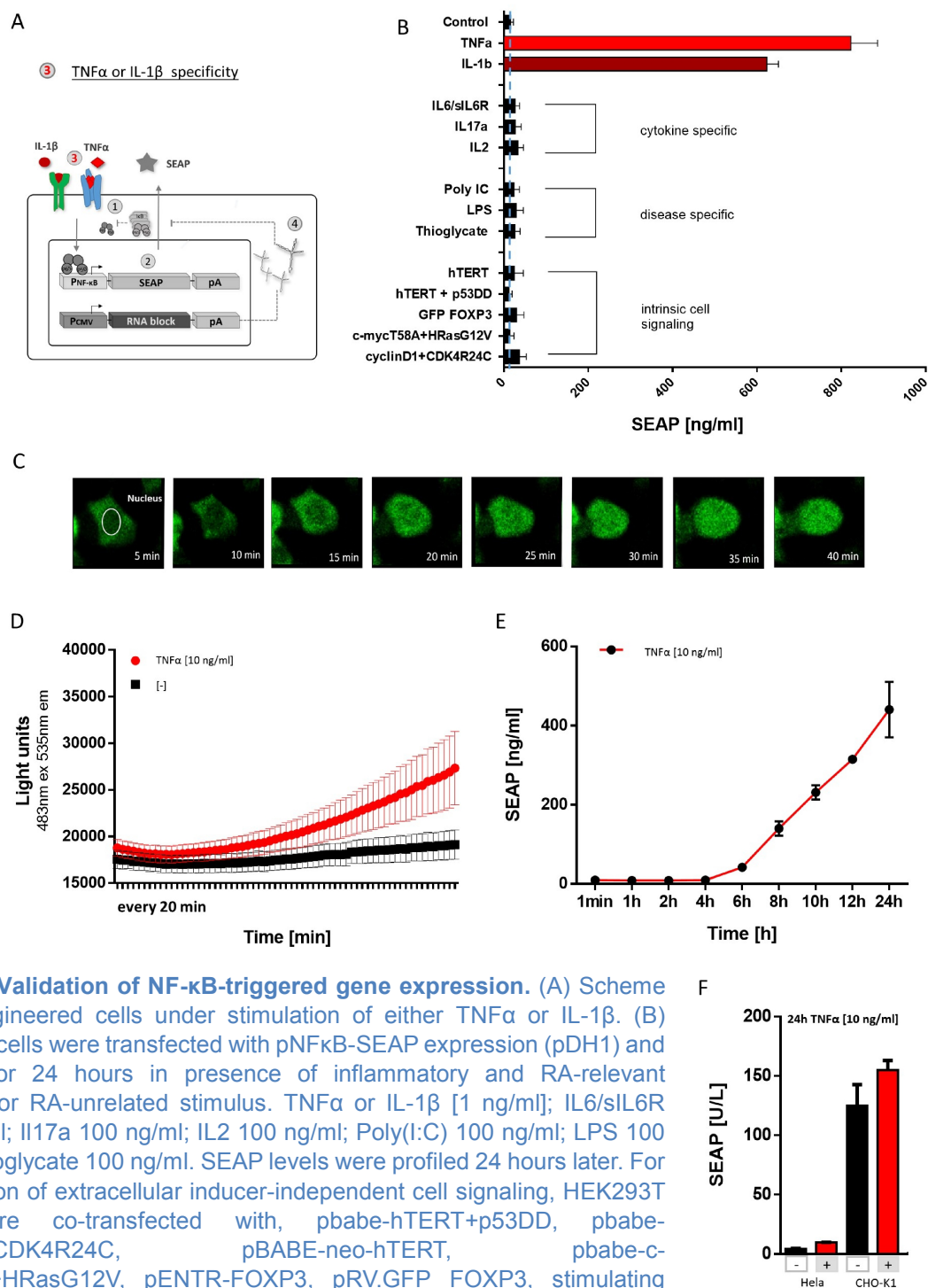


Figure 8. Validation of NF- κ B-triggered gene expression. (A) Scheme of the engineered cells under stimulation of either TNF α or IL-1 β . (B) HEK293T cells were transfected with pNF κ B-SEAP expression (pDH1) and cultured for 24 hours in presence of inflammatory and RA-relevant cytokines or RA-unrelated stimulus. TNF α or IL-1 β [1 ng/ml]; IL6/sIL6R 1000 ng/ml; IL17a 100 ng/ml; IL2 100 ng/ml; Poly(I:C) 100 ng/ml; LPS 100 ng/ml; Thioglycate 100 ng/ml. SEAP levels were profiled 24 hours later. For investigation of extracellular inducer-independent cell signaling, HEK293T cells were co-transfected with, pbabe-hTERT+p53DD, pbabe-cyclinD1+CDK4R24C, pbabe-neo-hTERT, pbabe-c-mycT58A+HRasG12V, pENTR-FOXP3, pRV.GFP FOXP3, stimulating intrinsically different signal transduction pathways. Unless otherwise stated all plasmids were co-transfected with filler plasmid (pDH79) to equalize amount of plasmids. (C) The kinetic of p50/p65 activation were analyzed in HEK293T cells transfected with pp65-EYFP-C1 encoding p65 fused with eYFP by real-time fluorescence microscopy. (D) and (E) To monitor the time dependent activation of the cytokine neutralizer in response to TNF α , HEK293T cells were either transfected with pNF κ B-tGFP-PEST (pDH38) for real-time analysis, or for accumulated expression profile with pNF κ B-SEAP (pDH1). (F) HeLa, CHO-K1 were transfected with pNF κ B-SEAP and cultured in response to TNF α . SEAP profile was detected 24 hours later. The experimental data of (B) are mean \pm SD of n=4 independent experiments and different passage of HEK293T cells. Each n stand for three independent experiments with one cell passage. The experimental data of (D), (E) and (F) are mean \pm SD of n=3 independent experiments.

Furthermore, we investigated the kinetic of NF- κ B-triggered expression of a rapidly destabilized tGFP variant (pNF κ B-tGFP; C-terminal PEST domain) (Figure 8D). Similarly the accumulation of SEAP was monitored (Figure 8E). Independently of the expressed gene (tGFP or SEAP), we observed the first expression starting after approximately 6 hours. Further controls should support this assertion of NF- κ B signaling in HEK293T cells and other cells. A previous investigation on Hela cells and CHO-K1 cells profiled significantly decreased SEAP levels and fold induction (Figure 8F).

Design and construction of p65-dependent activation of Gal4/UAS chimeric promoters

NF- κ B transcription factors enhance the expression of many different genes, mostly pro-inflammatory genes, depending on cell-type (Hoffmann *et al.*, 2002). To potentially influence the cell-type specific secretome of p50/p65 activated genes, we attempted to capture and rewire p50/p65 to a non-mammalian inducible promoter. Whereby the endogenous p50/p65 binding sites must be inhibited by another, later planned step using for example repressors or dynamic genome engineering by single RNA strands (Ausländer *et al.*, 2014). Figure 9 illustrates two synthetic promotor designs to harness and rewire p50/p65 to a Gal4 dependent promoter. The Gal4/UAS system of yeasts has been shown to work in mammalian cells. Furthermore, it has been demonstrated, that the transactivation domains of p65 fused to the Gal4 DNA-binding domain (Gal4DBD), enables gene expression in mammalian cells by Gal4/UAS dependent promoter (De Bosscher *et al.*, 2000, Seipel *et al.*, 1992). We redesigned those achievements using two strategies (design 1 and 2) to activate a Gal4/UAS dependent promoter through NF- κ B signaling in mammalian cells.

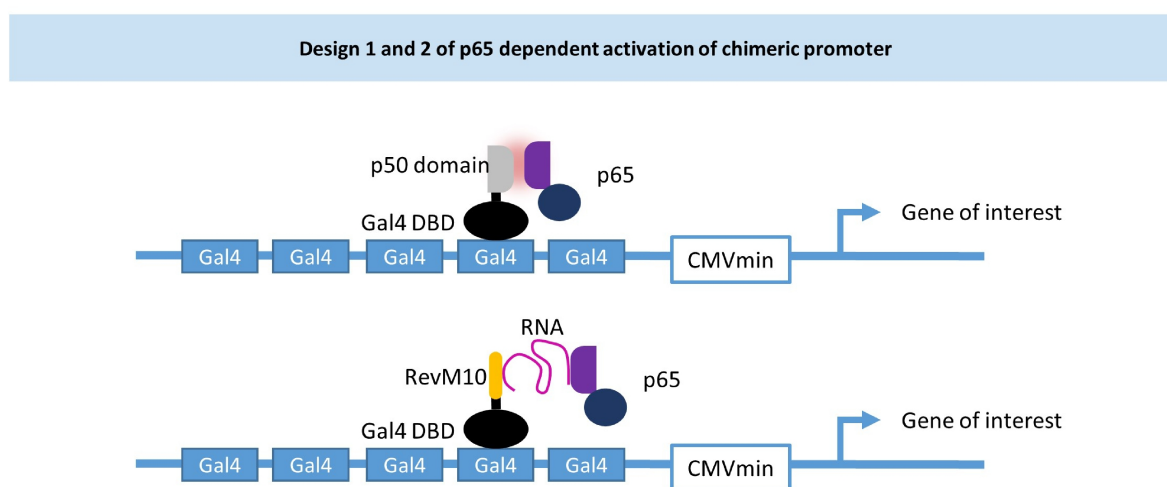


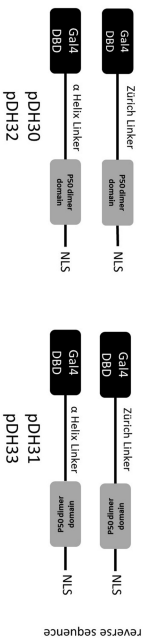
Figure 9. Design and construction overview of p65 dependent activation of Gal4/UAS chimeric promoters. Aim is to activate a non-mammalian promoter by NF- κ B signaling. Design 1: This strategy is similar to mammalian two hybrid assay and based on the high affinity heterodimer of p65 to p50 (Huxford *et al.*, 2002). Design 2: The combinations of HIV Rev Proteins (RevM10), which bind to specific RNA strands (RRE) and p50/p65 binding RNA elements (anti-p50 RNA and anti-p65 RNA binds to p50 and p65, respectively) are designed to create a mammalian three hybrid assay. Both approaches have the aim to recruit the transactivation domain of p65 through fusion proteins with a Gal4DBD tail to yeast Gal4 enhancer elements and at last to activate the chimeric promoter.

The p50/p65 heterodimer contains a C-terminal domain with strong nanomolar affinity to each other. Homodimers of p50/p50 or p65/p65 are also described, but the heterodimer form occurs most frequently. Through protein engineering, we fused the p50 dimer domain C-terminal to Gal4DBD. Here we used first the same linker previously published and second a steric spacer an α -helix linker (Seipel *et al.*, 1992, Arai *et al.*, 2001). This strategy is similar to the mammalian two-hybrid system and based on the dimerization of p50 and p65.

Four chimeric proteins were designed bioinformatically and based on X-ray structures (Gal4: PDB code 3COQ; p50/p65: PDB code 3GUT); they containing the p50 dimer domain fused to the Gal4DBD. Based on the fact that reverse sequences of amino acids may form similar structure motives and molecular surfaces, especially in small proteins with low enthalpy, we designed two experiments with the reverse sequence of p50. Reverse sequences are amino acids from N- to C-terminal in reverse order (ABCD→DCBA).

The strategy to use reversed sequences is disputed. For example, the one polypeptide chain of calmodulin show two similar domains encoded by two reverse sequences (PDB code 1CLL). Contrary results were previously evidenced by small peptides and challenged this strategy. For example, the penta-peptide YGGFL acts as opiate, the reverse sequence LFGGY not (Berg *et al.*, 2007).

In addition to predict secondary structure motives, all designs were validated using the online protein predict dashboard viewer (predictprotein.org) and compared with the native X-ray structures (Gal4: PDB code 3COQ; p50/p65: PDB code 3GUT). All established chimeric proteins have the aim to recruit the transactivation domain of p65 to yeast Gal4 enhancer elements and activate the chimeric promoter. Figure 10 gives an abstract design of the chimeric proteins used for design 1.



35

The second strategy (design 2) is similar to the mammalian three hybrid system. Using bioinformatics, we designed the chimeric protein RevM10-Gal4DBD, which has the aim to recruit the transactivation domain of p65 through interacting with non-coding RNAs as connector. RevM10 is a mutant of HIV-Rev proteins, which are known to bind the Rev response element (RRE) in a nanomolar way (Guzik *et al.*, 2001). The RRE is a non-coding RNA motive from HIV-1 and is necessary for virus replication (Fernandes *et al.*, 2012). The inserted mutation of RevM10 (M10) is localized in the nuclear export signal and therefore RevM10 cannot be transported to cytoplasm and permanently resides in the nucleus, while the nucleus localization signal and the RRE binding ability are still active (Guzik *et al.*, 2001).

RevM10 proteins are very small proteins (two α -Helixes in v-form by β -turn; PDB: 4PMI), but packed with many signal domains and the interactions with RRE constitute a major focus of HIV-based research (Suhasini *et al.*, 2009). α -helixes in proteins are steric structures which have a low enthalpy and fold predominantly. Therefore RevM10 proteins are predestined for fusion to Gal4DBD, which is also built up by α -helixes. Three different linker were used: The same linker previously published, a commonly used flexible GS-linker and again the steric α -helix linker (Seipel *et al.*, 1992, Reddy Chichili *et al.*, 2013, Arai *et al.*, 2001). Reverse sequences were also designed in combination with each linker, resulting in six engineered proteins.

For p50 and p65, the anti-p50 and anti-p65 RNA sequences described previously, structurally mimic DNA through double-stranded RNA and have high affinity to p50 and p65, respectively. A so called RNA-based T-cassette offers, through its low enthalpy structure, as an RNA-based fundament, a perfect platform for insertions and combinations of RNA motives (Wurster *et al.*, 2009). Engineered T-cassettes, consisting of RRE RNA and p50/p65-binding RNA, may link and bind RevM10 with the one arm and p50/p65 with the other arm. Two similar approaches have been previously published, using RevM10 and RRE, or a three-hybrid system with anti-p65 RNA (Putz *et al.*, 1996, Wurster *et al.*, 2009). To test more combinations, we calculated RNA structures using an online RNA structure prediction program (Mathew *et al.*, 2012-2017) and selected low enthalpy and combinations of RNA motives. RNA 2D structures have the major advantage that they are very predictable using bioinformatic calculations (Seetin *et al.*, 2012). Figure 11 illustrates the designs of non-coding RNA molecules and chimeric proteins.

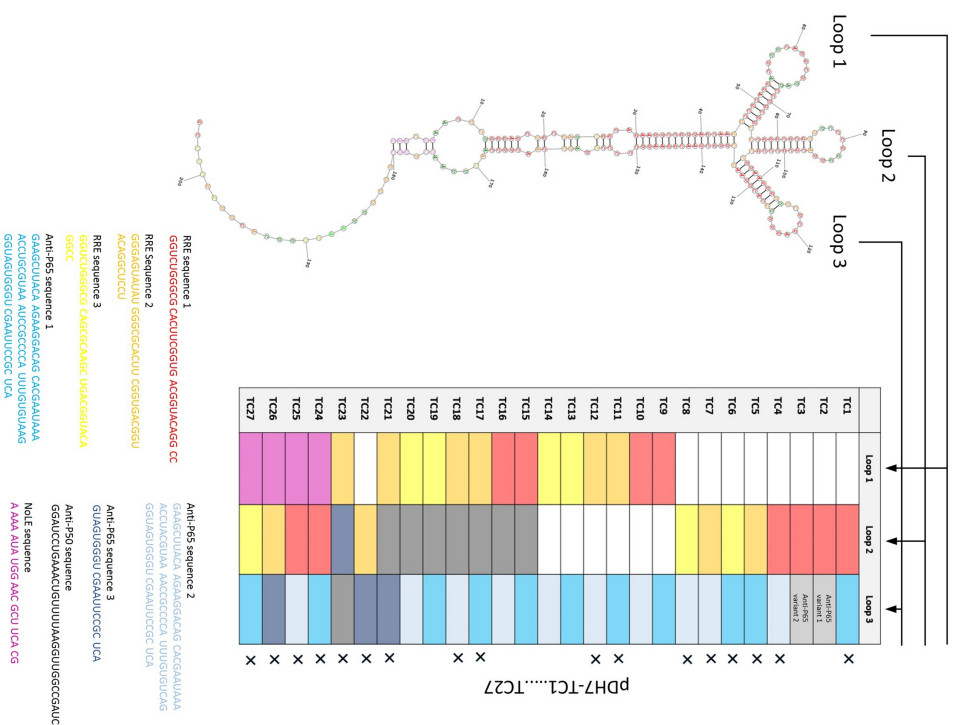
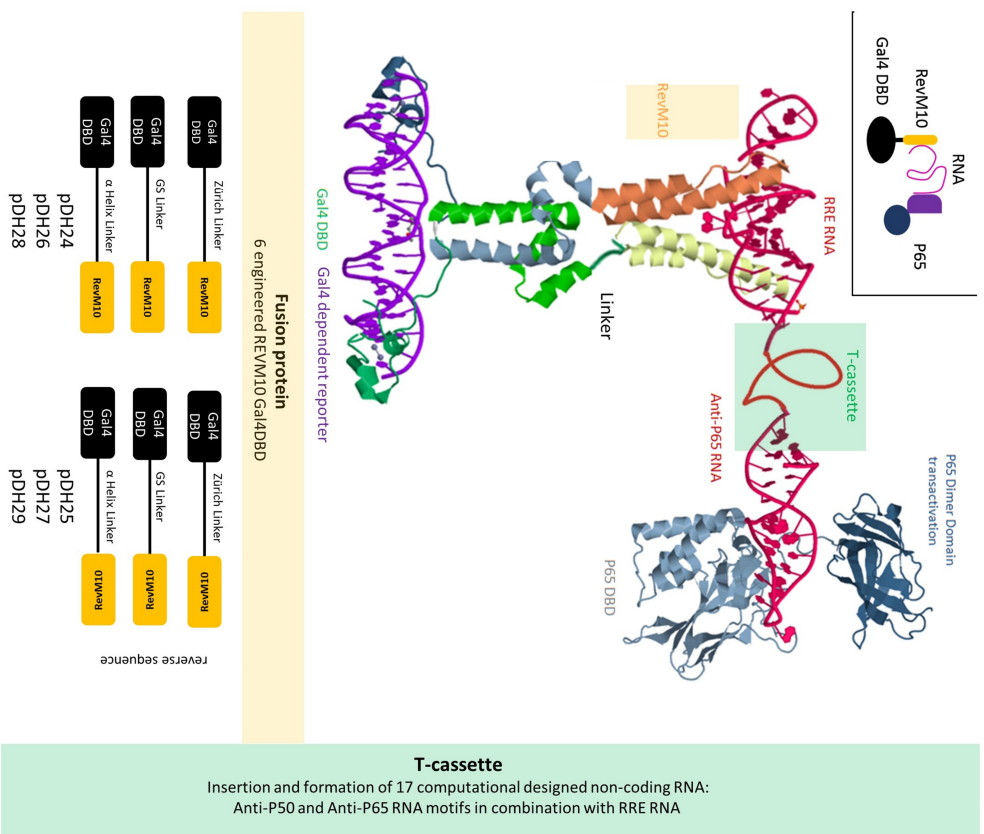


Figure 11. Design 2 of p65 dependent activation of chimeric promoter. On the left side, as an abstractive design we illustrated a non-real structure of the chimeric protein RevM10-Ga4DBD, which recruits the transactivation domain of p65 through an interacting RNA element and fusion protein Ga4DBD tail to yeast Ga4/UAS enhancer elements. Therefore this strategy is similar to mammalian three hybrid system, containing three interacting elements: (i) RevM10 is a mutant form belonging to HIV-Rev proteins, which are known to bind to (ii) RRE RNA sequences (Guzik *et al.*, 2001) and (iii) for p50 and p65 are anti-p50 and anti-p65 RNA sequences described, which bind to p50 and p65, respectively. The right side illustrates the design of the interacting, non-coding RNA using a so-called RNA T-cassette. An RNA T-cassette offers through its strong structure and its three loops, as a RNA based fundament a perfect platform for integration and combination of these to sequences (Wurster *et al.*, 2009). To test more combinations, we calculated RNA structures using an online RNA structure prediction program (Mathew *et al.*, 2012-2017).

Results of p65-dependent activation of chimeric Gal4/UAS promoter

We co-transfected plasmids encoding the constructed fusion proteins of design 1 (p50DD-Gal4DBD; Figure 10) and for recording their activity plasmids allowing Gal4/UAS-triggered SEAP expression (pGal4-SEAP; pDH6). The cells were cultured in presence (red bars) or absence (black bars) of TNF α presence and after 24 hours SEAP expression was analyzed (Figure 12A). The expression levels achieved with or without TNF α were significantly lower than for NF- κ B-driven SEAP (pNF- κ B-SEAP). Furthermore, we observed no detectable difference compared to the control (pDH6/pDH79).

For the second strategy (design 2) we co-transfected HEK293T cells with three plasmids encoding for (i) Gal4/UAS-regulated SEAP (pGal4-SEAP, pDH6), (ii) one of four different Gal4DBD-RevM10 fusion proteins (Figure 12B), and (iii) as connector to p65 one of 17 plasmids expressing selected non-coding RNAs. The different combinations total to 102 transfections (Figure 12B). The transfected cells were cultured in the presence (red bars) or absence (black bars) of TNF α and SEAP expressions were profiled after 24 hours. Almost all setups showed no SEAP expression, but all combinations of the two fusion proteins Gal4DBD-RevM10 with a reverse sequence (pDH25 and pDH29) did. Even when these detected results are paradoxical, because we detected strong activation without TNF α in some setups (pDH25/TC4; pDH29/TC18; pDH29/TC22). The setup (pDH6/pDH29/TC27) showed the best fold induction of 7 in response of TNF α .

The repeated occurrence of two plasmids pDH25 and pDH29 in these cases, which both encode for similarly designed RevM10-Gal4DBD variants, may imply a correlation. We therefore performed further investigations with pDH25 and pDH29. Another control refuted these correlations and the observed activation may be wrong or not explainable: Cells were co-transfected with only pDH6/pDH25 or pDH6/pDH29 and without RNA interaction. We observed strong activation in the absence of the RNA elements, which is not plausible (Figure 13A).

As another control and to verify potential unknown *in vivo* interactions in the RevM10 domain, we treated this setup with known inhibitors of HIV-Rev proteins. Proflavin and Neomycin B have been previously described to sensitively inhibit HIV-Rev proteins (Kirk *et al.*, 2000; Dejong *et al.*, 2003). As shown in Figure 13B, we detected an inhibition caused by Proflavin. However, Proflavin in a similar manner inhibits constitutive expressions of SEAP, indicating its toxic influence in general and is therefore insufficient.

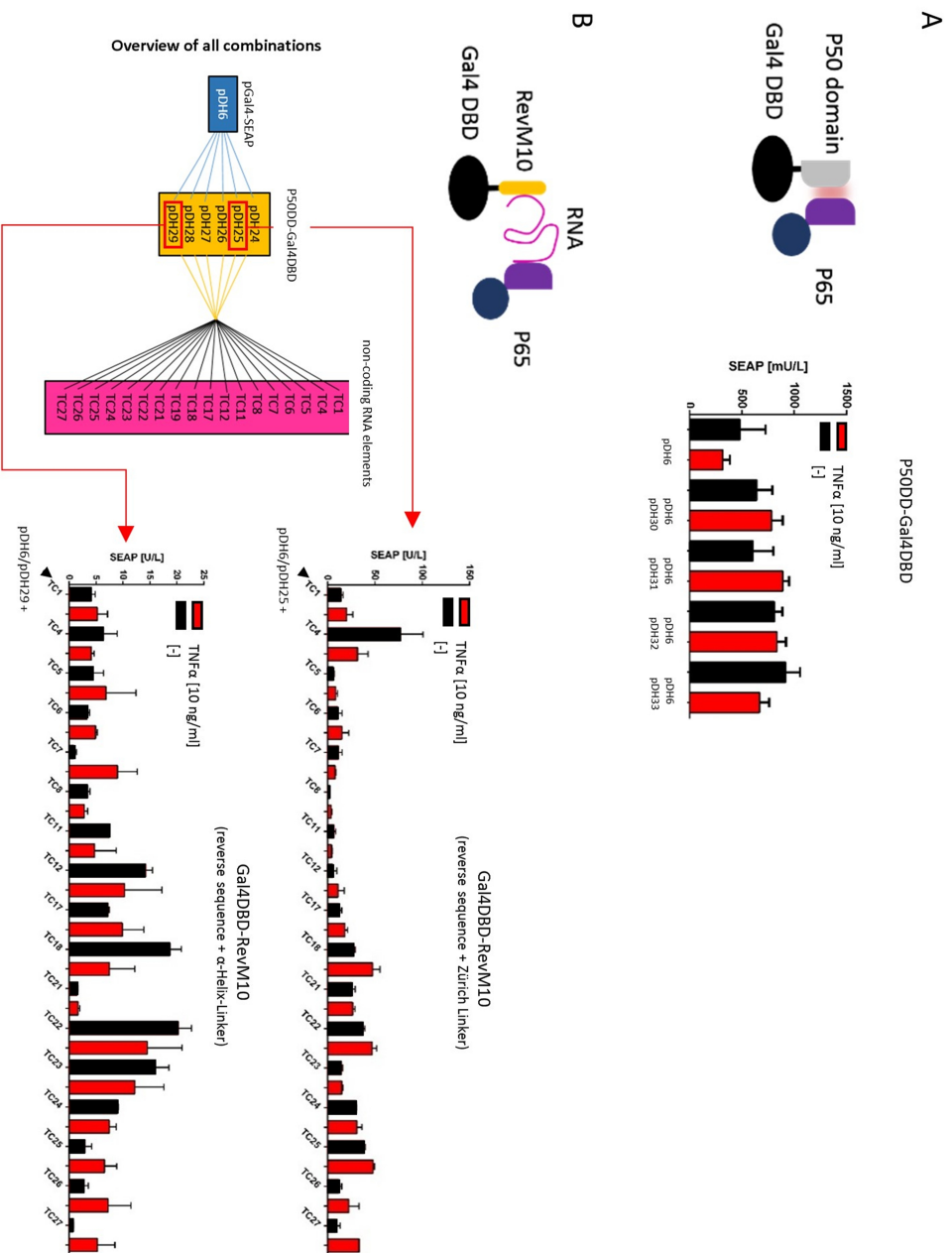


Figure 12. Results of the two designs to capture the transactivation domain of p65 and to recruit it to the Gal4 dependent promoter. (A) HEK293T cells were co-transfected with plasmids encoding for Gal4-triggered SEAP (pGal4-SEAP, PDH6) and the engineered fusion protein p50DD-Gal4DBD variants (pDH30-33). The cells were subsequently cultured in response to TNF α [10 ng/ml] for 24 hours to profile afterwards SEAP expression. **(B)** HEK293T cells were co-transfected with plasmids encoding for 17 synthetic non-coding RNAs (Figure 11; TC1-TC27) in combinations with the engineered fusion proteins RevM10-Gal4DBD variants (pDH24-29) and pGal4-SEAP (PDH6). The cells were also cultured in response to TNF α [10 ng/ml] for 24 hours and afterwards SEAP expression were measured. To reduce the excess of results only the combinations of PDH6/pDH25 or PDH6/pDH28 with the non-coding RNA's were shown. All other transfection combinations (a total of 102 combinations) did not provide any detectable SEAP profile and are not shown. All experimental data presented are mean \pm SD of 3 independent experiments.

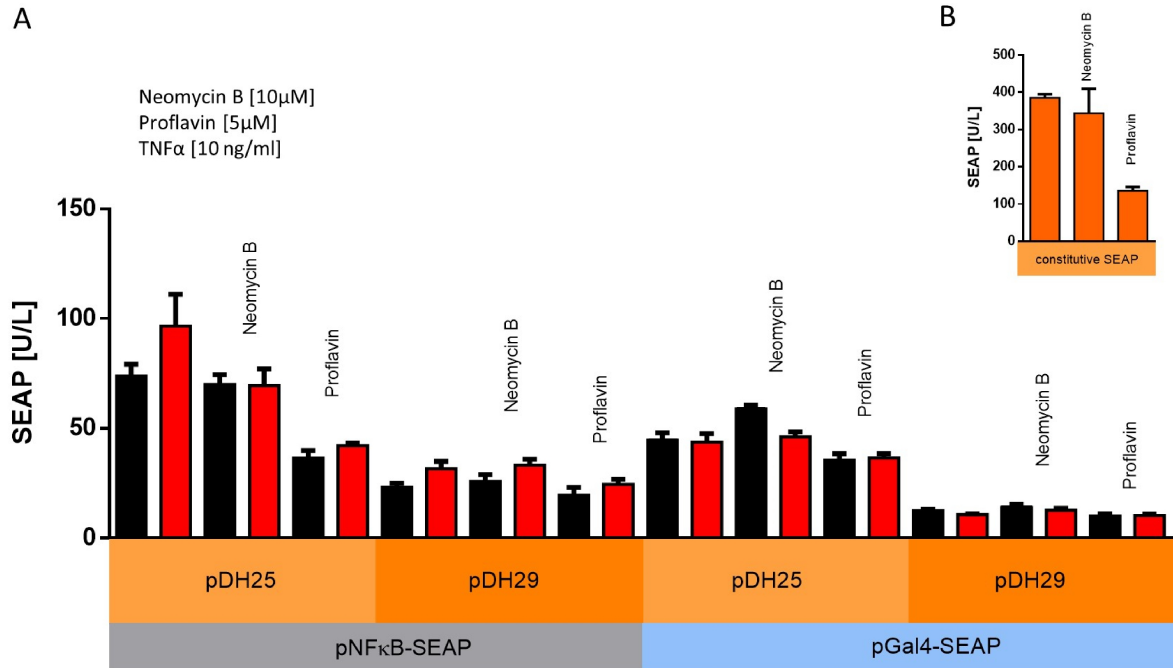


Figure 13. Controls of RevM10-Gal4DBD proteins pDH25 and pDH29. (A) HEK293T cells were co-transfected with pNF κ B-SEAP (pDH1) and with pDH25 or pDH29 and cultured in response to TNF α [10 ng/ml] together with neomycin B [10 μ M] or proflavin [5 μ M]. The same experiment were implemented with pGal4-SEAP (pDH6) instead of pNF κ B-SEAP (pDH1). SEAP profile were detected 24 hours later. (B) Validation of neomycin B and proflavin. HEK293T cells were transfected with SEAP2control and cultured in response to neomycin B [10 μ M] or proflavin [5 μ M]. All experimental data presented are mean \pm SD of 3 independent experiments.

Analysis and optimization of the NF- κ B-triggered gene expression

The general focuses within engineering inducible promoters are efforts to achieve dynamic on/off-switching between (i) strong expression after stimulation, (ii) low basal expression in off-state, and (iii) reversibility. To aspire to such dynamic efforts with inducible promoters, we investigated different interfering elements as a negative feedback in combination with NF- κ B-triggered expression. As Figure 3 illustrates, one strategy is to interfere post-transcriptional by using RNA interference. Complementary RNA molecules bind to target-mRNA and the resulting double stranded RNAs recruit cellular enzymes and form the so called RNA-induced silencing complex (RISC). The RISC degrades the double-stranded RNA what in turn leads to reduced translation. Hence, we designed single hairpin RNAs (shRNA) that are specific to the mRNA of SEAP (SEAP-shRNA).

We designed several SEAP-shRNAs with different blast results and used additionally one that has been previously published (Wooddell *et al.*, 2005). To adjust the shRNA expression, we further investigated two RNA polymerase II dependent promoter elements: A CMV-based one and CMV_{min}. CMV-based RNA expression levels have been demonstrated to be lower than Polymerase III dependent promoters such as U6 promoters (Kim *et al.*, 2010). Hence, we used CMV or CMV_{min} driven shRNA expression instead of U6 promoters, to induce only slight repressions. Plasmids encoding the described shRNAs were co-transfected with pNF κ B-SEAP (pDH1) and SEAP expression in response to TNF α was investigated (Figure 14B). The designed SEAP shRNAs were validated using constitutive driven SEAP expression (Figure 14C). CMV-driven shRNAs demonstrated superior suppressions in comparison to CMV_{min} expressed shRNAs (Figure 14B). With both promoter types, we observed a reduction in basal and in maximal expression, but with no better fold inductions compared to the control (pDH1/pDH79).

One major benefit of shRNA-induced RNA interference is its specificity to the target-mRNA. However, regarding sensor-effector cells, which express different biologicals, a more overlapping regulation of NF- κ B-triggered expression is highly desired. Another interesting approach is therefore to influence NF- κ B signal transduction by influencing p50/p65 directly by anti-transcription factor RNA aptamers.

The use of RNA double-strands mimicking binding sites for p50/p65 to antagonize the p50/p65-DNA interaction (Figure 3), so called anti-transcription factor RNA aptamers, is an interesting approach to interfere with NF- κ B signaling (Wurster *et al.*, 2009). For the NF- κ B transcription factors p50 and p65, so-called anti-transcription factor RNA aptamers have been previously published, binding to the subunits *in vitro* and *in vivo* in a nanomolar way (Wurster *et al.*, 2009). As shown in Figure 11, we designed and selected bioinformatically different combinations of p50/p65 binding site mimicking RNA motives.

In some designs (Figure 11), we additionally inserted anti-p50 RNA (TC15 – TC21) or RNA-based nucleus localizations sequences (TC24 - TC27). Focusing on the molecular level, previous publications have enlightened the core sequences using X-ray crystallography, which are responsible for binding to p65. Therefore, such core sequences were experimentally inserted (TC21, TC22, TC23, TC26). For a molecular platform, a so-called T-cassette was selected in order to combine and ensure more predictable RNA motives (Wurster *et al.*, 2009). More combinations were structurally calculated using an online RNA secondary structure prediction tool (Mathew *et al.*, 2012-2017). For more detailed information on the design, see Figure 11, or the cloning description Table 8.

Plasmids encoding the described RNAs were co-transfected with pNF κ B-SEAP (pDH1) and SEAP expression in response to TNF α was investigated (Figure 14D). All transfection combinations showed clearly decreased SEAP expression, but with increased fold inductions compared to the control (pDH1/pDH79). In fact, in almost all cases basal expression levels were clearly decreased. The results for TC21 showed the lowest basal SEAP expression and improved fold induction. The fold inductions for TC17, TC11 and TC24 were also acceptable (data not shown).

During reproduction and in comparison with the control TC21 repeatedly demonstrated strong repressions. As control, a RFP-encoding plasmid (pDH79) was co-transfected to equalize amount of plasmids. We therefore selected TC21 for further experiments. TC21 were validated using constitutive driven GPL or SEAP expression and the inhibition rate was compared to SEAP-shRNA (Figure 14E). Whereas the detailed function of this RNA molecule remains unclear and must be further investigated, it turned out to be a useful tool to adjust an improved balance between repressions, fold induction and decreasing the leakiness of the NF- κ B-dependent promoter (Figure 15D). For a better description, TC21 is in what follows described as “RNA block”. The 2D-structure prediction of the RNA block (Figure 15), which show the anti-p50 RNA (Wurster *et al.*, 2009) and a modified anti-p65 RNA (Figure 11), demonstrated stable folding of the designed structure (red-marked = 99%).

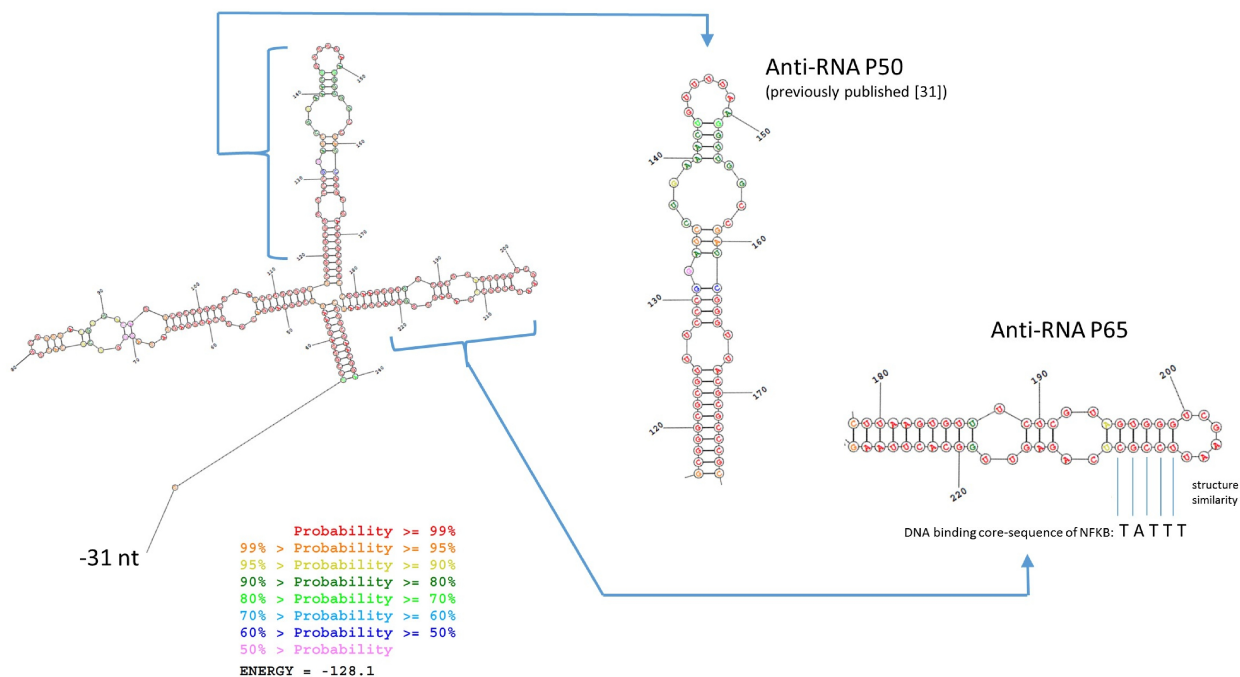
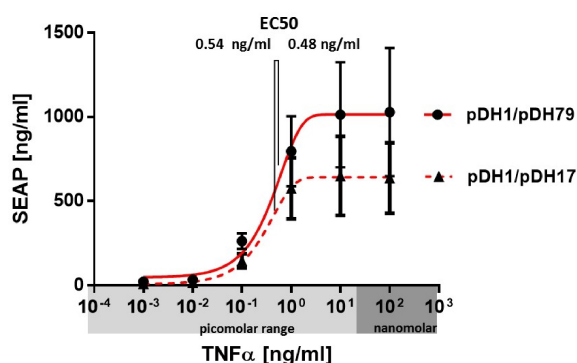


Figure 15. Prediction of secondary RNA structure of RNA block (pDH17). The structure of TC21 was calculated by an online RNA secondary structure prediction tool (Mathew *et al.*, 2012-2017). The RNA motives, anti-p50 and anti-p65 RNA, showed good stabilities (energy: -128.1 kcal/mol) and probabilities (red marked $\geq 99\%$). For more details see Figure 11.

Monitoring the sensitivity, we profiled the NF- κ B-triggered expression levels of SEAP (Figure 16A and B) in a dose-dependent manner using different amounts of TNF α and IL-1 β . For $\leq 5 \times 10^4$ cells gene expression starts with lower picomolar concentrations for both cytokines. The EC50 values of the SEAP profile were reached at 0.54 ng/ml TNF α and 0.48 ng/ml TNF α with RNA block (pDH17) and 0.56 ng/ml IL-1 β and 0.76 ng/ml IL-1 β with RNA block. Thus the presence of the RNA block had no relevance on the dose dependency of the NF- κ B-regulated response.

A



B

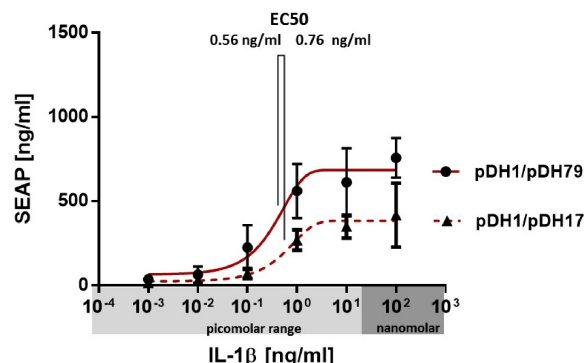


Figure 16. Sensitivity of NF- κ B-triggered SEAP expression. (A) and (B) show the sensitivity and EC50 values of NF- κ B-regulated SEAP expression. HEK293T cells were co-transfected either with pNF κ B-SEAP (pDH1) and RNA block (pDH17) or with filler plasmid (pDH79) and were subsequently exposed to titrated TNF α or IL-1 β concentrations. SEAP expression were profiled 24 hours later. All experimental data presented are mean \pm SD of n=3 independent experiments and different passage of HEK293T cells. Each n stand for three independent experiments with one cell passage.

3.2 Development of cytokine neutralizer cells

NF- κ B-regulated expression of biologicals and *in vitro* validation

As mentioned in the introduction, we planned to exploit TNF α - or IL-1 β -triggered NF- κ B signaling in order to achieve a therapeutic output. After the optimization and characterization of the NF- κ B-regulated promoter, we exchanged reporter genes (SEAP, tGFP) with therapeutic genes. The first construct TNFR2-Fc-GPL (pNF κ B-TNFR2-Fc-GPL; pDH40) is a fusion protein of the human TNFR2 ectodomain with the human IgG1 domain and a C-terminal Gaussia princeps luciferase (GpL) reporter domain, which mimics the approved therapeutic etanercept and can be easily quantified with the help of the GpL domain. Etanercept binds to TNF α and has been used for RA therapy for decades. We furthermore designed a codon-optimized construct encoding the antibody adalimumab (pNF κ B-anti-TNF α ; pDH67). Adalimumab is a powerful TNF α -specific monoclonal antibody and also used for treatment of RA for decades. By integrating IRES elements between the sequences encoding for the antibody light chain and heavy chain, we realized antibody expression from one expression cassette (Komar *et al.*, 2011). For more detailed information on etanercept or adalimumab, see pages 7-10. For a better description, the genetically modified cells, expressing neutralizing biologicals under the control of the NF- κ B-dependent promoter are in what follows described as “cytokine neutralizer cells”.

We co-transfected plasmids encoding the antibody adalimumab (pNF κ B-anti-TNF α ; pDH67) under the control of our NF- κ B-dependent promoter with RNA block. Again, the co-transfected RNA block (pDH17) reduced the leakiness of expression, and thus

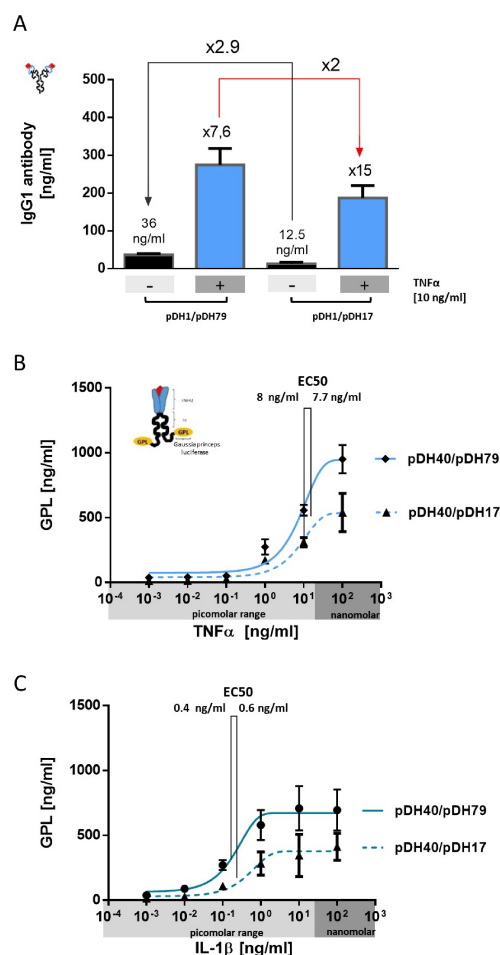


Figure 17. Therapeutic *in vitro* validation of the cytokine neutralizer cells. (A) HEK293T cells were transfected with pNF κ B-anti-TNF α (pDH67, aa sequence of adalimumab) either in combination with RNA block (pDH17) or as control, a RFP-encoding plasmid (pDH79, filler plasmid) was co-transfected to equalize amount of plasmids. (B) and (C) show the sensitivity and EC50 values of TNF α or IL-1 β -triggered expression of TNF α blocker TNFR2-Fc. HEK293T cells were co-transfected either with pNF κ B-TNFR2-Fc-GPL (pDH40, aa sequence of etanercept fused with GpL) and RNA block (pDH17) or with filler plasmid (pDH79). Subsequently the cells were exposed to titrated TNF α or IL-1 β concentrations and profiled for GPL expression 24 hours later.

improved fold induction values in response to TNF α (Figure 17A). Next, we co-transfected HEK293T with pNF κ B-TNFR2-Fc-GPL (pDH40), a NF- κ B-regulated construct encoding a fusion protein of the human TNFR2 ectodomain with the human IgG1 domain, and a C-terminal Gaussia princeps luciferase (GpL) reporter domain (Lang *et al.*, 2016) and profiled the NF- κ B-triggered expression levels of TNFR2-Fc-GpL (Figure 17B and C). The EC50 values of the TNFR2-Fc-GpL profile were reached at 8 ng/ml TNF α and 7.7 ng/ml TNF α with RNA block and 0.4 ng/ml IL-1 β and 0.6 ng/ml IL-1 β with RNA block.

By calculating the number density of inputs (TNF α or IL-1 β) and outputs (SEAP or TNFR2-Fc-GpL) and by correlating these particle numbers, we visualized the signal conversion and amplification profile of the drug delivery system (Figure 18), which is most powerfully in the lower picomolar range.

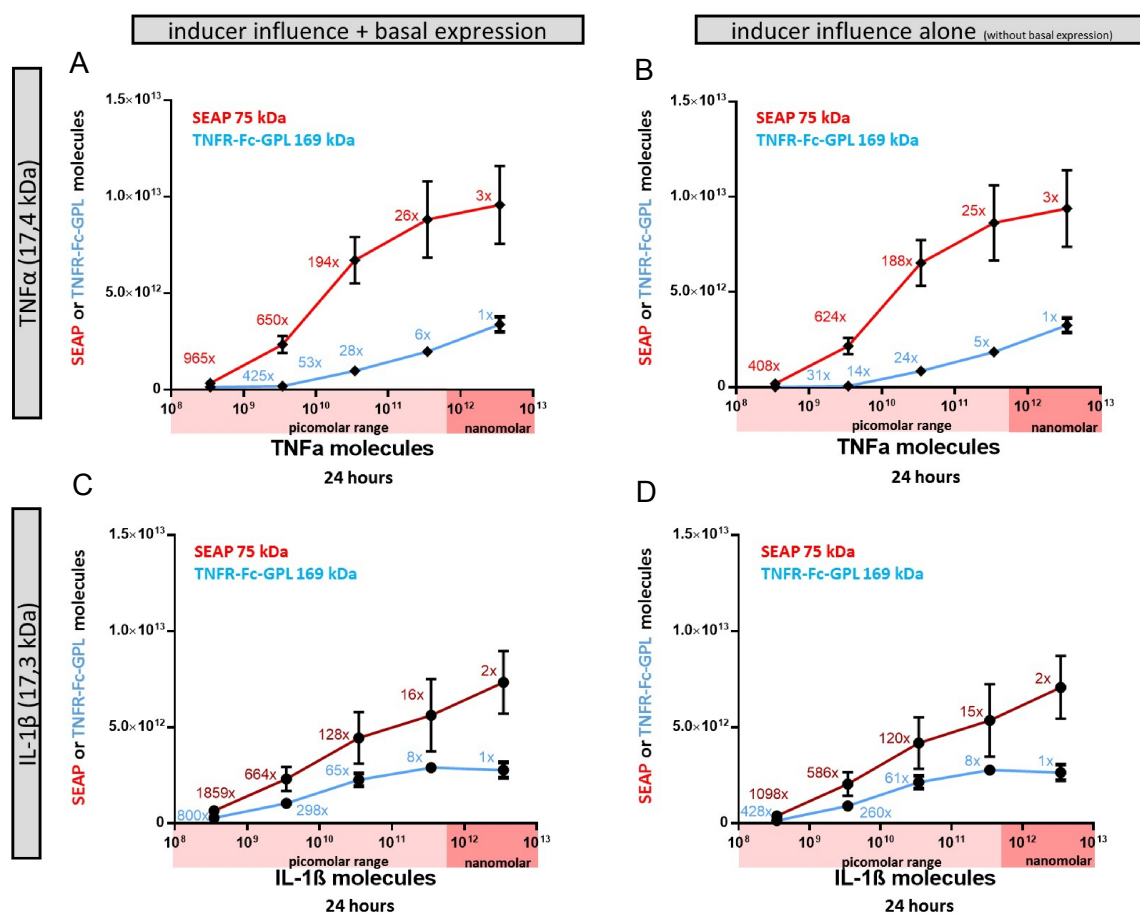


Figure 18. Signal amplifications by particles. Direct correlation of inputs and outputs. The particle density of input TNF α (A) and (B) or IL-1 β (C) and (D), and outputs - SEAP or TNFR2-Fc-GPL - were correlated and the corresponding fold inductions were highlighted. The right column, (B) and (D) show the same correlation but without basal expression. Particle numbers were calculated using the measured data of Figure 16A and B and Figure 17B and C (without RNA block), the molecular mass and Avogadro constant. TNF α (17.4 kDa); IL-1 β (17.3 kDa); SEAP (70 kDa) or TNFR-Fc-GPL (169 kDa).

To demonstrate the neutralization capacity of the sensor-effector cells, we cultured the cells for 24 hours with a mixture of RA-related cytokines (Cytokine mix: IL2, IL17a, IL6/sIL6R) in the presence and absence of TNF α and IL-1 β . In the case of experiments with TNF α , cells were transfected with plasmids encoding for NF- κ B-triggered expression of adalimumab or etanercept (pNF κ B-anti-TNF α , pDH67 or pNF κ B-TNFR2-Fc, pDH68) and for the experiments with IL-1 β with a plasmid encoding for anakinra (pNF κ B-IL1RA, pDH64). After 24 hours we transferred the supernatant to sensor cells transfected with the pNF κ B-SEAP plasmid (pDH1) in order to monitor the functionality of the NF- κ B-regulated biologicals (Figure 19B).

In all the experiments, the engineered cells neutralized the activity of TNF α or IL-1 β completely. This automated and self-induced neutralization of cytokines also remains active in the presence of the RNA block (Figure 20B and D). Furthermore, dose-dependent neutralization was observed with increased concentrations of TNF α or IL-1 β [10 ng/ml] (Figure 20C and D).

To compare the therapeutic neutralization capacity of the neutralizer cells with exogenously added adalimumab, we performed the same experiment with a titration curve of known adalimumab concentrations in the presence of constant TNF α [1 ng/ml]. We observed a dose dependent inhibition of TNF α activity with increase concentrations of exogenously added adalimumab and an IC50 value of 10.8 ng/ml (Figure 19C). Using cell culture inserts, we performed separated co-culture experiments. Through the co-culture of cytokine neutralizer cells with sensor cells transfected with pNF κ B-tGFP (pDH38), we analyzed and monitored simultaneously the neutralization of TNF α (Figure 19D). After 24 hours enough inhibitor was produced to inhibit the synthesis of tGFP. In a control experiment, we investigated the TNF α diffusion rate of the porous PET membrane with or without the cells in the inserts (Figure 21). We performed the same experiment, but using sensor cells transfected with pNF κ B-SEAP (pDH1) for quantification. Both results demonstrate the cross-talk of cytokine neutralizer cells and sensor cells through a porous and strong PET membrane.

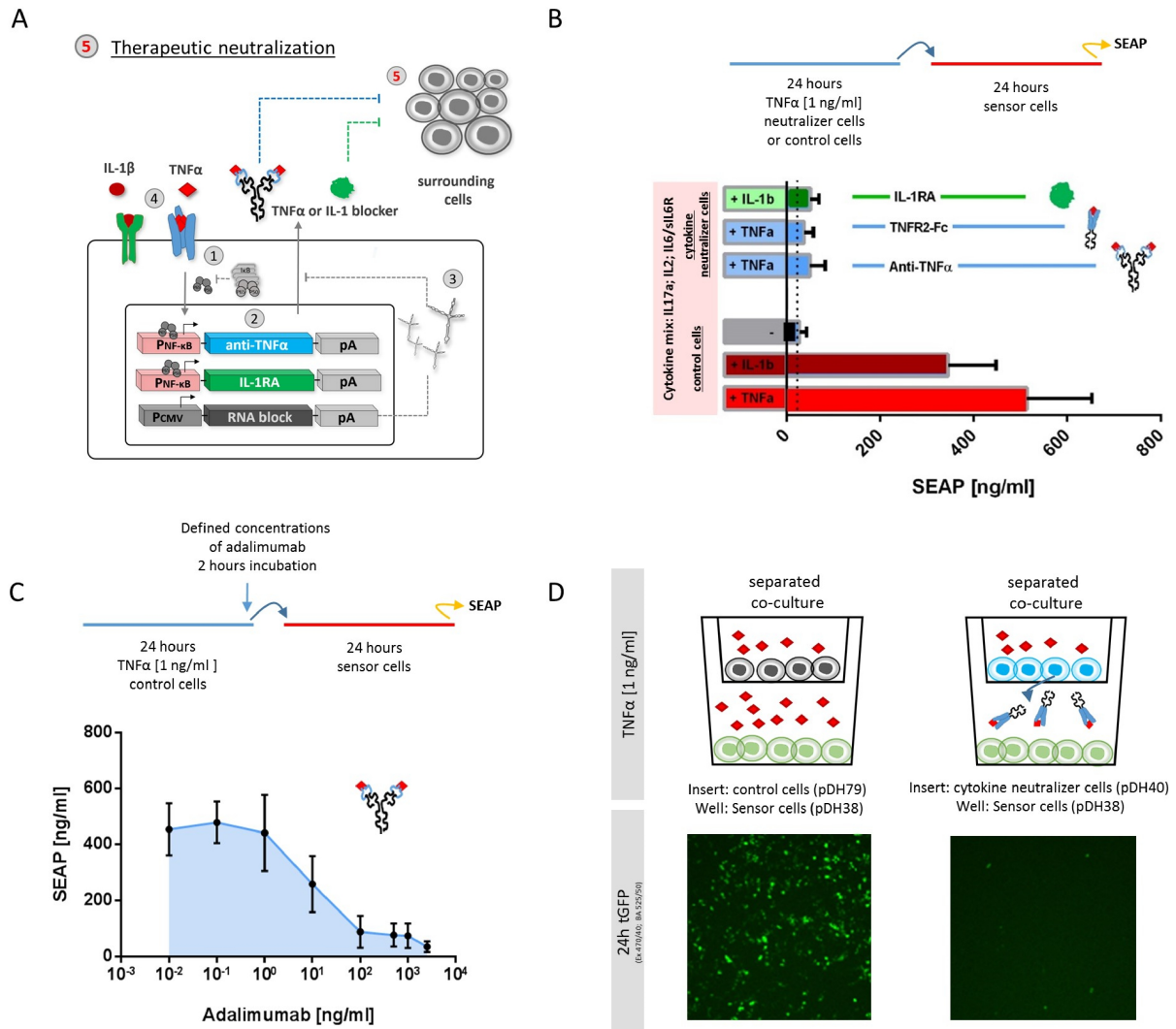


Figure 19. Therapeutic neutralization capacity. (A) Scheme of the engineered cells under stimulation of either TNF α or IL-1 β . (B) HEK293T transfected with pNFkB-anti-TNF α (pDH67) or pNFkB-TNFR2-Fc (pDH68) or pNFkB-IL-1RA (pDH64) were cultured for 24 hours in a cytokine mix (RA-related cytokines: IL-2, IL-17a, IL6, sIL6R) in presence or absence of TNF α [1 ng/ml] or IL-1 β [1 ng/ml]. Controls were HEK293T cells transfected with plasmids encoding RFP (pDH79) and treated with the same conditions. After 24 hours the medium was transferred to the sensor cells - HEK293T cells transfected with pNFkB-SEAP (pDH1) - and SEAP levels were profiled 24 hours later. (C) Control of the cell-based neutralization capacity with addition of adalimumab (anti-TNF α). We performed the same experiment with a titration curve of known adalimumab concentrations in the presence of constant TNF α [1 ng/ml]. Control cells - HEK293T cells transfected with pDH79, treated with TNF α [1 ng/ml] and after 24 hours and further 2 hours of incubation with defined concentrations of adalimumab, the medium were transferred to the sensor cells. All experimental data presented are mean \pm SD of n=3 independent experiments and different passage of HEK293T cells. Each n stand for three independent experiments with one cell passage. (D) Co-culture of sensor and cytokine neutralizer cells. Sensor cells: HEK293T cells were transfected with pNFkB-tGFP-PEST (pDH38). Cytokine neutralizer cells: HEK293T cells were transfected pNFkB-TNFR2-Fc (pDH68). Control cells: HEK293T cells were transfected with pDH79 encoding RFP. The cells in the inserts were treated with TNF α [1 ng/ml] and pNFkB-tGFP expressions were observed in the wells by fluorescence microscopy 24 hours later.

Figure 20. *In vitro* validation of the cytokine neutralizer cells.

Same experimental procedure like Figure 19B, but with or without co-transfection of RNA block (pDH17) or activation with increased concentration TNF α [10 ng/ml]. The upper row (A) and (B) was performed using 1 ng/ml TNF α and the lower row (C) and (D) with 10 ng/ml TNF α . The right column, (B) and (D) show the same experiment but with co-transfection of the RNA block (pDH17). Unless otherwise stated all plasmids were co-transfected with filler plasmid (pDH79) to equalize amount of plasmids. After 24 hours the medium was transferred to the sensor cells - HEK293T cells transfected with pNFkB-SEAP (pDH1) - and SEAP levels were profiled 24 hours later. All experimental data presented are mean \pm SD of 3 independent experiments.

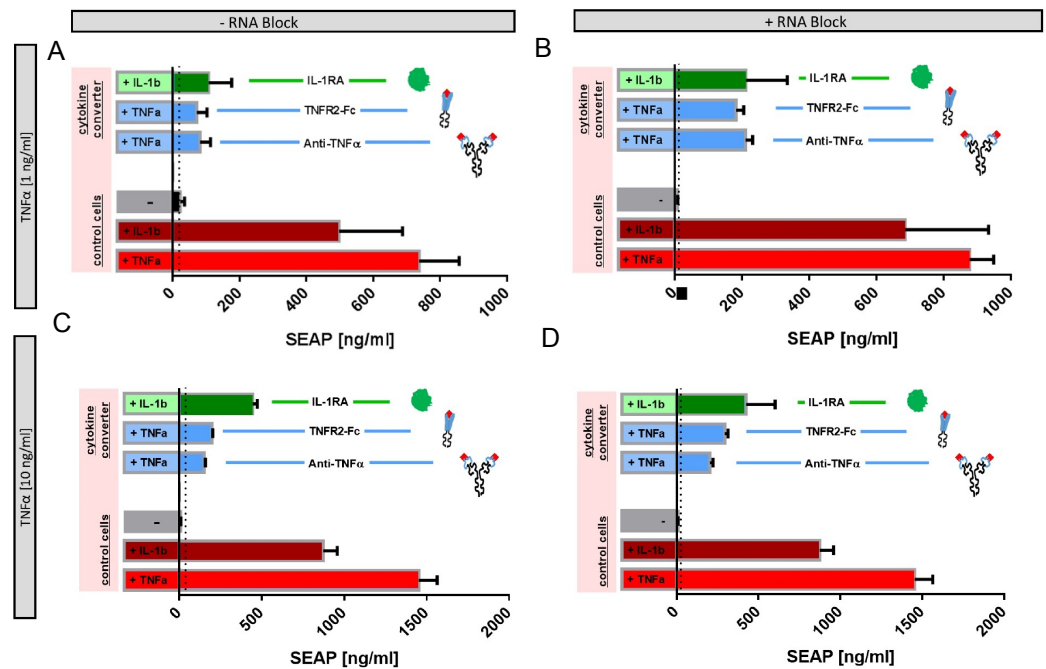
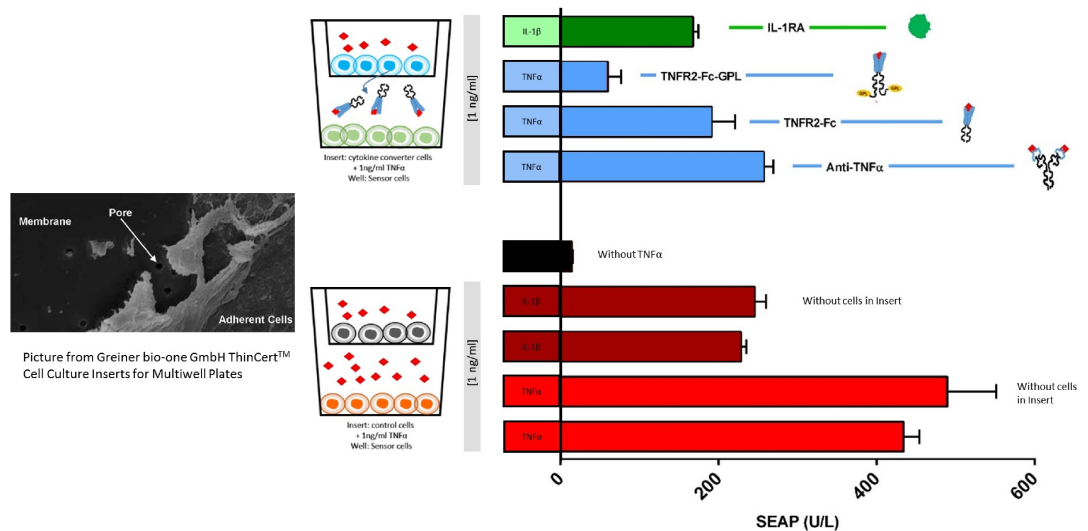


Figure 21. Co-culture of sensor and cytokine neutralizer cells. Co-cultures were performed using 1 μ m porous PET membrane of inserts (Thincert™). The cytokine neutralizer cells or control cells were cultured in inserts and sensor cells below in the wells.



Cytokine neutralizer cells: HEK293T cells transfected with pNFkB-anti-TNF α (pDH67), pNFkB-TNFR2-Fc (pDH68), pNFkB-TNFR2-Fc-GPL (pDH40), or pNFkB-IL-1RA (pDH64). Sensor cells: HEK293T cells transfected with pNFkB-SEAP (pDH1). The cells in the inserts were treated for 24 hours with TNF α or IL-1 β [1 ng/ml]. As control HEK293T cells were transfected with pDH79 encoding RFP and treated with the same conditions. To monitor any perfusion barriers by cells, same conditions were done in absence of cells. In all wells SEAP levels were profiled after 24h. All experimental data presented are mean \pm SD of 3 independent experiments.

Controllability of the cytokine neutralizer cells

The drug delivery of our cytokine neutralizer cells is self-regulated by an autocrine negative feedback loop (Figure 22). With increased IL-1 β or TNF α concentrations, we observed differences in the expression profiles for pNF κ B-TNFR2-Fc-GpL (pDH40). As already illustrated in Figure 16, TNF α activates pNF κ B-SEAP more powerfully than IL-1 β . However, replacing SEAP with TNFR2-Fc-GpL yielded rather reversed results. In Figure 22B we overlapped the TNF α and IL-1 β dose-dependent NF- κ B-triggered TNFR2-Fc-GpL profile of Figure 17B and C. The stimulation of IL-1 β compared to TNF α showed a strong shift to a higher sensitivity EC₅₀ value, from 0.4 ng/ml IL-1 β to 8 ng/ml TNF α . In case of TNF α stimulation, we furthermore detected a slightly reduced expression in the range of 0.01-0.1 ng/ml and an enhanced saturation profile (>100 ng/ml) in relation to the corresponding TNF α -triggered SEAP profile (Figure 16A). This finding suggests an autocrine negative feedback loop. Another indication is the co-culture of neutralizer cells with sensor cells (Figure 22C). The cells were transfected, either with pDH40 (neutralizer cells) or with pDH39 (sensor cells), and after the transfection procedure mixed together (1:1). The mixture of neutralizer cells and sensor cells was cultured afterwards in the presence of TNF α . Within 24 hours we observed no NF κ B-dependent tGFP expression (just few single clones), while in the control, a mixture of sensor cells with RFP-transfected cells, showed strong GFP expression (Figure 22C). Such closed-loop regulations are highly desirable for gene therapy or designer cells and thus for prospective *in vivo* implants (Saxena *et al.*, 2017).

For potential future therapeutic implants, genetically modified cells need to stay under constant control. E.g. CAR T-cells are apt to overstimulate and induce a cytokine storm, which leads to fatal immune reaction and toxicity (Barrett *et al.*, 2014). The integrated interfering modules, the RNA block and the autocrine inducer-blocking mechanism are autonomic cell-based regulations ensuring such a control. The controllability can furthermore be extended by non-genetic means, namely the use of inhibitors of NF- κ B signaling such as for example TPCA-1. TPCA-1 is known to bind and inhibit at nanomolar concentrations I κ B kinase-2 (IKK2), the central signaling hub of the classical NF- κ B signaling pathway (Nan *et al.*, 2014). Indeed, it has been shown that a 20 mg/kg oral dose of TPCA-1 administered twice daily to mice significantly reduced the clinical score and disease severity in a collagen-induced arthritis (CIA) model (Podolin *et al.*, 2005).

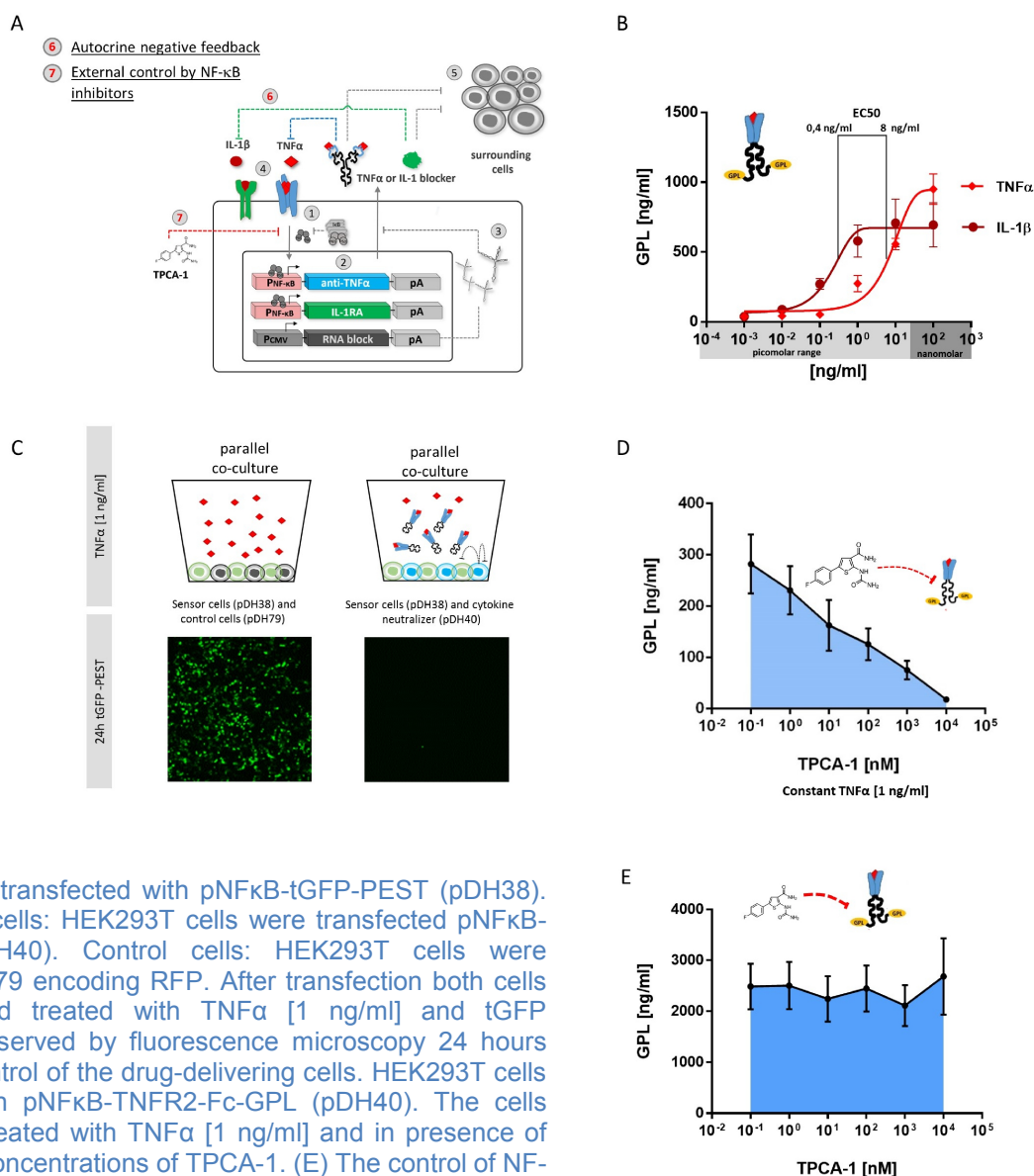
By inhibiting the interception point IKK complex of NF- κ B signaling, we used TPCA-1 as an external control element for the cytokine neutralizer cells (Figure 22D). Cytokine neutralizer cells transfected with pNF κ B-TNFR2-Fc-GpL (pDH40) were treated with increased concentrations of TPCA-1 and consequently exposed to TNF α [1 ng/ml]. Already with 1 nM TPCA-1, we observed first inhibition of TNFR2-Fc-GpL induction and the IC₅₀ value was 40 nM. To exclude any side

effects of solvents and, to prove the specificity to IKK, we controlled and repeated the titration with cells transfected with pCMV-TNFR2-Fc-GPL (pDH41) which express TNFR2-Fc-GpL constitutively. No influences were detected (Figure 22E). In addition to the autonomous control, we extended the adjustability of the genetically modified cells using a small molecule (TPCA-1), regulating the drug delivery.

Figure 22. Controllability of the neutralizer cells.

(A) Schematic overview of TNF α or IL-1 β -triggered and controllable delivery of neutralizing biologicals. (B) Autocrine negative feedback loop of induced TNF α -blocker. HEK293T cells transfected with pNFkB-TNFR2-Fc-GPL (pDH40) show the dose-dependent expression profile and strong EC50 shift after TNF α or IL-1 β stimulus. GPL levels were measured 24 hours later. (C) Co-culture by mixed sensor and cytokine neutralizer cells. Sensor cells:

HEK293T cells were transfected with pNFkB-tGFP-PEST (pDH38). Cytokine neutralizer cells: HEK293T cells were transfected pNFkB-TNFR2-Fc-GPL (pDH40). Control cells: HEK293T cells were transfected with pDH79 encoding RFP. After transfection both cells were mixed 1:1 and treated with TNF α [1 ng/ml] and tGFP expressions were observed by fluorescence microscopy 24 hours later. (D) External control of the drug-delivering cells. HEK293T cells were transfected with pNFkB-TNFR2-Fc-GPL (pDH40). The cells were consequently treated with TNF α [1 ng/ml] and in presence of different nanomolar concentrations of TPCA-1. (E) The control of NF-kB-specific inhibition of TPCA-1 were performed with constitutive expression of CMV-TNFR2-Fc-GPL, (pDH41), showing the specificity to NF-kB signaling and the cell viability. HEK293T cells were transfected with pDH41 and equally treated like (D). All experimental data presented are mean \pm SD of n=3 independent experiments and different passage of HEK293T cells. Each n stand for three independent experiments with one cell passage.



Dynamic and reversibility of NF- κ B-triggered gene expression

As previously mentioned in the introduction, NF- κ B signaling is influenced by the exposure time of one inducer and different inducers activate at different intensities (Hoffmann *et al.*, 2002, Hellweg *et al.*, 2006). Thus, we investigated the dynamics of NF- κ B-triggered SEAP expression over three days (Figure 23). The first long-time experiments were performed with pulse times of 24 hours and 1 ng/ml TNF α . We co-transfected cells with pNF κ B-SEAP (pDH1) and with or without the RNA block (pDH1/pDH17).

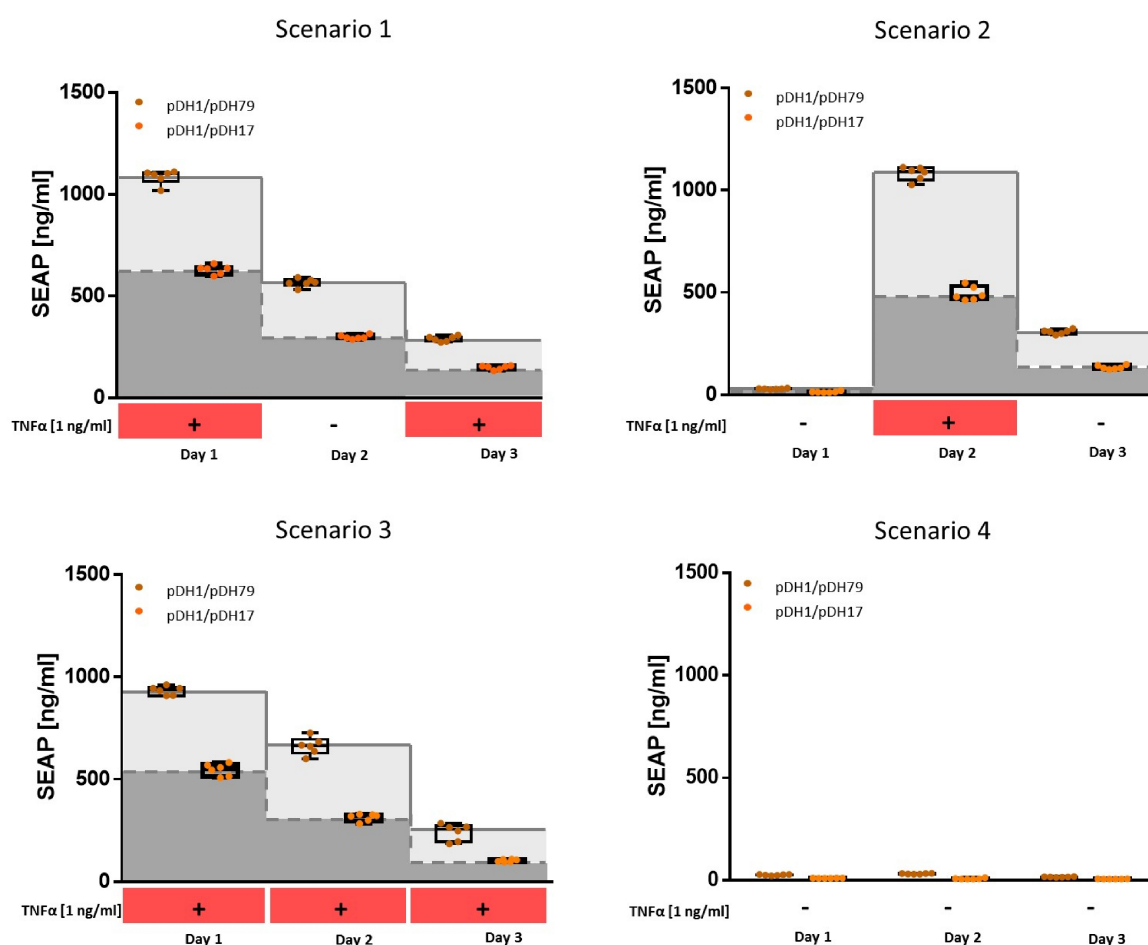


Figure 23. Dynamic and Reversibility of NF- κ B-triggered gene expression. HEK293T cells were transfected with pNF κ B-SEAP (pDH1) and either co-transfected with RNA block (pDH17) or with filler plasmid (pDH79) as control and to equalize amount of plasmids. Four different scenarios (alteration every 24 hours) were tested over 3 days. After incubation with TNF α [1 ng/ml] for 24 hours, the supernatant was replaced, SEAP expression was measured and new fresh media was added. SEAP profile was measured over 3 days. Example of scenario 1: Day 1 (first activation); day 2 (off-state, exchange with fresh media); day 3 (second activation). All experimental data presented are mean \pm SD of n=2 independent experiments and different passage of HEK293T cells. Each n stand for 3 independent experiments with one cell passage.

Four different experiments were performed, called: Scenario 1-4. These experiments investigate to which extent an already activated signal may be silenced and conversely to which extent NF- κ B signaling may be able to reactivate the NF- κ B-dependent promoter after inducer removal (scenario 1 and 2). Scenario 3 is the constant activation, while scenario 4 is the complete off-state as a control with fresh media.

Under each of the conditions, the RNA block suppressed permanently. The activation after off-state leads to SEAP expression (scenario 2) and the controls (scenario 4) were permanently silenced. However, we observed a continuous, decreased SEAP profile in reversibility 3 and no reactivation in reversibility 1. FACS analysis of transfected cells with plasmids encoding a degradable tGFP under the control of the NF- κ B-dependent promoter (pNF κ B-tGFP-PEST, pDH38) demonstrated off-switched expression of new-synthesized tGFP at day 2 (Figure 24), after activation (day 1) and inducer removal (day 2).

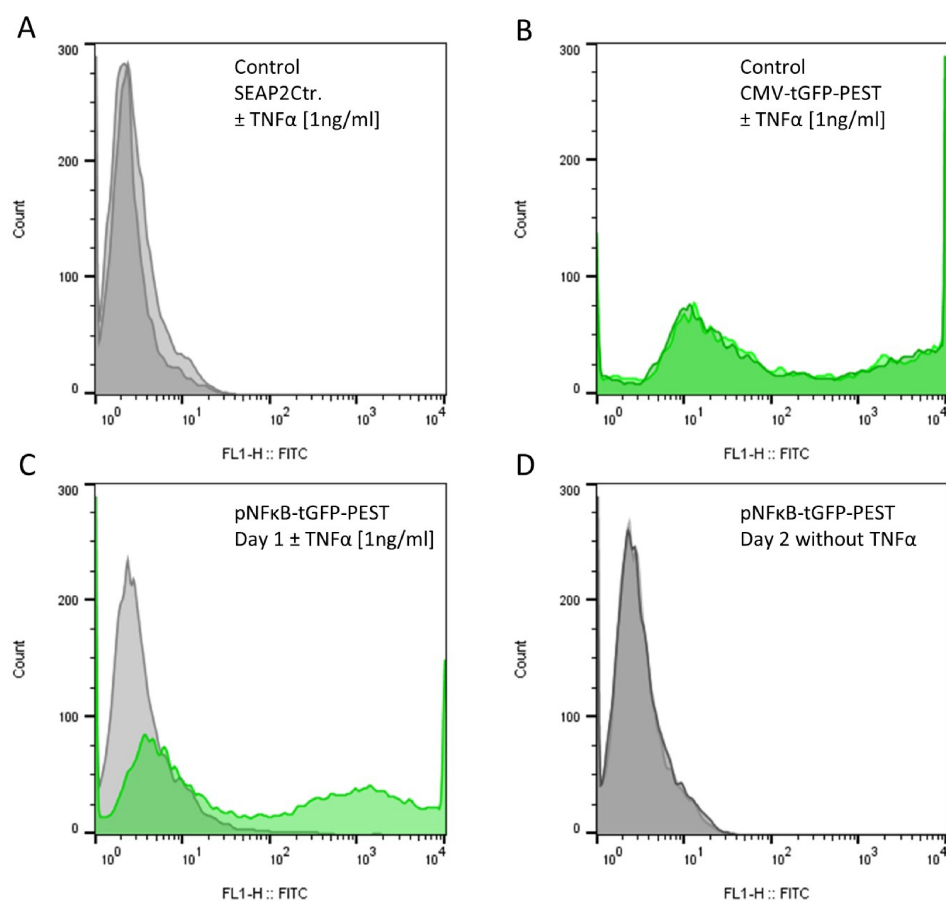


Figure 24. Validation of NF- κ B-dependent promoter activation. HEK293T cells were transfected (A) with SEAP2Ctr. as negative control, (B) with CMV-tGFP-PEST as a positive control, (C) and (D) with pNF κ B-tGFP-PEST. (C) Day 1: The cells were treated with (green) or without (grey) TNF α [1 ng/ml] and FACS analysis with fluorescence detection were performed 24 hours later. (D) Day 2: The inducer and medium were removed and refilled with fresh medium and FACS analysis with fluorescence detection were again performed 24 hours later.

Regarding the impact of the pulse time of inducers, we repeated reversibility 1 with different pulse times of the inducer TNF α (Figure 25). Four different pulse times were used: 2 hours, 4 hours, 8 hours and 10 hours. After each pulse time, the media was replaced by new, pre-warmed media and the removed media was analyzed for SEAP quantifications (SEAP levels after 2 hours, 4 hours, 8 hours and 10 hours). After fixed time points - day 1, 2 and 3 - SEAP expression were again measured and the resulting amounts were added to the corresponding initial SEAP levels of the pulse times to achieve total SEAP expression level (for example, SEAP level after 10 hours pulse time plus SEAP expression after 24 hours).

Interestingly, we observed different results compared with the 24 hours pulse time experiment (Figure 23). With reduced pulse times, NF- κ B-regulated SEAP showed enhanced reactivation and faster decreases after activation of NF- κ B signaling. However, the decreased pulse times and the increased media removals influence the cell viability. We also counted the cell numbers after day 3 (Table 14) and detected decreased cell numbers in comparison to the control (1.1 mio cells/ml after day 3) where no pulse times were used.

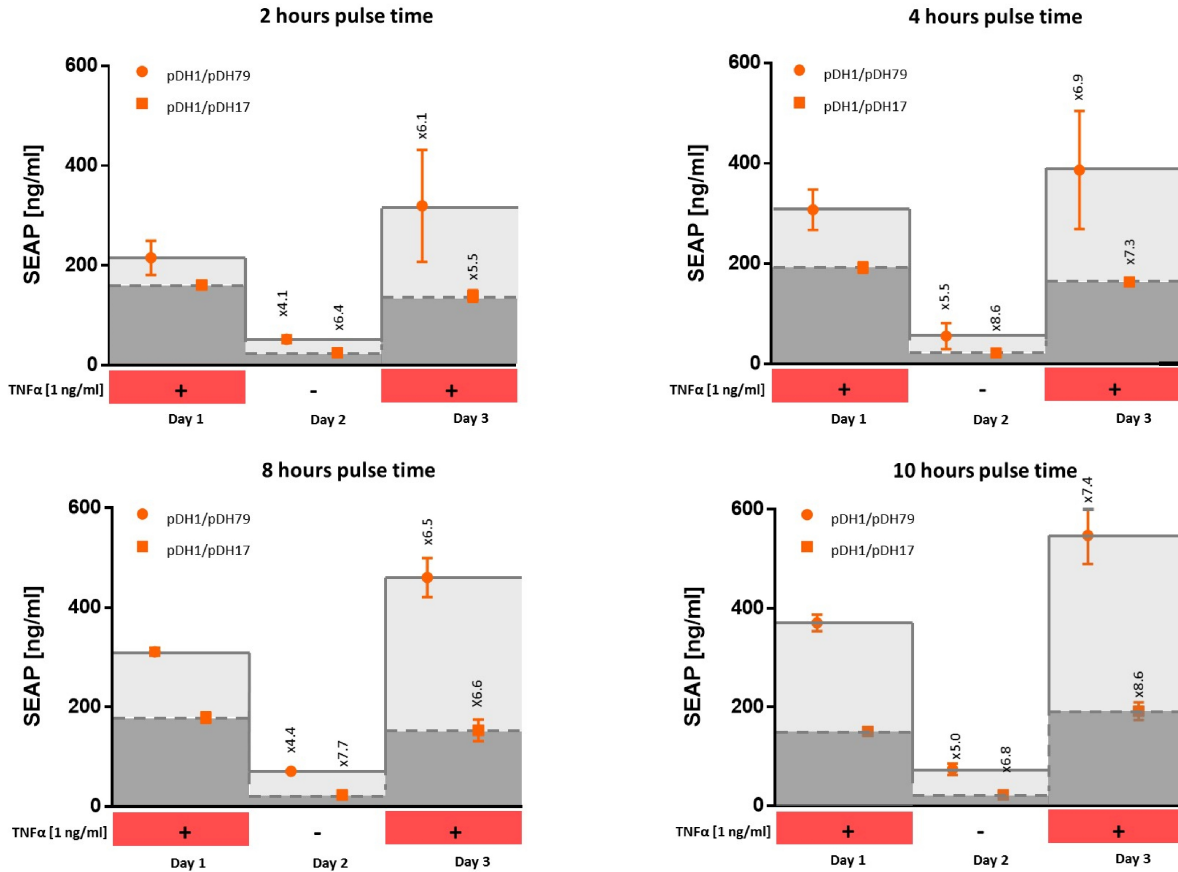


Figure 25. Dynamic and reversibility of NF-κB-triggered gene expression. HEK293T cells were co-transfected with pNFκB-SEAP and either with RNA block (pDH17) or with filler plasmid (pDH79) as control and to equalize amount of plasmids. In comparison to Figure 23 only one scenario (scenario 1) were performed over 3 days. However, the pulse time of TNFα varied. After induction with TNFα [1 ng/ml] for corresponding pulse time: 2 hours induction; 4 hours induction; 8 hours induction; and 10 hours induction, supernatant was replaced, SEAP expression profiles were measured and new fresh media were added. SEAP profile were additionally measured after solid time points of 24 hours. Day 1 (first activation); day 2 (off-state, exchange with fresh media); day 3 (second activation). Considering SEAP expressions while the pulse time, readings were added to the data of solid time points, respectively. All experimental data presented are mean ± SD of 3 independent experiments.

Transfection setup	Control (pDH1/pDH79)	RNA block (pDH1/pDH17)
Pulse time 2 hours	4.35*10 ⁵ cells/ml	3*10 ⁵ cells/ml
Pulse time 4 hours	5.8*10 ⁵ cells/ml	3.8*10 ⁵ cells/ml
Pulse time 8 hours	4.7*10 ⁵ cells/ml	4.9*10 ⁵ cells/ml
Pulse time 10 hours	4.8*10 ⁵ cells/ml	4.8*10 ⁵ cells/ml

Table 14. Cell numbers after reversibility. At the beginning 8*10⁴ cells/ml were seeded. The control without media exchanges after 3 days was 1.1 *10⁶ cells/ml.

The pulse time of 4 hours showed good expression levels and dynamics. We therefore reproduced and manifested those results and adopted the experiment for the cytokine neutralizer cells (Figure 26). We were able to stepwise increase the dynamic of NF- κ B-triggered gene expression by the integration of the following interfering modules: (i) The RNA block, (ii) the autocrine negative feedback loop of TNF α blockers, and (iii) the combination of both, which improved dynamics and reversibility.

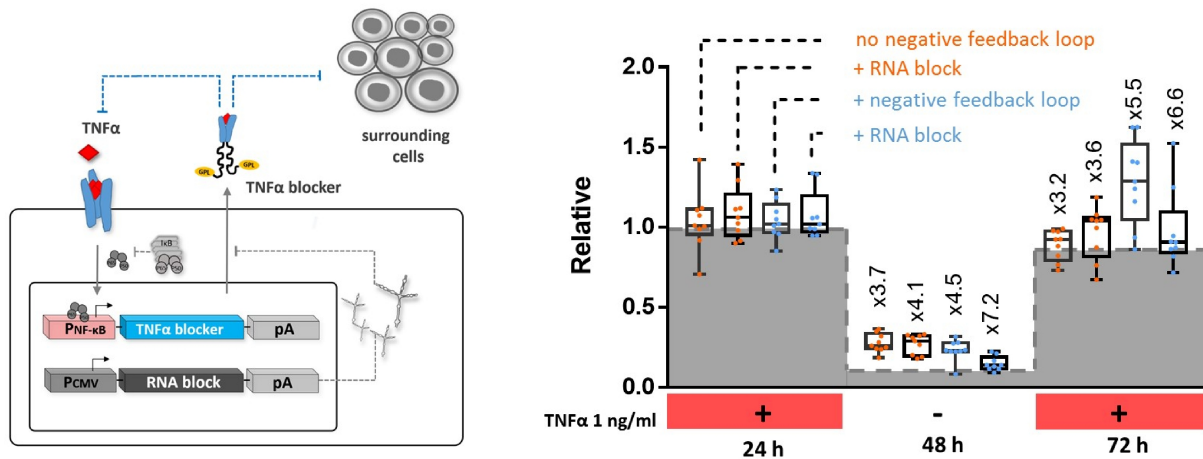


Figure 26. Dynamic and reversibility of cytokine neutralizer cells. To measure the dynamic and reversibility of the cytokine neutralizer by comparing the interfering elements, HEK293T cells were co-transfected with plasmids encoding for the following genes: (i) pNF κ B-SEAP (pDH1) co-expression with or without RNA block (pDH17), or (ii) co-transfected with plasmids encoding pNF κ B-TNFR2-Fc-GPL (pDH40) co-expression with or without RNA block (pDH17). As control, a RFP-encoding plasmid (pDH79) was co-transfected to equalize amount of plasmids. After pulse time of 4 hours TNF α [1 ng/ml], supernatant was replaced, expression profiles were measured and new fresh media was added. SEAP profiles of pNF κ B-SEAP or GPL profiles of pNF κ B-TNFR2-Fc-GPL were additionally measured after solid time points of 24 hours. Day 1 (first activation); day 2 (off-state, exchange with fresh media for 24 hours); day 3 (second activation). Considering SEAP and GPL expressions while the pulse time of 4 hours, readings were added to the data of solid time points. Detected expressions for all combinations were relativized to 1 after the first activation, allowing for the different gene expressions of pNF κ B-SEAP (pDH1) and pNF κ B-TNFR2-Fc-GPL (pDH40). All experimental data presented are mean \pm SD of n=3 independent experiments and different passage of HEK293T cells. Each n stand for three independent experiments with one cell passage.

3.3 Outlook for *in vivo* implantations

Validation of NF- κ B-regulated gene expression of alginate encapsulated cells

In view of future *in vivo* trials, genetically modified allogenic cells, as a local drug delivery depot, must be protected from the host's immune system and conversely the recipient from that of the cells. The most frequently used strategy is encapsulation and here, the polymer alginate is commonly applied. Alginate encapsulation has the significant advantage of simple handling. Water-solved alginate suspends cells in desired concentrations and the cell-alginate suspensions can cure in CaCl_2 or BaCl_2 solutions drop by drop, generating microcapsules. Furthermore, alginate has demonstrated *in vivo* auto-vascularization for promoting nutrients supply. However, the alginate-based cell encapsulation and its release profile is not suitable for large drug payloads such as antibodies. Smaller biologicals like the here used anakinra or antibody fragments like single-domain antibodies may overcome better this alginate barrier. There also exist strategies without encapsulation using engineered and heterologously expressed MHC molecules on cells, preventing NK-mediated lysis (Claudia Mitchell *et al.*, 2012-2017). However, here the recipient remains unprotected from the genetically modified cells, which may be problematic.

We encapsulated cells, transfected with either pNF κ B-tGFP-PEST for localization or with pNF κ B-SEAP for quantification (Figure 27). As a control, we performed the same procedure with constitutive expressed hCMV-tGFP-PEST. In response to TNF α , we observed after 48 hours the first induced tGFP. No detection was observed after 24 hours. For SEAP quantification, we detected first SEAP expressions in the supernatant after 180 hours (Figure 27C). These belated expressions are probably caused by the diffusion rate of (i) the incoming of TNF α through the alginate and (ii) the activation and secretion of SEAP.

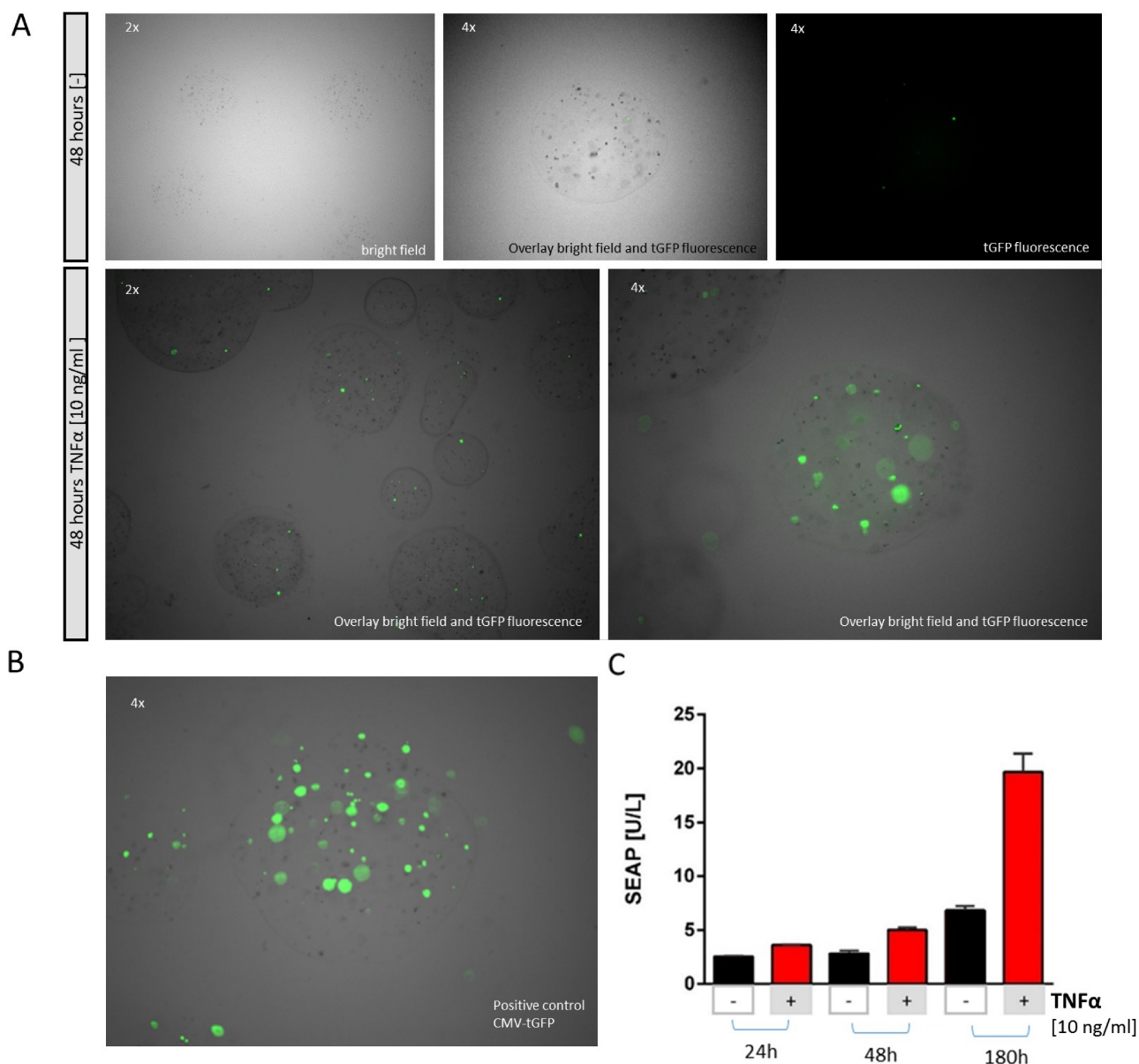


Figure 27. Validation of NF-κB-regulated gene expression of alginate encapsulated cells. (A) HEK293T cells transfected with pNFκB-tGFP-PEST (pDH38) were encapsulated and cultured for 48 hours in absence or presence of TNFα [10 ng/ml]. **(B)** As a positive control HEK293T cells were transfected with pCMV-tGFP-PEST (pDH39) and afterwards encapsulated. Microscopy images were recorded after 48 hours. **(C)** To quantify gene expression in supernatant HEK293T cells were transfected with pNFκB-SEAP (pDH1), encapsulated and cultured in absence (black bars) or presence (red bars) of TNFα [10 ng/ml]. SEAP expressions were profiled 24 hours; 48 hours and 180 hours later. All experimental data presented are mean ± SD of each triplicates.

Regardless, the findings proved the cross-talking of encapsulated cells within the microenvironment. The co-culture of human blood cells and encapsulated designer cells has also been previously published (Lin *et al.*, 2015). However, a conflicting fact observed during this research is that cells may escape the alginate capsule. Alginate capsules have a gel-like consistency and are not impassable.

Figure 28 shows encapsulated cells escaping and outgrowing one capsule. These facts have to be considered and controversially discussed, especially considering planned *in vivo* trials.

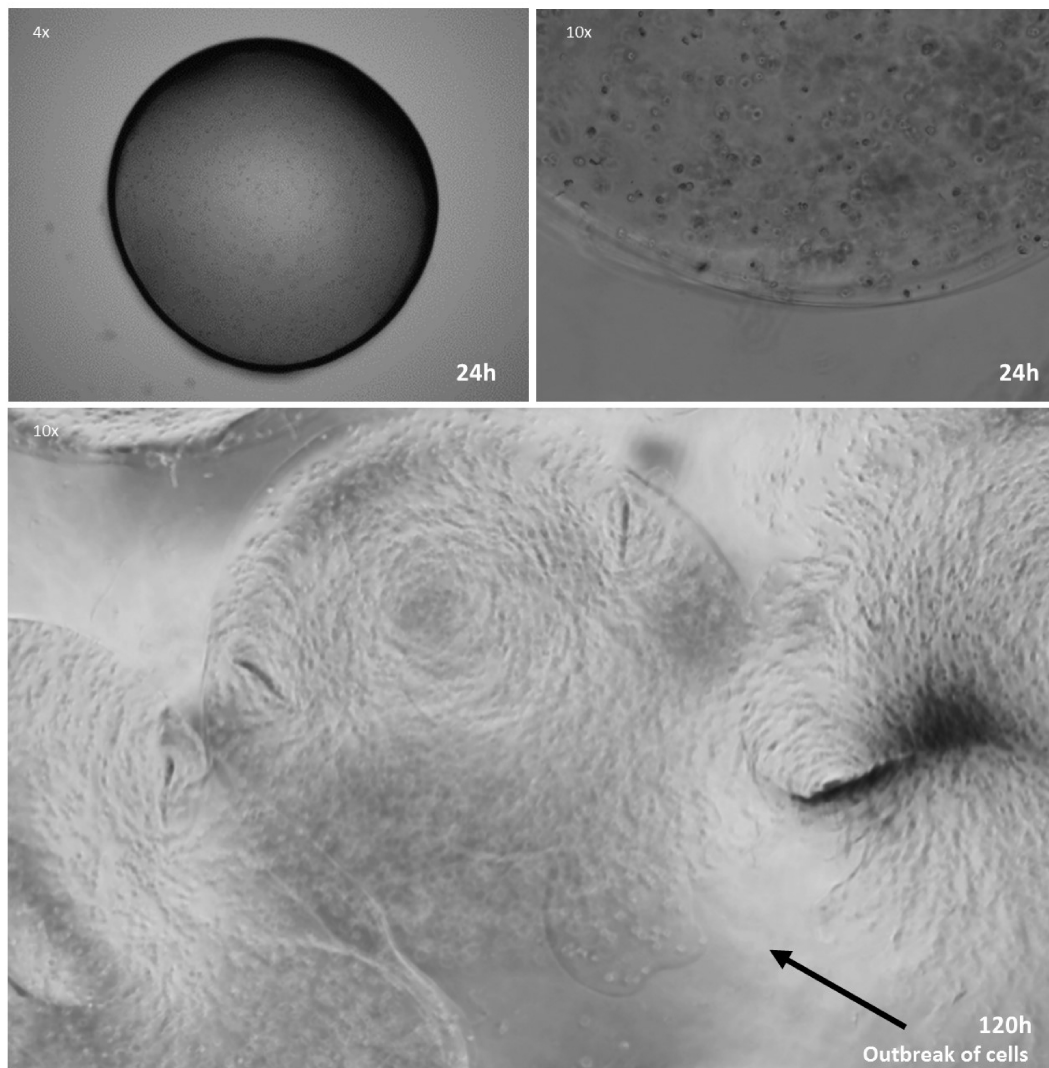


Figure 28. Long-term culture of alginate encapsulated cells. HEK293T cells (1 mio/ml in 1.5% alginate ddH_2O) were encapsulated by droplets in CaCl solution (1%). Encapsulated HEK293T cells were cultured in DMEM media and recorded after 24 hours and 120 hours. After 120 hours, at some capsules we observed a burst open of the capsule and an outbreak of cells. The released cells were able to form little islets on the well bottom (black arrow).

The NF- κ B-regulated promoter works in blood plasma and synovial liquids

We tested pNF κ B-SEAP transfected cells (with or without RNA block) for cell viability and NF- κ B activation in blood plasma or synovial liquids (Figure 29). The blood plasma was from a healthy control and the synovial liquid from an arthrosis patients (several years old and origin unknown). For the synovial liquids, we performed only two dilutions with cell media because of the small sample size of 1 ml.

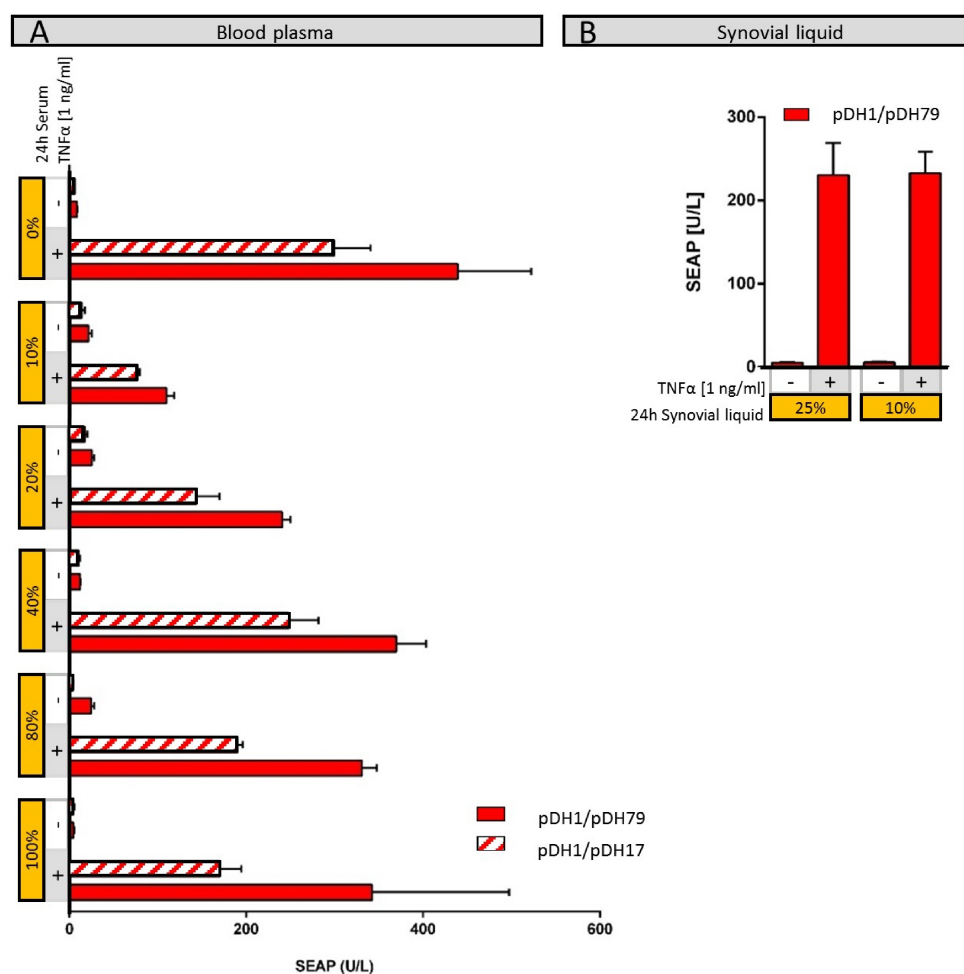


Figure 29. Analysis of NF- κ B-regulated promoter using human samples. HEK293T cells were transfected with pNF κ B-SEAP (pDH1) and exposed to human blood plasma or synovial liquids. **(A)** All cells were either cultured in absence or presence of TNF α [1 ng/ml] together with increased concentrations of human blood plasma or **(B)** together with increased concentrations of human synovial liquids. All experimental data presented are mean \pm SD of 3 independent experiments.

In all the conditions, we observed an increased SEAP expression in response to TNF α , demonstrating NF- κ B-dependent promoter activation even with culture in 100% blood plasma. The diluted synovial liquid sample also showed activation of NF- κ B-regulated SEAP expression. When comparing the cell numbers after treatment, we detected a decreased number within increased blood plasma concentrations (Table 15).

Blood plasma/DMEM ratio	Cell number/ml
0/100	$3.2 \cdot 10^5$
10/90	$1 \cdot 10^5$
20/80	$1.8 \cdot 10^5$
40/60	$2.5 \cdot 10^5$
80/20	$2.4 \cdot 10^5$
100/0	$2.2 \cdot 10^5$

Table 15. Cell numbers in human blood cultures.

NF-κB-regulated gene expression induced by murine TNFα

Animal trials for the research of RA are often prepared using mice. Transfected HEK293T cells respond to murine TNFα as well (Figure 30). A fact that becomes necessary when using non-humanized mice for a proof of concept like e.g. collagen-induced arthritis (CIA).

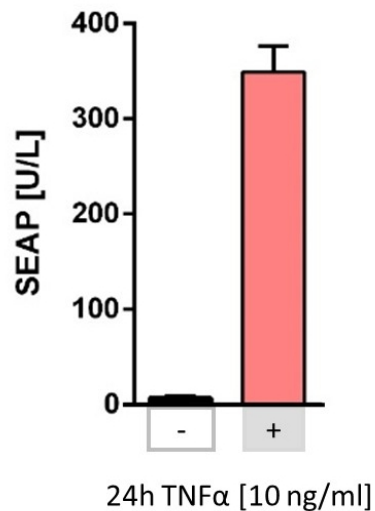


Figure 30. Xenogeneic NF-κB-regulated gene expression by murine TNFα. HEK293T cells were transfected with pNFκB-SEAP (pDH1) and exposed to 10 ng/ml murine TNFα. After 24 hours SEAP expression were profiled. All experimental data presented are mean ± SD of 3 independent experiments.

IV. Discussion

Characteristics of NF- κ B-regulated gene expression

NF- κ B signaling is the basis of the cytokine neutralizer cells developed here. The self-regulated and dynamic characteristics of NF- κ B transcription factors are predestined as molecular on/off-switcher of gene expression. NF- κ B signaling demonstrates a strong negative feedback loop through the expression of its inhibitor I κ Ba, induced by p50/p65 itself.

Previous publications have investigated the dynamic behavior of NF- κ B-triggered gene expression in different cells. NF- κ Bs have showed here different behavioral patterns depending on (i) the exposure time of inducers, which influences the NF- κ B-dependent expression profile, (ii) different inducer stimuli with different strengths and (iii) the cell type or the cellular differentiation (Hoffmann *et al.*, 2002, Hellweg *et al.*, 2006).

In this thesis, we first analyzed NF- κ B-triggered gene expression in HEK293T cells. We also tested other cell lines (Figure 8F), but HEK293T seemed to be best suited to achieve good NF- κ B-triggered gene expression. In standby mode, we detected an excess of I κ Ba by seeing YFP labeled p65 in the cytoplasm. Here we artificially increased the intracellular amounts of p65 by transfection of plasmids that drive the constitutive expression of p65-YFP, and yet most p65-YFP remained in the cytoplasm. This finding indicates a strong influence of I κ Ba. The translocation of p65-YFP to the nucleus starts within minutes (Figure 8C) after TNF α stimulation and the first NF- κ B-triggered protein expression was observed after 6 hours (Figure 8D and E).

When analyzing pulse time and reversibility over 3 days (Figure 23), we observed a continuous, decreased SEAP profile in scenario 3 (permanent activation) and no reactivation in scenario 1 (day 1 activation, day 2 off-state, day 3 reactivation). A possible interpretation is, that NF- κ B transcription factors reach a latent state through the ligand-induced receptor internalization and degradation after 24 hours of pulse times. High p50/p65-induced I κ Ba expression may also influence the changes. However, the fact that residual SEAP levels were detected even in the off-state (scenario 1, day 2), argues for receptor internalizations and p50/p65 temporary remaining active. By the non-detected expression of NF- κ B-regulated and short-lived tGFP at day 2 (Figure 24), we observed the deactivation of NF- κ B-triggered expression under 24 hours in off-state after preceded 24 hours activation. A time-lapse analysis recording a longer time line and more time points should substantiate these findings and observe the oscillation of NF- κ Bs or receptor reconstitution. Other more sensitive methods should confirm the findings, which may validate the detection limit of FACS analysis. Hypothetical strong reduced gene expressions may be still

active, which may explain the residual SEAP levels in scenario 1, day 2 in Figure 23. SEAP expression levels are more sensitive than destabilized tGFP profiles, because of the stability and accumulation of SEAP. However, evidences for a long-term desensitization of the NF- κ B signaling would be problematic for sensor-effector cell therapies.

By reducing the pulse times of TNF α , a different gene expression pattern of NF- κ Bs has been previously observed: Hoffmann *et al.*, (2002) detected an hourly oscillation of NF- κ Bs from cytoplasm to the nucleus. We also observed an increased reduction of the remaining SEAP expression in the off-state after we reduced pulse times (Figure 25; Figure 26). The strong correlations between pulse time, receptor activation and internalization, I κ Bs degradation and new synthesis, which influence all NF- κ B signaling should be analyzed in more detail under real-time conditions. Further investigations, including proteome-based methods, should analyze the dynamic behavior of NF- κ Bs and its network without the use of interrupting reporter genes, such as SEAP or tGFP. The use of single cell analysis could highlight the clonal and cell-specific behavior of NF κ B-signaling.

NF- κ B-dependent activation of chimeric Gal4/UAS promoter

To influence the cell type-specific secretome of the p50/p65 dependent gene expressions, we planned to capture and rewire p65 to a non-mammalian inducible promoter using two different strategies (design 1 and 2). Whereby the endogenous p50/p65 binding sites must be inhibited by another, later planned step using for example repressors or dynamic genome engineering by single RNA strands (Ausländer *et al.*, 2014). Neither designs 1 nor 2 (Figure 12A and B) achieved the desired expression levels or fold inductions. In design 2 almost all setups showed no SEAP expression, but all combinations of the two fusion proteins Gal4DBD-RevM10 with a reverse sequence (pDH25 and pDH29) did. Even when these detected results are paradoxical, because we detected activation without RNA interaction: HEK293T cells were co-transfected with only pDH6/pDH25 or pDH6/pDH29 and we observed strong activation in the absence of the RNA elements, which is not plausible (Figure 13A). In fact, some structural analyses show that Rev proteins can accumulate in cells to an enormous degree by binding to each other (Dimattia *et al.*, 2016). This publication demonstrate, that the N-terminal domains become necessary for dimerization and the C-terminal domains become partially ordered in the context of filaments. These findings may correlate with the repeated occurrence of two plasmids pDH25 and pDH29, both of which encode for reversed sequences of RevM10-Gal4DBD. Such reversed sequences may mimic the N-terminal domain of the Rev proteins. Such possible structure in combination

with DNA binding motives through the fused Gal4DBD could theoretically rearrange plasmid configurations and synergistically influence the transcriptions machinery.

Even if Rev proteins are described as trans-activating proteins essential for the regulation of HIV-1 gene expressions, no published transactivation domains for Rev proteins interacting directly with the transcription machinery exist yet. Native Rev protein improve the export of mRNA into the cell nucleus and thus increase protein translation. Whether the chimeric protein RevM10-Gal4DBD enables mRNA export remains unexplored. However, we have not taken this into further consideration, because it is far from our focus to develop autonomous cytokine neutralizer cells.

Optimization of NF- κ B-triggered gene expression

As intracellular negative feedback, we also co-transfected different plasmids constitutively expressing single hairpin RNAs (shRNA) that are specific to the mRNA of SEAP (shRNA-SEAP) using different promoters (Figure 14B). However, we detected a too strong repression with none improved fold induction. One major benefit of shRNA-induced RNA interference is its specificity to the target mRNA. However, regarding sensor-effector cells, which express different biologicals, a more overlapping or unspecific regulation of NF- κ B-triggered expression is highly desired.

The designed RNA-based DNA mimicry elements of design 2 (Figure 11) are useful tools for influencing NF- κ B-triggered gene expression. We co-transfected a plasmid encoding a constitutively transcribed small non-coding RNA molecule as an interfering regulator (RNA block, pDH17). The RNA block contains a previously published anti-p50 RNA sequence and an engineered core sequence of an anti-p65 RNA sequence (Figure 15). Whereas the detailed function of this RNA molecule remains unclear and must be further investigated, it turned out to be a useful tool to adjust an improved balance between repressions, fold induction, and decreasing the leakiness of the NF- κ B-dependent promoter (Figure 14D). The RNA block (pDH17) consequently improved the NF- κ B promoter with different genes of interest (Figure 14D, 17A, 17B and C, and 27).

Characteristics and *in vitro* validation of the cytokine neutralizer cells

By rewiring NF- κ B signaling to RA-related biologicals (etanercept, adalimumab, or anakinra), we may tailor potential cell and gene therapies for RA. The cytokine neutralizer cells described in this work are capable of processing therapeutic outputs by sensing and responding to TNF α or IL-1 β cytokines. Using the RNA block described above, we achieved increased fold inductions and dynamics of NF- κ B-triggered biologicals (Figure 17 and 26). Furthermore, we observed a

closed-loop circuit using TNF α -induced expressions of TNF α -blocking biologicals, (Figure 22B). As already illustrated in Figure 3, TNF α activates NF κ B-regulated SEAP more powerfully than IL-1 β . However, replacing SEAP with TNF α blocker yielded rather reversed results. We detected an EC50 sensitivity for TNF α -triggered TNF α blocking of 8 ng/ml, which increased dramatically when using IL-1 β -triggered TNF α blocking to EC50 0.4 ng/ml. This finding suggests an autocrine negative feedback loop. Another indication is the co-culture in presence of TNF α of neutralizer cells (NF κ B-regulated TNF α blocker) with sensor cells (NF κ B-regulated tGFP) (Figure 22C). Within 24 hours we observed no NF κ B-dependent tGFP expression (just few single clones), while in the control, a mixture of sensor cells with RFP-transfected cells, showed strong GFP expression (Figure 22C). Such closed-loop regulations are highly desirable for gene therapy or designer cells and thus for prospective *in vivo* implants (Saxena *et al.*, 2017).

The controllability can furthermore be extended by non-genetic means, namely the use of inhibitors of the classical NF- κ B signaling such as for example TPCA-1. Already with 1 nM TPCA-1, we observed first inhibition of TNFR2-Fc-GpL induction and the IC50 value was 40 nM (Figure 22D).

Another important feature of NF- κ B signaling is the strong transactivation domain of p65 (O'Shea *et al.*, 2008; Wan *et al.*, 2009), which enables strong inducible gene expression. In systemic treatments, low levels of injected biologicals *in vivo* are therapeutically insufficient. The drugs delivered from the cytokine neutralizer cells also undergo pharmacokinetics. We postulate, that with a local release of drugs near the origin of the inflammation (for example, the knee), a lower dose might be sufficient. Otherwise, we might be able to upscale to higher drug concentrations with increased amounts of cytokine neutralizer cells. Which, of course, would have to be shown first.

With regard to scaling up, the sensitivity to signal input and the strength of input-output conversion is more decisive in the development of sensor-effector cells. Interestingly, when studying the direct correlation of in- and outputs, we observed increased fold inductions when using decreased input levels (Figure 18). We correlated the particle numbers of inputs (TNF α or IL-1 β) and outputs (SEAP or TNFR2-Fc-GPL) and highlighted the corresponding fold inductions. Hereby we differentiated between with basal expressions and without to verify the tight interdependency of in- and output. From clinical point of view, the basal expression is naturally included. This inverse proportionality of the amount of inducer and fold inductions, highlights the best signal amplifications of the cytokine neutralizer cells in response to the lower particles of inducers.

In an *in vivo*-situation, a complex mixture of cytokines and other soluble proteins will affect the cytokine neutralizer cells. Regarding HEK293T cells, we only monitored responses to IL-1 β and TNF α (Figure 8B), even though a wider spectrum of cytokines should further substantiate this finding. Especially for the pathogenesis of RA, however, the correlation between TNF α and IL-1 β has been repeatedly confirmed. *In vivo*, TNF α strongly triggers the expression of IL-1 β , emphasizing TNF α as a main trigger of an inflammatory cascade (Butler *et al.*, 1995). Furthermore, the transgene expression of TNF α or the depletion of the interleukin receptor antagonist IL-1Ra in mice, cause RA symptoms with up 100% efficacy (Keffer *et al.*, 1991; Akitsu *et al.*, 2015). Regarding the *in vivo* dependency on IL-1 β and TNF α , therapeutic cells with NF- κ B-regulated IL-1 β or TNF α blocking biologicals (cytokine neutralizer cells), may be perhaps tailored for prospective RA treatment.

Regarding the complexity of *in vivo* situations, we performed all cell cultures and activations in the presence of 5% non-heat inactivated FCS. The cell culture in blood plasma or with synovial fluids of an arthrosis patient demonstrated the feasibility of the sensor circuit using additive TNF α (Figure 29). Of course, these results must be confirmed and proven by reproduction and ideally by large scale samples from RA patients. In addition, cytokine levels (TNF α , IL-1 β or others) should be investigated in such human specimens. The culture in the blood plasma has a limited supply of nutrients (for example, limited glucose levels), and large batch-to-batch variations (Yao *et al.*, 2017). We thus observed decreased cell viability in the presence of blood plasma (Table 15). Hence, we recommend a blood plasma supply using continuous cultures, to overcome these limitations, or switching to *in vivo* animal trials to investigate the first proof of concept for the cytokine neutralizer cells.

Challenge and problems

Outlook for *in vivo* trials

In view of planned *in vivo* trials, genetically engineered cells must be protected from the host's immune system and, conversely, the recipient from the cells. The most frequently used strategy is encapsulation, and here, the polymer alginate is commonly applied. More decisively, implanted cellular drug depots, such as alginate-encapsulated cytokine sensor-effector cells may allow long-term monitoring of treatment compliance as previously shown in mice for insulin producing beta cells (Vegas *et al.*, 2016). We started to investigate the sensor-effector capabilities of the transfected and encapsulated cells (Figure 27).

The results demonstrated the cross-talk between TNF α and SEAP release profile of encapsulated cells within the microenvironment, albeit very delayed. The SEAP profile only increased after 180 hours.

The findings showed the cross-talk between TNF α and SEAP release profile of encapsulated cells within the microenvironment. However, the alginate-based cell encapsulation and its release profile is not suitable for large drug payloads such as antibodies. Smaller biologicals like the here used anakinra or antibody fragments like single-domain antibodies may overcome this alginate barrier. In addition, alginate capsules have a gel-like consistency and are not impassable. Figure 28 shows encapsulated cells escaping and outgrowing one capsule. These facts have to be considered and controversially discussed, especially considering planned *in vivo* trials.

The encapsulation process performed here was handmade, while it normally is standardized by encapsulation machines (Lina *et al.*, 2016). This fact must be considered as well. Furthermore, there are commercial providers of cell encapsulation, such as the Canadian firm Sernova, that produce cell pouches with FDA-approved materials combining alginate polymers (Philip Toleikis *et al.*, 2001-2017). Such cell pouches might be an alternative for demonstrating the therapeutic benefit of cytokine neutralizer cells.

For long-term therapies a stable cell line would be preferable and *in vitro* long-term experiments should investigate further pulse times and reversibilities to safely exclude desensitization of NF- κ B-regulated sensor-effector cell therapies. The combination of virus-based large T-antigen and the replication of Ori, allow episomal replications for up to 30 days (Silla *et al.*, 2005; Mahon *et al.*, 2011). A first proof of concept previously published, which sensed TNF α and delivered immune suppressive proteins by alginate encapsulated and genetically modified cells, used transiently transfected cells (Lina *et al.*, 2015). In the design of this publication, first *in vivo* animal trials using alginate encapsulation and smaller biologicals (e.g. anakinra) could be done for the cytokine neutralizer cells as a proof of concept of the therapeutic benefit.

Rheumatoid arthritis disease models

In vivo trials for the research of RA are often prepared using mice. There are many different mice models for developing RA, but the general aim of an animal disease model is to mimic human situations as closely as possible. The collagen-induced arthritis (CIA) model is the one most frequently used for *in vivo* trials (Hirose *et al.*, 2011). Injections of collagen and adjuvants cause mice to spontaneously develop arthritis. There are also genetically modified mice developing RA. Transgene expression of hTNF α induce RA in mice with 100 % incidence and are used for investigations of TNF α -blocking biologicals (Keffer *et al.*, 1991). Another promising established

model is the genetic integration of HLA-DR4 subtypes, which correlate strongly with collagen-based peptides and active autoreactive T cells (Danner *et al.*, 2011).

For a first proof of concept of cytokine neutralizer cells, mice models are preferred with transgene expression of human TNF α : (i) They develop RA with 100 % incidence (ii) adalimumab binds only human TNF α , and (iii) the conventional treatment with adalimumab is standardized in these mice and thus useful for positive controls (Pahl, 2017). However, the constitutive driven human TNF α in mice may in general generate a non-natural *in vivo*-situation. Thus, CIA mice may stay in a more natural disorder through its spontaneous development. The fact that the here described cytokine neutralizer cells can respond to murine TNF α (Figure 30) and etanercept blocks murine TNF α , too, CIA mice may become also suitable for a proof of concept.

In addition, the therapeutic range of TNF α -blocking biologicals is constantly increasing and now covers psoriatic arthritis, ankylosing spondylitis, Crohn's disease, ulcerative colitis, and plaque psoriasis (Scheinfeld *et al.*, 2003, Maxwell *et al.*, 2015, Baumgart, 2009, Sandborn *et al.*, 2012, Croom *et al.*, 2009). Hence, the potential therapeutic benefit of the cytokine neutralizer cells could also be discussed for other diseases models.

Outlook of RA patients - TNF α or IL-1 β are suitable *in vivo* biomarkers?

TNF α and IL-1 have major influences in many immune-based regulations and diseases (Marks *et al.*, 2008). Furthermore is evidenced that TNF α blockade has been proved to influence strongly the levels of IL-1 β *in vivo*, demonstrating a close correlation between these two cytokines and highlighting TNF α as a main trigger for of inflammation (Butler *et al.*, 1995).

Because of their short half-life time in the body, TNF α and IL-1 β concentrations in the blood are highly dynamic and differ from person to person and day to day. In the body the blood is flowing and pulsing, which dilutes the concentrations immediately and causes the cytokines to rapidly undergo metabolism and renal excretion. Some publications, which analyzed the TNF α or IL-1 β concentrations in the blood of RA patients, vary enormously with the only tendency being that RA patients have higher concentrations than healthy persons. Moreover, most studies have included RA patients, who began treatment with drugs, which in turn has led to great variations. Drug responder of TNF α -blocking treatment, demonstrated decreased TNF α levels (Zhao *et al.*, 2014). Previously published investigations differ on the severity grade of patients (Tetta *et al.*, 1990). Here, upregulated TNF α concentrations have been observed in acute RA (active < 1 ng/ml; severe > 6 ng/ml TNF α). Increased concentrations of IL-1 β (asymmetric knee involvement: 519

± 226 pg/ml) have also been found in the synovial liquids of inflamed knees (Rooney *et al.*, 1990). However, the results were based on a small group.

Regarding the great variations, other larger studies have focused on TNF α levels in the synovium, moving closer to the origin of inflammation and incorporating the correlation to TNF α -blocking therapy and drug responder (Wijbrandts *et al.*, 2008). The researchers indicate that, if the patient is correctly classified into a subgroup, TNF α synovial levels may be suitable as biomarkers in the clinic. In sum, with correct classification of RA patients (in treatment, no treatment, drug responder, non-responder, etc.) and local sampling, TNF α or IL-1 β levels may be useful biomarkers. These local-released disease markers may perhaps activate the cytokine neutralizer cells and make their *in vivo* implantation promising.

Closing words: Vision of intelligent and self-regulated medicine for recurring autoimmune diseases

The use of biologicals revolutionized the medicine since more than 30 years and biologicals became the blockbusters of pharma industry. The efficacy of adalimumab or etanercept is undisputed, however, the therapy costs of them are doubtful. In the period from January 1, 2005 and June 30, 2009, the mean annual TNF-blocker costs per treated patient was \$15,345 for etanercept and \$18,046 for adalimumab (Bonafede *et al.*, 2012). New released patents extensions will remain the situation unchanged (Mullard, 2017). Even though the costs are questionable and probably based on economic reasons, the intravenous injection of adalimumab or etanercept are efficient.

By synthetic biology-based cell therapies, local drug production and delivery may be possible and open doors to overcome overcharged prices. Apart from that, cell therapies may reduce personal expenses or exclude expensive purifications processes towards drug formulations. And more decisive, the implanted drug depots may guarantee long-term treatment compliance. The sensor-effector circuit further may provide a dose dependent drug delivery and may offer a more personalized medicine than calculated drug dosing based on body weight. Furthermore, the real-time regulated drug delivery that appears possible with the cytokine neutralizer cells described in this work, could directly repress the inflammation process and interfere with disease before symptoms occur, which may result in prevention rather than disease treatment. To prove such hypothesis, a lot of future research is required.

V. References

- Akitsu A, Ishigame H, Kakuta S, Chung SH, Ikeda S, Shimizu K, Kubo S, Liu Y, Umemura M, Matsuzaki G, Yoshikai Y, Saijo S, Iwakura Y.** IL-1 receptor antagonist-deficient mice develop autoimmune arthritis due to intrinsic activation of IL-17-producing CCR2(+)V γ 6(+) $\gamma\delta$ T cells. *Nat Commun.* 2015 Jun 25;6:7464. doi: 10.1038/ncomms8464. PMID: 26108163
- Ali T, Kaitha S, Mahmood S, Ftesi A, Stone J, Bronze MS.** Clinical use of anti-TNF therapy and increased risk of infections. *Drug, Healthcare and Patient Safety.* 2013 Mar 28; 5: 79-99 PMID: 23569399, DOI: 10.2147/DHPS.S28801
- Allen-Hoffmann BL, Schlosser SJ, Ivarie CA, Sattler CA, Meisner LF, O'Connor SL.** Normal growth and differentiation in a spontaneously immortalized near-diploid human keratinocyte cell line, NIKS. *J Invest Dermatol.* 2000 Mar;114(3):444-55. PMID: 10692102
- Apolo AB, Infante JR, Balmanoukian A, Patel MR, Wang D, Kelly K, Mega AE, Britten CD, Ravaud A, Mita AC, Safran H, Stinchcombe TE, Srdanov M, Gelb AB, Schlichting M, Chin K, Gulley JL.** Avelumab, an Anti-Programmed Death-Ligand 1 Antibody, In Patients With Refractory Metastatic Urothelial Carcinoma: Results From a Multicenter, Phase Ib Study. *J Clin Oncol.* 2017 Jul 1;35(19):2117-2124. doi: 10.1200/JCO.2016.71.6795. Epub 2017 Apr 4. PMID: 28375787
- Arai R, Ueda H, Kitayama A, Kamiya N, Nagamune T.** Design of the linkers which effectively separate domains of a bifunctional fusion protein. *Protein Eng.* 2001 Aug;14(8):529-32. PMID: 11579220
- Aubin F, Carbonnel F, Wendling D.** The complexity of adverse side-effects to biological agents. *J Crohns Colitis.* 2013 May;7(4):257-62. doi: 10.1016/j.crohns.2012.06.024. Epub 2012 Jul 20. Review. PMID: 22819590
- Ausländer S, Ausländer D, Fussenegger M.** Synthetic Biology-The Synthesis of Biology. *Angew Chem Int Ed Engl.* 2017 Jun 1;56(23):6396-6419. doi: 10.1002/anie.201609229. Epub 2017 Apr 25. Review. PMID: 27943572
- Ausländer S, Fussenegger M.** Synthetic biology. Dynamic genome engineering in living cells. *Science.* 2014 Nov 14;346(6211):813-4. doi: 10.1126/science.aaa1246. No abstract available. PMID: 25395523
- Ausländer S, Wieland M, Fussenegger M.** Smart medication through combination of synthetic biology and cell microencapsulation. *Metab Eng.* 2012 May;14(3):252-60. doi: 10.1016/j.ymben.2011.06.003. PMID: 21722748
- Badr C, Niers JM, Tjon-Kon-Fat LA, Noske DP, Wurdinger T, Tannous BA.** Real-time monitoring of NF-kappaB activity in cultured cells and in animal models. *Molecular imaging.* 2009 Sep-Oct; 8(5): 278-290 , PMID: 19796605
- Barrett DM, Teachey DT, Grupp SA.** Toxicity management for patients receiving novel T-cell engaging therapies. *Current opinion in pediatrics.* 2014 Feb; 26(1): 43-49 PMID:24362408
- Baumgart DC.** The Diagnosis and Treatment of Crohn's Disease and Ulcerative Colitis. *Deutsches Ärzteblatt International.* 2009 Feb 20; 106(8): 123-133, PMID: 19568370, DOI: 10.3238/arztebl.2009.0123
- Bhattacharyya S, Ratajczak CK, Vogt SK, Kelley C, Colonna M, Schreiber RD, Muglia LJ.** TAK1 targeting by glucocorticoids determines JNK and I κ B regulation in Toll-like receptor-stimulated macrophages. *Blood.* 2010 Mar 11; 115(10): 1921-1931 , PMID: 20065289, DOI: 10.1182/blood-2009-06-224782
- Bode JG, Albrecht U, Häussinger D, Heinrich PC, Schaper F.** Hepatic acute phase proteins--regulation by IL-6- and IL-1-type cytokines involving STAT3 and its crosstalk with NF-kB-dependent signaling. *Eur J Cell Biol.* 2012 Jun-Jul;91(6-7):496-505. doi: 10.1016/j.ejcb.2011.09.008. Epub 2011 Nov 16. Review. PMID: 22093287
- Boisson B, Puel A, Picard C, Casanova JL.** Human I κ B α Gain of Function: a Severe and Syndromic Immunodeficiency. *J Clin Immunol.* 2017 Jul;37(5):397-412. doi: 10.1007/s10875-017-0400-z. Epub 2017 Jun 9. Review. PMID: 28597146
- Bollrath J, Greten FR.** IKK/NF-kappaB and STAT3 pathways: central signalling hubs in inflammation-mediated tumour promotion and metastasis. *EMBO Rep.* 2009 Dec;10(12):1314-9. doi: 10.1038/embor.2009.243. Epub 2009 Nov 6. Review. PMID: 19893576
- Bolon B, Campagnuolo G, Zhu L, Duryea D, Zack D, Feige U.** Interleukin-1beta and tumor necrosis factor-alpha produce distinct, time-dependent patterns of acute arthritis in the rat knee. *Vet Pathol.* 2004 May;41(3):235-43. PMID: 15133172
- Bonafede MM, Gandra SR, Watson C, Princic N, Fox KM.** Cost per treated patient for etanercept, adalimumab, and infliximab across adult indications: a claims analysis. *Adv Ther.* 2012 Mar;29(3):234-48. doi: 10.1007/s12325-012-0007-y. Epub 2012 Mar 9. PMID: 22411424
- Brennan FM, Chantry D, Jackson A, Maini R, Feldmann M.** Inhibitory effect of TNF alpha antibodies on synovial cell interleukin-1 production in rheumatoid arthritis. *Lancet.* 1989 Jul 29; 2(8657):244-7. PMID: 2569055
- Bruening W, Giasson B, Mushynski W, Durham HD.** Activation of stress-activated MAP protein kinases up-regulates expression of transgenes driven by the cytomegalovirus immediate/early promoter. *Nucleic Acids Research.* 1998 Jan 15; 26(2): 486-489 , PMID: 9421504

- Butler DM, Maini RN, Feldmann M, Brennan FM.** Modulation of proinflammatory cytokine release in rheumatoid synovial membrane cell cultures. Comparison of monoclonal anti TNF-alpha antibody with the interleukin-1 receptor antagonist. *Eur Cytokine Netw.* 1995 Jul-Dec;6(4):225-30. PMID: 8789287
- Cao S, Zhang X, Edwards JP, Mosser DM.** NF-kappaB1 (p50) homodimers differentially regulate pro- and anti-inflammatory cytokines in macrophages. *J Biol Chem.* 2006 Sep 8;281(36):26041-50. Epub 2006 Jul 11. PMID: 16835236
- Caskey M, Lefebvre F, Filali-Mouhim A, Cameron MJ, Goulet JP, Haddad EK, Breton G, Trumpfheller C, Pollak S, Shimeliovich I, Duque-Alarcon A, Pan L, Nelkenbaum A, Salazar AM, Schlesinger SJ, Steinman RM, Sékaly RP.** Synthetic double-stranded RNA induces innate immune responses similar to a live viral vaccine in humans. *J Exp Med.* 2011 Nov 21;208(12):2357-66. doi: 10.1084/jem.20111171. Epub 2011 Nov 7. PMID: 22065672
- Chabaud M, Fossiez F, Taupin JL, Miossec P.** Enhancing effect of IL-17 on IL-1-induced IL-6 and leukemia inhibitory factor production by rheumatoid arthritis synoviocytes and its regulation by Th2 cytokines. *J Immunol.* 1998 Jul 1;161(1):409-14. PMID: 9647250
- Chames P, Van Regenmortel M, Weiss E, Baty D.** Therapeutic antibodies: successes, limitations and hopes for the future. *British Journal of Pharmacology.* 2009 May; 157(2): 220-233 , PMID: 19459844, DOI: 10.1111/j.1476-5381.2009.00190.x
- Chapman TM, Keating GM.** Basiliximab: a review of its use as induction therapy in renal transplantation. *Drugs.* 2003;63(24):2803-35. Review. PMID: 14664658
- Chen FE, Huang DB, Chen YQ, Ghosh G.** Crystal structure of p50/p65 heterodimer of transcription factor NF-kappaB bound to DNA. *Nature.* 1998 Jan 22;391(6665):410-3. PMID: 9450761
- Counter CM, Hahn WC, Wei W, Caddle SD, Beijersbergen RL, Lansdorp PM, Sedivy JM, Weinberg RA.** Dissociation among in vitro telomerase activity, telomere maintenance, and cellular immortalization. *Proceedings of the National Academy of Sciences of the United States of America.* 1998 Dec 8; 95(25): 14723-14728, PMID: 9843956
- Croom KF, McCormack PL.** Adalimumab: in plaque psoriasis. *Am J Clin Dermatol.* 2009;10(1):43-50. doi: 10.2165/0128071-200910010-00008. Review. PMID: 19170412
- Danner R, Chaudhari SN, Rosenberger J, Surls J, Richie TL, Brumeanu TD, Casares S.** Expression of HLA Class II Molecules in Humanized NOD.Rag1KO.IL2RgcKO Mice Is Critical for Development and Function of Human T and B Cells. *PLoS ONE.* 2011 May 17; 6(5): e19826, PMID: 21611197, DOI: 10.1371/journal.pone.0019826
- Das DS, Wadhwa N, Kunj N, Sarda K, Pradhan BS, Majumdar SS.** Dickkopf homolog 3 (DKK3) plays a crucial role upstream of WNT/ β -CATENIN signaling for Sertoli cell mediated regulation of spermatogenesis. *PLoS One.* 2013 May 7;8(5):e63603. doi:10.1371/journal.pone.0063603. Print 2013. PMID: 23667645
- De Bosscher K, Vanden Berghe W, Vermeulen L, Plaisance S, Boone E, Haegeman G.** Glucocorticoids repress NF-kB-driven genes by disturbing the interaction of p65 with the basal transcription machinery, irrespective of coactivator levels in the cell. *Proceedings of the National Academy of Sciences of the United States of America.* 2000 Apr 11; 97(8): 3919-3924, PMID: 10760263
- DeJong ES, Chang CE, Gilson MK, Marino JP.** Proflavine acts as a Rev inhibitor by targeting the high-affinity Rev binding site of the Rev responsive element of HIV-1. *Biochemistry.* 2003 Jul 8;42(26):8035-46. PMID: 12834355
- Delfino F, Walker WH.** Hormonal regulation of the NF-kappaB signaling pathway. *Mol Cell Endocrinol.* 1999 Nov 25;157(1-2):1-9. Review. PMID: 10619392
- Della Vittoria Scarpatti G, Fusciello C, Perri F, Sabbatino F, Ferrone S, Carlomagno C, Pepe S.** Ipilimumab in the treatment of metastatic melanoma: management of adverse events. *OncoTargets and therapy.* 2014 Feb 19; 7: 203-209, PMID: 24570590, DOI: 10.2147/OTT.S57335
- DiMattia MA, Watts NR, Cheng N, Huang R, Heymann JB, Grimes JM, Wingfield PT, Stuart DI, Steven AC.** The Structure of HIV-1 Rev Filaments Suggests a Bilateral Model for Rev-RRE Assembly. *Structure (London, England : 1993).* 2016 Jun 2; 24(7): 1068-1080, PMID: 27265851, DOI: 10.1016/j.str.2016.04.015
- Dinarello CA, Simon A, van der Meer JW.** Treating inflammation by blocking interleukin-1 in a broad spectrum of diseases. *Nature reviews. Drug discovery.* 2012 Aug; 11(8): 633-652, PMID: 22850787, DOI: 10.1038/nrd3800
- Du R, Zhao H, Yan F, Li H.** IL-17+Foxp3+ T cells: an intermediate differentiation stage between Th17 cells and regulatory T cells. *J Leukoc Biol.* 2014 Jul;96(1):39-48. doi: 10.1189/jlb.1RU0114-010RR. Epub 2014 Apr 17. Review. PMID: 24744433
- Emery P.** Treatment of rheumatoid arthritis. *BMJ : British Medical Journal.* 2006 Jan 21; 332(7534): 152-155, PMID: 16424492, DOI: 10.1136/bmj.332.7534.152
- Esensten JH, Wofsy D, Bluestone JA.** Regulatory T cells as therapeutic targets in rheumatoid arthritis. *Nature reviews. Rheumatology.* 2009 Oct; 5(10): 560-565, PMID: 19798031, DOI: 10.1038/nrrheum.2009.183

- Farahnik B, Beroukhim K, Abrouk M, Nakamura M, Zhu TH, Singh R, Lee K, Bhutani T, Koo J.** Brodalumab for the Treatment of Psoriasis: A Review of Phase III Trials. *Dermatology and Therapy*. 2016 May 25; 6(2): 111-124, PMID: 27221323, DOI: 10.1007/s13555-016-0121-x
- Feldmann M, Brennan FM, Maini RN.** Role of cytokines in rheumatoid arthritis. *Annu Rev Immunol*. 1996;14:397-440. Review. PMID: 8717520
- Fernandes J, Jayaraman B, Frankel A.** The HIV-1 Rev response element: An RNA scaffold that directs the cooperative assembly of a homo-oligomeric ribonucleoprotein complex. *RNA Biology*. 2012 Jan 1; 9(1): 6-11, PMID: 22258145, DOI: 10.4161/rna.9.1.18178
- Fleischmann RM, Schechtman J, Bennett R, Handel ML, Burmester GR, Tesser J, Modafferi D, Poulakos J, Sun G.** Anakinra, a recombinant human interleukin-1 receptor antagonist (r-metHuIL-1ra), in patients with rheumatoid arthritis: A large, international, multicenter, placebo-controlled trial. *Arthritis Rheum*. 2003 Apr;48(4):927-34. PMID: 12687534
- Fossiez F, Djossou O, Chomarat P, Flores-Romo L, Ait-Yahia S, Maat C, Pin JJ, Garrone P, Garcia E, Saeland S, Blanchard D, Gaillard C, Das Mahapatra B, Rouvier E, Golstein P, Banchereau J, Lebecque S.** T cell interleukin-17 induces stromal cells to produce proinflammatory and hematopoietic cytokines. *J Exp Med*. 1996 Jun 1;183(6):2593-603. PMID: 8676080
- Friedman R, Hughes AL.** Molecular evolution of the NF-kappaB signaling system. *Immunogenetics*. 2002 Feb;53(10-11):964-74. Epub 2002 Jan 9. PMID: 11862396
- Furst DE, Breedveld FC, Kalden JR, Smolen JS, Burmester GR, Bijlsma JW, Dougados M, Emery P, Keystone EC, Klareskog L, Mease PJ.** Updated consensus statement on biological agents, specifically tumour necrosis factor {alpha} (TNF{alpha}) blocking agents and interleukin-1 receptor antagonist (IL-1ra), for the treatment of rheumatic diseases, 2005. *Ann Rheum Dis*. 2005 Nov;64 Suppl 4:iv2-14. Review. No abstract available. PMID: 16239380
- Garlanda C, Dinarello CA, Mantovani A.** THE INTERLEUKIN-1 FAMILY: BACK TO THE FUTURE. *Immunity*. 2013 Dec 12; 39(6): 1003-1018, PMID: 24332029, DOI: 10.1016/j.immuni.2013.11.010
- Gossen M, Bujard H.** Tight control of gene expression in mammalian cells by tetracycline-responsive promoters. *Proc Natl Acad Sci U S A*. 1992 Jun 15;89(12):5547-51. PMID: 1319065
- Guzik BW, Levesque L, Prasad S, Bor YC, Black BE, Paschal BM, Rekosh D, Hammarskjöld ML.** NXT1 (p15) is a crucial cellular cofactor in TAP-dependent export of intron-containing RNA in mammalian cells. *Mol Cell Biol*. 2001 Apr;21(7):2545-54. PMID: 11259602
- Haraoui B, Bykerk V.** Etanercept in the treatment of rheumatoid arthritis. *Therapeutics and Clinical Risk Management*. 2007 Mar; 3(1): 99-105, PMID: 18360618
- Harris LJ, Skaletsky E, McPherson A.** Crystallographic structure of an intact IgG1 monoclonal antibody. *J Mol Biol*. 1998 Feb 6;275(5):861-72. PMID: 9480774
- Haworth C, Brennan FM, Chantry D, Turner M, Maini RN, Feldmann M.** Expression of granulocyte-macrophage colony-stimulating factor in rheumatoid arthritis: regulation by tumor necrosis factor-alpha. *Eur J Immunol*. 1991 Oct; 21(10):2575-9. PMID: 1915559
- Hayden MS, Ghosh S.** Signaling to NF-kappaB. *Genes Dev*. 2004 Sep 15;18(18):2195-224. Review. PMID: 15371334
- Hayden MS, West AP, Ghosh S.** NF-kappaB and the immune response. *Oncogene*. 2006. Oct 30;25(51):6758-80. Review. PMID: 17072327
- Hellweg CE, Arenz A, Bogner S, Schmitz C, Baumstark-Khan C.** Activation of nuclear factor kappa B by different agents: influence of culture conditions in a cell-based assay. *Ann N Y Acad Sci*. 2006 Dec;1091:191-204. PMID: 17341614
- Henderson B, Pettipher ER.** Arthritogenic actions of recombinant IL-1 and tumour necrosis factor alpha in the rabbit: evidence for synergistic interactions between cytokines in vivo. *Clin Exp Immunol*. 1989 Feb;75(2):306-10. PMID: 2784740
- Hirose J, Tanaka S.** [Animal models for bone and joint disease. CIA, CAIA model]. *Clin Calcium*. 2011 Feb;21(2):253-9. doi: CliCa1102253259. Review. Japanese. PMID: 21289422
- Ho SC, Bardor M, Feng H, Mariati, Tong YW, Song Z, Yap MG, Yang Y.** IRES-mediated Tricistronic vectors for enhancing generation of high monoclonal antibody expressing CHO cell lines. *J Biotechnol*. 2012 Jan;157(1):130-9. doi: 10.1016/j.jbiotec.2011.09.023. Epub 2011 Oct 17. PMID: 22024589
- Hoffmann A, Levchenko A, Scott ML, Baltimore D.** The IkappaB-NF-kappaB signaling module: temporal control and selective gene activation. *Science*. 2002 Nov 8;298(5596):1241-5. PMID: 12424381
- Horiuchi T, Mitoma H, Harashima SI, Tsukamoto H, Shimoda T.** *Rheumatology (Oxford, England)*. 2010 Mar 1; 49(7): 1215-1228 PMID: 20194223
- Hu S, Liang S, Guo H, Zhang D, Li H, Wang X, Yang W, Qian W, Hou S, Wang H, Guo Y, Lou Z.** Comparison of the Inhibition Mechanisms of Adalimumab and Infliximab in Treating Tumor Necrosis Factor α -Associated Diseases from a Molecular View. *The Journal of Biological Chemistry*. 2013 Aug 13; 288(38): 27059-27067, PMID: 23943614, DOI: 10.1074/jbc.M113.491530

- Huxford T, Mishler D, Phelps CB, Huang DB, Sengchanthalangsy LL, Reeves R, Hughes CA, Komives EA, Ghosh G.** Solvent exposed non-contacting amino acids play a critical role in NF-kappaB/IkappaBalpha complex formation. *J Mol Biol.* 2002 Dec 6;324(4):587-97. PMID: 12460563
- Jacobs MD, Harrison SC.** Structure of an IkappaBalpha/NF-kappaB complex. *Cell.* 1998 Dec 11;95(6):749-58. PMID: 9865693
- Janda A, Bowen A, Greenspan NS, Casadevall A.** Ig Constant Region Effects on Variable Region Structure and Function. *Frontiers in Microbiology.* 2016 Feb 4; 7: 22. PMID: 26870003, DOI: 10.3389/fmicb.2016.00022
- Jenneck C, Novak N.** The safety and efficacy of alefacept in the treatment of chronic plaque psoriasis. *Therapeutics and Clinical Risk Management.* 2007 Jun; 3(3): 411-420, PMID: 18488075
- Keating GM.** Abatacept: a review of its use in the management of rheumatoid arthritis. *Drugs.* 2013 Jul;73(10):1095-119. doi: 10.1007/s40265-013-0080-9. Review. PMID: 23794171
- Keffer J, Probert L, Cazlaris H, Georgopoulos S, Kaslaris E, Kioussis D, Kollias G.** Transgenic mice expressing human tumour necrosis factor: a predictive genetic model of arthritis. *EMBO J.* 1991 Dec;10(13):4025-31. PMID:1721867
- Kendall SD, Linardic CM, Adam SJ, Counter CM.** A network of genetic events sufficient to convert normal human cells to a tumorigenic state. *Cancer Res.* 2005 Nov 1;65(21):9824-8. PMID: 16267004
- Kim JH, Jin HM, Kim K, Song I, Youn BU, Matsuo K, Kim N.** The mechanism of osteoclast differentiation induced by IL-1. *J Immunol.* 2009 Aug 1;183(3):1862-70. doi: 10.4049/jimmunol.0803007. Epub 2009 Jul 8. PMID: 19587010
- Kim SM, Lee KN, Lee SJ, Ko YJ, Lee HS, Kweon CH, Kim HS, Park JH.** Multiple shRNAs driven by U6 and CMV promoter enhances efficiency of antiviral effects against foot-and-mouth disease virus. *Antiviral Res.* 2010 Sep;87(3):307-17. doi: 10.1016/j.antiviral.2010.06.004. Epub 2010 Jun 16. PMID: 20561543
- Kirk SR, Luedtke NW, Tor Y.** Neomycin-Acridine Conjugate: A Potent Inhibitor of Rev-RRE Binding. *J Am Chem Soc.* 2000;122(5):980-981
- Kohno T, Tam LT, Stevens SR, Louie JS.** Binding characteristics of tumor necrosis factor receptor-Fc fusion proteins vs anti-tumor necrosis factor mAbs. *J Invest Dermatol Symp Proc.* 2007 May;12(1):5-8. PMID: 17502862
- Kollias G, Kontoyiannis D.** Role of TNF/TNFR in autoimmunity: specific TNF receptor blockade may be advantageous to anti-TNF treatments. *Cytokine Growth Factor Rev.* 2002 Aug-Oct;13(4-5):315-21. Review. PMID: 12220546
- Komar AA, Hatzoglou M.** Cellular IRES-mediated translation: The war of ITAFs in pathophysiological states. *Cell Cycle.* 2011 Jan 15; 10(2): 229-240 , PMID: 21220943, DOI: 10.4161/cc.10.2.14472
- Krogh A, Larsson B, von Heijne G, Sonnhammer EL.** Predicting transmembrane protein topology with a hidden Markov model: application to complete genomes. *J Mol Biol.* 2001 Jan 19;305(3):567-80. PMID: 11152613
- Kroot EJ, Huisman AM, Van Zeben J, Wouters JM, Van Paassen HC.** Oral pulsed dexamethasone therapy in early rheumatoid arthritis: a pilot study. *Ann N Y Acad Sci.* 2006 Jun;1069:300-6. PMID: 16855157
- Lam D, Harris D, Qin Z.** Inflammatory mediator profiling reveals immune properties of chemotactic gradients and macrophage mediator production inhibition during thioglycollate elicited peritoneal inflammation. *Mediators Inflamm.* 2013;2013:931562. doi: 10.1155/2013/931562. Epub 2013 Mar 31. PMID: 23606798
- Lancet and collaborators.** GBD 2013 Mortality and Causes of Death Collaborators. Global, regional, and national age-sex specific all-cause and cause-specific mortality for 240 causes of death, 1990-2013: a systematic analysis for the Global Burden of Disease Study 2013. 2015 Jan 10;385(9963):117-71. doi: 10.1016/S0140-6736(14)61682-2. Epub 2014 Dec 18. PMID: 25530442
- Lang I, Füllsack S, Wyzgol A, Fick A, Trebing J, Arana JA, Schäfer V, Weisenberger D, Wajant H.** Binding Studies of TNF Receptor Superfamily (TNFRSF) Receptors on Intact Cells. *J Biol Chem.* 2016 Mar 4;291(10):5022-37. doi:10.1074/jbc.M115.683946. Epub 2015 Dec 31. PMID: 26721880
- Lee LF, Xu B, Michie SA, Beilhack GF, Warganich T, Turley S, McDevitt HO.** The role of TNF-alpha in the pathogenesis of type 1 diabetes in the nonobese diabetic mouse: analysis of dendritic cell maturation. *Proc Natl Acad Sci U S A.* 2005 Nov 1;102(44):15995-6000. Epub 2005 Oct 24. PMID: 16247001
- Leipe J, Grunke M, Dechant C, Reindl C, Kerzendorf U, Schulze-Koops H, Skapenko A.** Role of Th17 cells in human autoimmune arthritis. *Arthritis Rheum.* 2010 Oct;62(10):2876-85. doi: 10.1002/art.27622. PMID: 20583102
- Li X, Zhao X, Fang Y, Jiang X, Duong T, Fan C, Huang CC, Kain SR.** Generation of destabilized green fluorescent protein as a transcription reporter. *J Biol Chem.* 1998 Dec 25;273(52):34970-5. PMID: 9857028
- Liu JK.** The history of monoclonal antibody development – Progress, remaining challenges and future innovations. *Annals of Medicine and Surgery.* 2014 Sep 11; 3(4): 113-116, PMID: 25568796, DOI: 10.1016/j.amsu.2014.09.001
- Liu Y, Zhao H.** A computational approach for ordering signal transduction pathway components

from genomics and proteomics Data.BMC Bioinformatics. 2004 Oct 25; 5: 158, PMID: 15504238, DOI: 10.1186/1471-2105-5-158

Long M, Park SG, Strickland I, Hayden MS, Ghosh S. Nuclear factor-kappaB modulates regulatory T cell development by directly regulating expression of Foxp3 transcription factor. *Immunity*. 2009 Dec 18;31(6):921-31. doi: 10.1016/j.immuni.2009.09.022. PMID: 20064449

Magdolen U, Schmitt M, Hildebrandt B, Diehl P, Schauwecker J, Saldamli B, Burgkart R, Tübel J, Gradinger R, Royer-Pokora B. Spontaneous in vitro transformation of primary human osteoblast-like cells. *Cancer Genomics Proteomics*. 2010 Mar-Apr;7(2):61-6. PMID: 20335519

Mahon MJ. Vectors bicistronically linking a gene of interest to the SV40 large T antigen in combination with the SV40 origin of replication enhance transient protein expression and luciferase reporter activity. *BioTechniques*. 2011 Aug; 51(2): 119-128 , PMID: 21806556, DOI: 10.2144/000113720

Maitra A, Arking DE, Shivapurkar N, Ikeda M, Stastny V, Kassaei K, Sui G, Cutler DJ, Liu Y, Brimble SN, Noaksson K, Hyllner J, Schulz TC, Zeng X, Freed WJ, Crook J, Abraham S, Colman A, Sartipy P, Matsui S, Carpenter M, Gazdar AF, et al. Genomic alterations in cultured human embryonic stem cells. *Nat Genet*. 2005. Oct;37(10):1099-103. Epub 2005 Sep 4. PMID: 16142235

Margaret E. Ackerman, Falk Nimmerjahn. Reichert JM. Antibody Fc: Linking Adaptive and Innate Immunity. *mAbs*. 2014 Mar 21; 6(3): 619-621 , PMID: 0, DOI: 10.4161/mabs.28617

Maxwell LJ, Zochling J, Boonen A, Singh JA, Veras MM, Tanjong Ghogomu E, Benkhalti Jandu M, Tugwell P, Wells GA. TNF-alpha inhibitors for ankylosing spondylitis. *Cochrane Database Syst Rev*. 2015 Apr 18;(4):CD005468. doi:10.1002/14651858.CD005468.pub2. Review. PMID: 25887212

McInnes IB, al-Mughales J, Field M, Leung BP, Huang FP, Dixon R, Sturrock RD, Wilkinson PC, Liew FY. The role of interleukin-15 in T-cell migration and activation in rheumatoid arthritis. *Nat Med*. 1996 Feb;2(2):175-82. PMID: 8574962

McInnes IB, Schett G. The pathogenesis of rheumatoid arthritis. *N Engl J Med*. 2011 Dec 8;365(23):2205-19. doi: 10.1056/NEJMra1004965. Review. No abstract available. PMID: 22150039

Mease PJ. Adalimumab in the treatment of arthritis. *Therapeutics and Clinical Risk Management*. 2007 Mar; 3(1): 133-148, PMID: 18360621

Mertens M, Singh JA. Anakinra for rheumatoid arthritis. *Cochrane Database Syst Rev*. 2009 Jan 21;(1):CD005121. doi: 10.1002/14651858.CD005121.pub3. Review. PMID: 19160248

Monaco C, Nanchahal J, Taylor P, Feldmann M. Anti-TNF therapy: past, present and future.

International Immunology. 2014 Nov 19; 27(1): 55-62 PMID: 25411043 DOI: 10.1093/intimm/dxu102

Moritz B, Becker PB, Göpfert U. CMV promoter mutants with a reduced propensity to productivity loss in CHO cells. *Scientific Reports*. 2015 Nov 19; 5: 16952, PMID: 26581326, DOI: 10.1038/srep16952

Mullard A. Bracing for the biosimilar wave. *Nat Rev Drug Discov*. 2017 Mar 1;16(3):152-154. doi: 10.1038/nrd.2017.36. Review. PMID: 28248938

Nan J, Du Y, Chen X, Bai Q, Wang Y, Zhang X, Zhu N, Zhang J, Hou J, Wang Q, Yang J. TPCA-1 is a direct dual inhibitor of STAT3 and NF-κB and regresses mutant EGFR-associated human non-small cell lung cancers. *Mol Cancer Ther*. 2014 Mar;13(3):617-29. doi: 10.1158/1535-7163.MCT-13-0464. Epub 2014 Jan 8. PMID: 24401319

Ogata Y, Kukita A, Kukita T, Komine M, Miyahara A, Miyazaki S, Kohashi O. A novel role of IL-15 in the development of osteoclasts: inability to replace its activity with IL-2. *J Immunol*. 1999 Mar 1;162(5):2754-60. PMID: 10072521

Oh H, Ghosh S. NF-κB: roles and regulation in different CD4(+) T-cell subsets. *Immunol Rev*. 2013 Mar;252(1):41-51. doi: 10.1111/imr.12033. Review. PMID: 23405894

O'Shea JM, Perkins ND. Regulation of the RelA (p65) transactivation domain. *Biochem Soc Trans*. 2008 Aug;36(Pt 4):603-8. doi: 10.1042/BST0360603. Review. PMID: 18631125

Overington JP, Al-Lazikani B, Hopkins AL. How many drug targets are there? *Nat Rev Drug Discov*. 2006 Dec;5(12):993-6. Review. PMID: 17139284

Pescovitz MD. Rituximab, an anti-cd20 monoclonal antibody: history and mechanism of action. *Am J Transplant*. 2006 May;6(5 Pt 1):859-66. Review. PMID: 16611321

Plaksin D, Baeuerle PA, Eisenbach L. KBF1 (p50 NF-kappa B homodimer) acts as a repressor of H-2Kb gene expression in metastatic tumor cells. *J Exp Med*. 1993 Jun 1;177(6):1651-62. PMID: 8496683

Podolin PL, Callahan JF, Bolognese BJ, Li YH, Carlson K, Davis TG, Mellor GW, Evans C, Roshak AK. Attenuation of murine collagen-induced arthritis by a novel, potent, selective small molecule inhibitor of IkappaB Kinase 2, TPCA-1(2-[(aminocarbonyl)amino]-5-(4-fluorophenyl)-3-thiophenecarboxamide), occurs via reduction of proinflammatory cytokines and antigen-induced T cell Proliferation. *J Pharmacol Exp Ther*. 2005 Jan;312(1):373-81. Epub 2004 Aug 17. PMID: 15316093

Qiu D, Zhao G, Aoki Y, Shi L, Uyei A, Nazarian S, Ng JC, Kao PN. Immunosuppressant PG490 (triptolide) inhibits T-cell interleukin-2 expression at the level of purine-box/nuclear factor of activated T-cells and NF-kappaB transcriptional activation. *J Biol Chem*. 1999 May 7;274(19):13443-50. PMID: 10224109

- Reddy Chichili VP, Kumar V, Sivaraman J.** Linkers in the structural biology of protein-protein interactions. *Protein Sci.* 2013 Feb;22(2):153-67. doi: 10.1002/pro.2206. Epub 2013 Jan 8. Review. PMID: 23225024
- Roca FJ, Mulero I, López-Muñoz A, Sepulcre MP, Renshaw SA, Meseguer J, Mulero V.** Evolution of the inflammatory response in vertebrates: fish TNF- α is a powerful activator of endothelial cells but hardly activates phagocytes. *J Immunol.* 2008 Oct 1;181(7):5071-81. PMID: 18802111
- Rooney M, Symons JA, Duff GW.** Interleukin 1 beta in synovial fluid is related to local disease activity in rheumatoid arthritis. *Rheumatol Int.* 1990;10(5):217-9. PMID: 2075374
- Rosman Z, Shoenfeld Y, Zandman-Goddard G.** Biologic therapy for autoimmune diseases: an update. *BMC Medicine.* 2013 Apr 4; 11: 88 , PMID: 23557513, DOI: 10.1186/1741-7015-11-88
- Ruder WC, Lu T, Collins JJ.** Synthetic biology moving into the clinic. *Science.* 2011 Sep 2;333(6047):1248-52. doi: 10.1126/science.1206843. Review. PMID: 21885773
- Sandborn WJ, van Assche G, Reinisch W, Colombel JF, D'Haens G, Wolf DC, Kron M, Tighe MB, Lazar A, Thakkar RB.** Adalimumab induces and maintains clinical remission in patients with moderate-to-severe ulcerative colitis. *Gastroenterology.* 2012 Feb;142(2):257-65.e1-3. doi: 10.1053/j.gastro.2011.10.032. Epub 2011 Nov 4. PMID: 22062358
- Sandborn WJ, van Assche G, Reinisch W, et al.** Adalimumab in the Treatment of Moderate-to-Severe Ulcerative Colitis: ULTRA 2 Trial Results. *Gastroenterology & Hepatology.* 2013 May; 9(5): 317-320, PMID: 23943669
- Sanford M.** Blinatumomab: first global approval. *Drugs.* 2015 Feb;75(3):321-7. doi: 10.1007/s40265-015-0356-3. Review. PMID: 25637301
- Saxena P, Bojar D, Fussenegger M.** Design of Synthetic Promoters for Gene Circuits in Mammalian Cells. *Methods Mol Biol.* 2017;1651:263-273. doi: 10.1007/978-1-4939-7223-4_19. PMID: 28801913
- Scheinfeld N.** Adalimumab (HUMIRA): a review. *J Drugs Dermatol.* 2003 Aug;2(4):375-7. Review. PMID: 12884458
- Schett G, Teitelbaum SL.** Osteoclasts and arthritis. *J Bone Miner Res.* 2009 Jul;24(7):1142-6. doi: 10.1359/jbmr.090533. Review. No abstract available. PMID: 19557892
- Schiff MH, DiVittorio G, Tesser J, Fleischmann R, Schechtman J, Hartman S, Liu T, Solinger AM.** The safety of anakinra in high-risk patients with active rheumatoid arthritis: six-month observations of patients with comorbid conditions. *Arthritis Rheum.* 2004 Jun;50(6):1752-60. PMID: 15188350
- Schiff MH.** Durability and rapidity of response to anakinra in patients with rheumatoid arthritis. *Drugs.* 2004;64(22):2493-501. Review. PMID: 15516150
- Schimmer BP, Tsao J, Cordova M, Mostafavi S, Morris Q, Scheys JO.** Contributions of Steroidogenic Factor 1 to the Transcription Landscape of Y1 Mouse Adrenocortical Tumor Cells. *Molecular and cellular endocrinology.* 2010 Nov 25; 336(1-2): 85-91 PMID: 21111771, DOI: 10.1016/j.mce.2010.11.024
- Schukur L, Geering B, Fussenegger M.** Human whole-blood culture system for ex vivo characterization of designer-cell function. *Biotechnol Bioeng.* 2016 Mar;113(3):588-97. doi: 10.1002/bit.25828. Epub 2015 Sep 30. PMID: 26348251
- Schukur L, Geering B, Charpin-El Hamri G, Fussenegger M.** Implantable synthetic cytokine converter cells with AND-gate logic treat experimental psoriasis. *Sci Transl Med.* 2015 Dec 16;7(318):318ra201. doi: 10.1126/scitranslmed.aac4964. PMID: 26676608
- Sedlák E, Schaefer JV, Marek J, Gimeson P, Plückthun A.** Advanced analyses of kinetic stabilities of iggs modified by mutations and glycosylation. *Protein Sci.* 2015 Jul;24(7):1100-13. doi: 10.1002/pro.2691. Epub 2015 Jun 11. PMID: 25966898
- Seetin MG, Mathews DH.** RNA structure prediction: an overview of methods. *Methods Mol Biol.* 2012;905:99-122. doi: 10.1007/978-1-61779-949-5_8. Review. PMID: 22736001
- Seipel K, Georgiev O, Schaffner W.** Different activation domains stimulate transcription from remote ('enhancer') and proximal ('promoter') positions. *The EMBO Journal.* 1992 Dec; 11(13): 4961-4968 , PMID: 1464321
- Sethi G, Ahn KS, Pandey MK, Aggarwal BB.** Celastrol, a novel triterpene, potentiates TNF-induced apoptosis and suppresses invasion of tumor cells by inhibiting NF-kappaB-regulated gene products and TAK1-mediated NF-kappaB activation. *Blood.* 2007 Apr 1;109(7):2727-35. Erratum in: *Blood.* 2013 Aug 15;122(7):1327. PMID: 17110449
- Sharma RR, Pollock K, Hubel A, McKenna D.** Mesenchymal stem or stromal cells: a review of clinical applications and manufacturing practices. *Transfusion.* 2014 May;54(5):1418-37. doi: 10.1111/trf.12421. Epub 2013 Oct 16. Review. PMID: 24898458
- Silla T, Hääl I, Geimanen J, Janikson K, Abroi A, Ustav E, Ustav M.** Episomal maintenance of plasmids with hybrid origins in mouse cells. *J Virol.* 2005 Dec;79(24):15277-88. PMID: 16306599
- Singh JA, Christensen R, Wells GA, Suarez-Almazor ME, Buchbinder R, Lopez-Olivo MA, Tanjong Ghogomu E, Tugwell P.** Biologics for rheumatoid arthritis: an overview of Cochrane reviews. *Cochrane Database Syst Rev.* 2009 Oct

7;(4):CD007848. doi: 10.1002/14651858.CD007848.pub2. PMID: 19821440

Soule HD, Maloney TM, Wolman SR, Peterson WD Jr, Brenz R, McGrath CM, Russo J, Pauley RJ, Jones RF, Brooks SC. Isolation and characterization of a spontaneously immortalized human breast epithelial cell line, MCF-10. *Cancer Res.* 1990 Sep 15;50(18):6075-86. PMID: 1975513

Suhasini M, Reddy TR. Cellular proteins and HIV-1 Rev function. *Curr HIV Res.* 2009 Jan;7(1):91-100. Review. PMID: 19149558

Takahashi K, Sawasaki Y, Hata J, Mukai K, Goto T. Spontaneous transformation and immortalization of human endothelial cells. *In Vitro Cell Dev Biol.* 1990 Mar;26(3Pt 1):265-74. PMID: 1690702

Tan SY, Grimes S. Paul Ehrlich (1854-1915): man with the magic bullet. *Singapore Med J.* 2010 Nov;51(11):842-3. No abstract available. PMID:21140107

Tetta C, Camussi G, Modena V, Di Vittorio C, Baglioni C. Tumour necrosis factor in serum and synovial fluid of patients with active and severe rheumatoid arthritis. *Annals of the Rheumatic Diseases.* 1990 Sep; 49(9): 665-667, PMID: 1700672

Torres M, Casadevall A. The immunoglobulin constant region contributes to affinity and specificity. *Trends Immunol.* 2008 Feb;29(2):91-7. doi:10.1016/j.it.2007.11.004. Epub 2008 Jan 10. Review. PMID: 18191616

van de Loo AA, van den Berg WB. Effects of murine recombinant interleukin 1 on synovial joints in mice: measurement of patellar cartilage metabolism and joint inflammation. *Ann Rheum Dis.* 1990 Apr;49(4):238-45. PMID: 2339905

van der Bruggen T, Nijenhuis S, van Raaij E, Verhoef J, Sweder van Asbeck B. Lipopolysaccharide-Induced Tumor Necrosis Factor Alpha Production by Human Monocytes Involves the Raf-1/MEK1-MEK2/ERK1-ERK2 Pathway. *Infection and Immunity.* 1999 Aug; 67(8): 3824-3829, PMID: 10417144

van Leeuwen MA, Westra J, van Riel PL, Limburg PC, van Rijswijk MH. IgM, IgA, and IgG rheumatoid factors in early rheumatoid arthritis predictive of radiological progression? *Scand J Rheumatol.* 1995;24(3):146-53. PMID: 7777825

Vegas AJ, Veiseh O, Gürtler M, Millman JR, Pagliuca FW, Bader AR, Doloff JC, Li J, Chen M, Olejnik K, Tam HH, Jhunjhunwala S, Langan E, Aresta-Dasilva S, Gandham S, McGarrigle JJ, Bochenek MA, Hollister-Lock J, Oberholzer J, Greiner DL, Weir GC, Melton DA, et al. Long-term glycemic control using polymer-encapsulated human stem cell-derived beta cells in immune-competent mice. *Nat Med.* 2016 Mar;22(3):306-11. doi: 10.1038/nm.4030. Epub 2016 Jan 25. Erratum in: *Nat Med.* 2016 Apr;22(4):446. PMID: 26808346

Vos Theo T Lancet and Collaborators. Global, regional, and national incidence, prevalence, and

years lived with disability for 310 diseases and injuries, 1990–2015: a systematic analysis for the Global Burden of Disease Study 2015. *GBD 2015 Disease and Injury Incidence and Prevalence* (London, England). 2016 Oct 8; 388(10053): 1545-1602, PMID: 27733282, DOI: 10.1016/S0140-6736(16)31678-6

Wajant H, Pfizenmaier K, Scheurich P. Tumor necrosis factor signaling. *Cell Death Differ.* 2003 Jan;10(1):45-65. Review. PMID: 12655295

Wan F, Lenardo MJ. Specification of DNA Binding Activity of NF- κ B Proteins. *Cold Spring Harbor Perspectives in Biology.* 2009 Oct; 1(4): a000067, PMID: 20066093, DOI: 10.1101/cshperspect.a000067

Wang D, Li Y, Liu Y, Shi G. The role of autoreactive T cell in the pathogenesis of rheumatoid arthritis and implications for T cell targeted vaccine therapy. *Minerva Med.* 2015 Jun;106(3):157-67. Review. PMID: 26057192

Watakabe A, Ohtsuka M, Kinoshita M, Takaji M, Isa K, Mizukami H, Ozawa K, Isa T, Yamamori T. Comparative analyses of adeno-associated viral vector serotypes 1, 2, 5, 8 and 9 in marmoset, mouse and macaque cerebral cortex. *Neurosci Res.* 2015 Apr;93:144-57. doi: 10.1016/j.neures.2014.09.002. Epub 2014 Sep 18. PMID: 25240284

Wijbrandts CA, Dijkgraaf MG, Kraan MC, Vinkenoog M, Smeets TJ, Dinant H, Vos K, Lems WF, Wolbink GJ, Sijpkens D, Dijkmans BA, Tak PP. The clinical response to infliximab in rheumatoid arthritis is in part dependent on pretreatment tumour necrosis factor α expression in the synovium. *Annals of the Rheumatic Diseases.* 2007 Nov 29; 67(8): 1139-1144, PMID: 18055470, DOI: 10.1136/ard.2007.080440

Wildner G, Kaufmann U. What causes relapses of autoimmune diseases? The etiological role of autoreactive T cells. *Autoimmun Rev.* 2013 Sep;12(11):1070-5. doi: 10.1016/j.autrev.2013.04.001. Epub 2013 May 16. Review. PMID: 23685277

Wooddell CI, Van Hout CV, Reppen T, Lewis DL, Herweijer H. Long-term RNA interference from optimized siRNA expression constructs in adult mice. *Biochem Biophys Res Commun.* 2005 Aug 19;334(1):117-27. PMID: 15993838

Wu Y, Borde M, Heissmeyer V, Feuerer M, Lapan AD, Stroud JC, Bates DL, Guo L, Han A, Ziegler SF, Mathis D, Benoist C, Chen L, Rao A. FOXP3 controls regulatory T cell function through cooperation with NFAT. *Cell.* 2006 Jul 28;126(2):375-87. PMID: 16873067

Wurster SE, Bida JP, Her YF, Maher LJ III. Characterization of anti-NF- κ B RNA aptamer-binding specificity in vitro and in the yeast three-hybrid system. *Nucleic Acids Research.* 2009 Aug 20; 37(18): 6214-6224, PMID: 19696077, DOI: 10.1093/nar/gkp670

Wurster SE, Maher LJ III. Selection and characterization of anti-NF- κ B p65 RNA aptamers. *RNA*. 2008 Jun; 14(6): 1037-1047, PMID: 18426920, DOI: 10.1261/rna.878908

Yao Z, Painter SL, Fanslow WC, Ulrich D, Macduff BM, Spriggs MK, Armitage RJ. Human IL-17: a novel cytokine derived from T cells. *J Immunol*. 1995 Dec 15;155(12):5483-6. PMID: 7499828

Yao, Tatsuma, Asayama, Yuta

Animal-cell culture media: History, characteristics, and current issues *Reprod Med Biol*. 2017. 16 IS - 2 1447-0578

Yost J, Gudjonsson JE. The role of TNF inhibitors in psoriasis therapy: new implications for associated comorbidities. *F1000 Medicine Reports*. 2009 May 8; 1: 30 , PMID: 20948750, DOI: 10.3410/M1-30

Youn HS, Lee JY, Fitzgerald KA, Young HA, Akira S, Hwang DH. Specific inhibition of MyD88-independent signaling pathways of TLR3 and TLR4 by resveratrol: molecular targets are TBK1 and RIP1 in TRIF complex. *J Immunol*. 2005 Sep 1;175(5):3339-46. PMID: 16116226

Zhang J, Wang X, Zhao Y, Chen B, Suo G, Dai J. Neoplastic transformation of human diploid fibroblasts after long-term serum starvation. *Cancer Lett*. 2006 Nov 8;243(1):101-8. Epub 2006 Feb 20. PMID: 16488534

Zhao PW, Jiang WG, Wang L, Jiang ZY, Shan YX, Jiang YF. Plasma levels of IL-37 and correlation with TNF- α , IL-17A, and disease activity during DMARD treatment of rheumatoid arthritis. *PLoS One*. 2014 May 1;9(5):e95346. doi: 10.1371/journal.pone.0095346. eCollection 2014. PMID: 24788826

Books and Internet

Alberts B, Johnson A, Lewis J, et al. Molecular Biology of the Cell. 4th edition. New York: Garland Science; 2002. The Generation of Antibody Diversity. Available from:
<https://www.ncbi.nlm.nih.gov/books/NBK26860/>

Berg J, Tymoczko J, Stryer L. Stryer Biochemie. 2007. 6. edition. Page 37 and 90.

Marks F, Klingmüller U, Müller-Decker K. Cellular signal processing: an introduction to the molecular mechanism of signal transduction. 2008. Page 227

Mathews D. RNAstructure Web Servers for RNA Secondary Structure Prediction, Mathews group. 2012-2017.

URL: <https://rna.urmc.rochester.edu/RNAstructureWeb/Servers/Predict1/Predict1.html>.

(October. 2017)

Mitchell, Claudia and Russell, David. Universal Cells Inc. 2012-2017.

URL: <http://www.universalcells.com/>

(October. 2017)

Murphy K, Travers P, Walport M. Janeway Immunologie. 2009. 7. edition. Page 40.

Pahl, Andreas. Heidelberg Pharma

On-Demand Webinar: Human TNF α Transgenic Mouse Model of Spontaneous Arthritis

URL: <https://www.taconic.com/resources/webinars/human-tnf-alpha-transgenic-mouse-model-of-spontaneous-arthritis.html>

(November 2017)

Skerra, Arne. Lecture therapeutic proteins SS2012.

URL: <https://www.biologische-chemie.userweb.mwn.de/Lehre/Lehre.html>

Toleikis, Philip. Sernova Corp. 2001-2017.

URL: <http://www.sernova.com/>

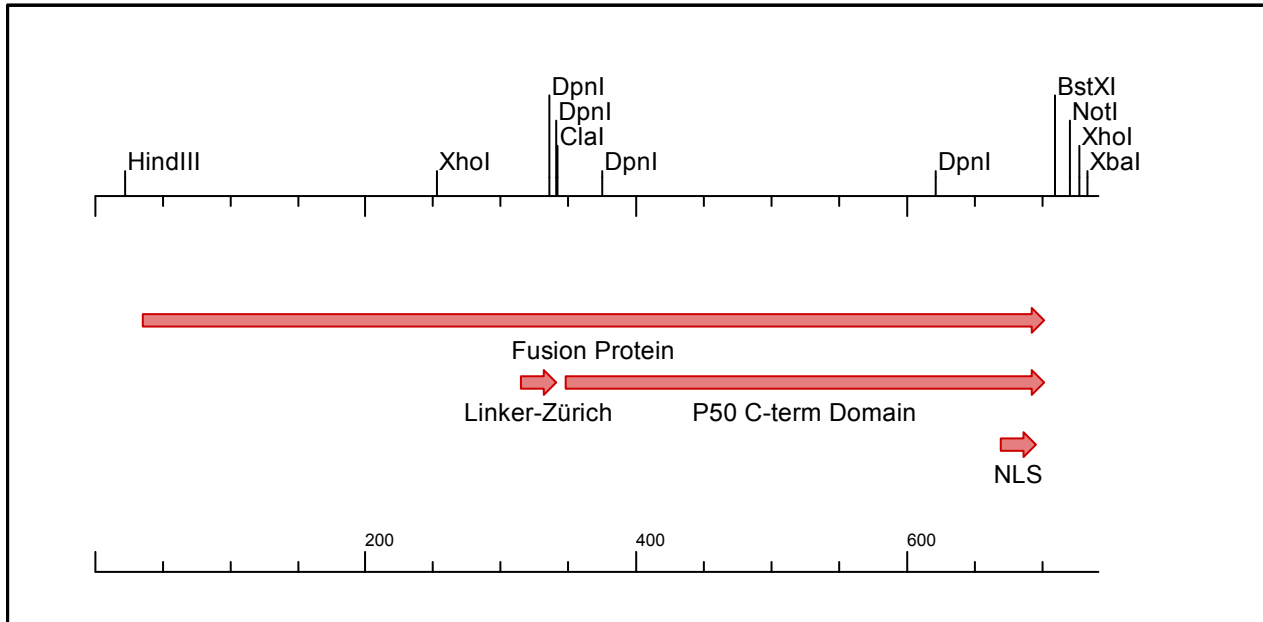
(October 2017)

Tony H, Feuchtenberger M, Gromnica-Ihle E, Kern P, Kleinert S, Kneitz C, Krüger K, Nigg A, Scharbatke C, Schulze-Koops H, Semmler M, Störk S. Langzeittherapie der rheumatoiden Arthritis. 2010. 1. edition. Page 36

VI. DNA sequences

DNA sequences of synthetic proteins or non-coding RNAs of design 1 and 2

Design 1



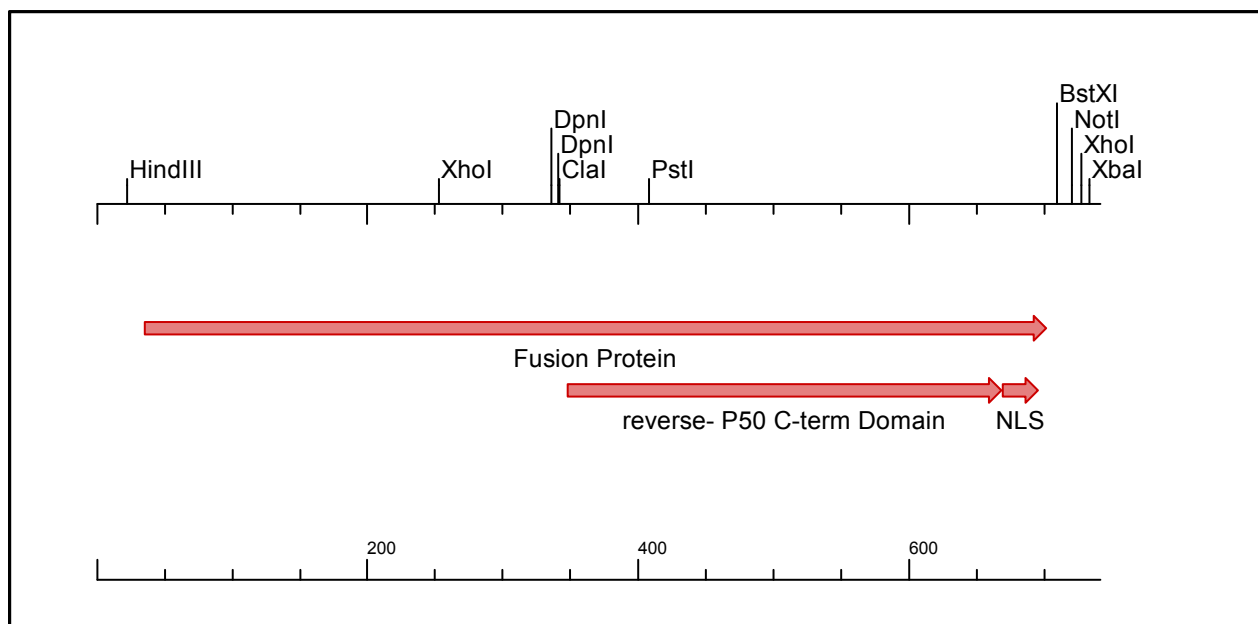
Molecule: pDH30-CMV-Gal4BD-c-term-p50, 741 bps DNA

Start	End	Name
36	701	Fusion Protein
315	341	Linker-Zrich
348	701	P50 C-term Domain
669	695	NLS

```

1  ggcaatggta ctgttggttaa agaagcttgc ccaccatgaa actgctgtct
51  tctatcgaac aagcatgcga tatttgccga cttaaaaaagc tcaagtgtct
101 caaagaaaaa ccgaagtgcg ccaagtgtct gaagaacaac tgggagtgtc
151 gctactctcc caaaaccaa aggtctccgc tgactagggc acatctgaca
201 gaagtggaat caaggctaga aagactggaa cagctatttc tactgatttt
251 tcctcgagaa gaccttgaca tgattttgaa aatggattct ttacaggata
301 taaaagcatt gttaggcacc ccggcggcgg cgattgatcc gatcgatgcg
351 agcaacctga aaattgtgcg catggatcgc accgcgggct gcgtgaccgg
401 cggcgaagaa atttatctgc tgtgcgataa agtgcagaaa gatgatattc
451 agattcgctt ttatgaagaa gaagaaaacg gcggcgtgtg ggaaggcttt
501 ggcgatttta gcccgaccga tgtgcatcgc cagtttgcca ttgtgtttta
551 aaccccgaaa tataaagata ttaacattac caaacccggc agcgtgtttg
601 tgcagctgcg ccgcaaaagc gatctggaaa ccagcgaacc gaaaccgttt
651 ctgtattatc cggaaattgg taccoccaa agagaagcgca aggtgtgatg
701 aaatctatcc agcacagtgg cggccgctcg agtctagagg g

```



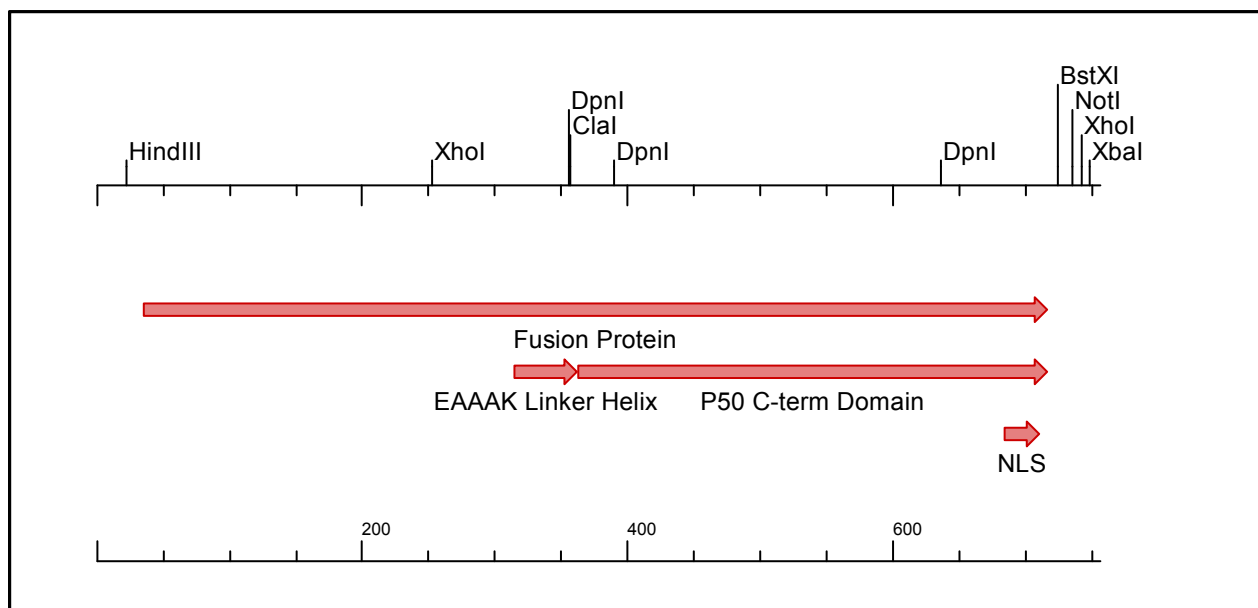
Molecule: pDH31-CMV-Gal4BD-reverse-c-term-p50, 741 bps DNA

Start	End	Name
36	701	Fusion Protein
348	668	reverse- P50 C-term Domain
669	695	NLS

```

1  ggcaatggta ctggttggtaa agaagcttgc ccaccatgaa actgctgtct
51  tctatcgaa aagcatgcga tatttgccga cttaaaaagc tcaagtgtct
101 caaagaaaaa ccgaagtgcg ccaagtgtct gaagaacaac tgggagtgtc
151 gctactctcc caaaaccaa aggtctccgc tgactagggc acatctgaca
201 gaagtggaat caaggctaga aagactggaa cagctatttc tactgatttt
251 tcctcgagaa gaccttgaca tgattttgaa aatggattct ttacaggata
301 taaaagcatt gttaggcacc ccggcggcgg cgattgatcc gatcgatatt
351 gaaccgtatt atctgtttcc gaaaccggaa agcaccgaac tggatagcaa
401 acgcgcgctg caggtgtttg tgagcgcgcc gaaaaccatt aacattgata
451 aatataaacc gaccaaattt gtgattgcgt ttcagcgcca tgtggatacc
501 ccgagctttg atggctttgg cgaatgggtg ggcggcaacg aagaagaaga
551 atattttcgc attcagattg atgataaaca ggtgaaagat tgctgtgtgt
601 atattgaaga aggcggcacc gtgtgcggcg cgaccgcgca tatgcgcgtg
651 attaaactga acagcgcggg taccctcaag aagaagcgca aggtgtgatg
701 aaatctatcc agcacagtgg cggccgctcg agtctagagg g

```



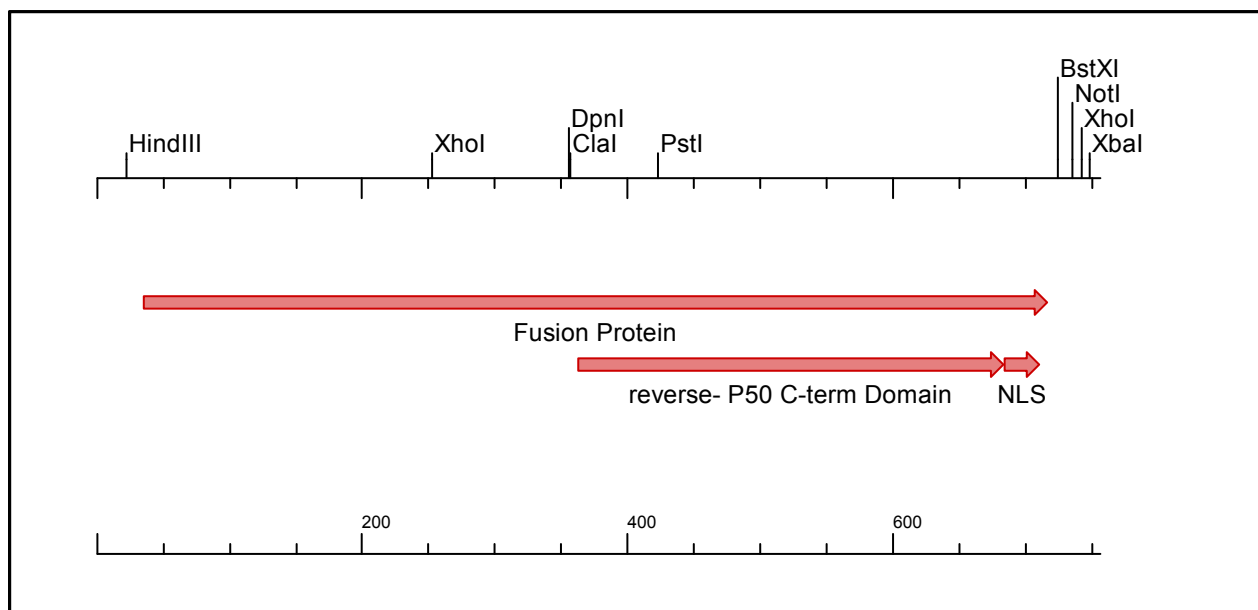
Molecule: pDH32-CMV-Gal4BD-c-term-p50-helixlinker, 756 bps DNA

Start	End	Name
36	716	Fusion Protein
315	362	EAAAK Linker Helix
363	716	P50 C-term Domain
684	710	NLS

```

1  ggcaatggta ctgttggttaa agaagcttgc ccaccatgaa actgctgtct
51  tctatcgaac aagcatgcga tatttgccga cttaaaaaagc tcaagtgtct
101 caaagaaaaa ccgaagtgcg ccaagtgtct gaagaacaac tgggagtgtc
151 gctactctcc caaaaccaa aggtctccgc tgactagggc acatctgaca
201 gaagtggaa caaggctaga aagactggaa cagctatttc tactgatttt
251 tcctcgagaa gaccttgaca tgattttgaa aatggattct ttacaggata
301 taaaagcatt gttagcggaa gcggcggcga aagaagcggc ggcgaaaagc
351 gcggcgatcg atgcgagcaa cctgaaaatt gtgcgcgatg atcgacaccg
401 gggctgcgtg accggcggcg aagaaattta tctgctgtgc gataaaagtgc
451 agaaagatga tattcagatt cgcttttatg aagaagaaga aaacggcggc
501 gtgtgggaag gctttggcga ttttagcccg accgatgtgc atcgccagtt
551 tgcgattgtg tttaaaacc cgaaatataa agatattaac attaccaaac
601 cggcgagcgt gtttgtgcag ctgcgccgca aaagcgatct ggaaaccagc
651 gaaccgaac cgtttctgta ttatccggaa attggtaccc ccaagaagaa
701 gcgcaaggtg tgatgaaatc tatccagcac agtggcgggc gtcgagttct
751 agaggg

```



Molecule: pDH33-CMV-Gal4BD-reverse-c-term-p50-helix-linker, 756 bps DNA

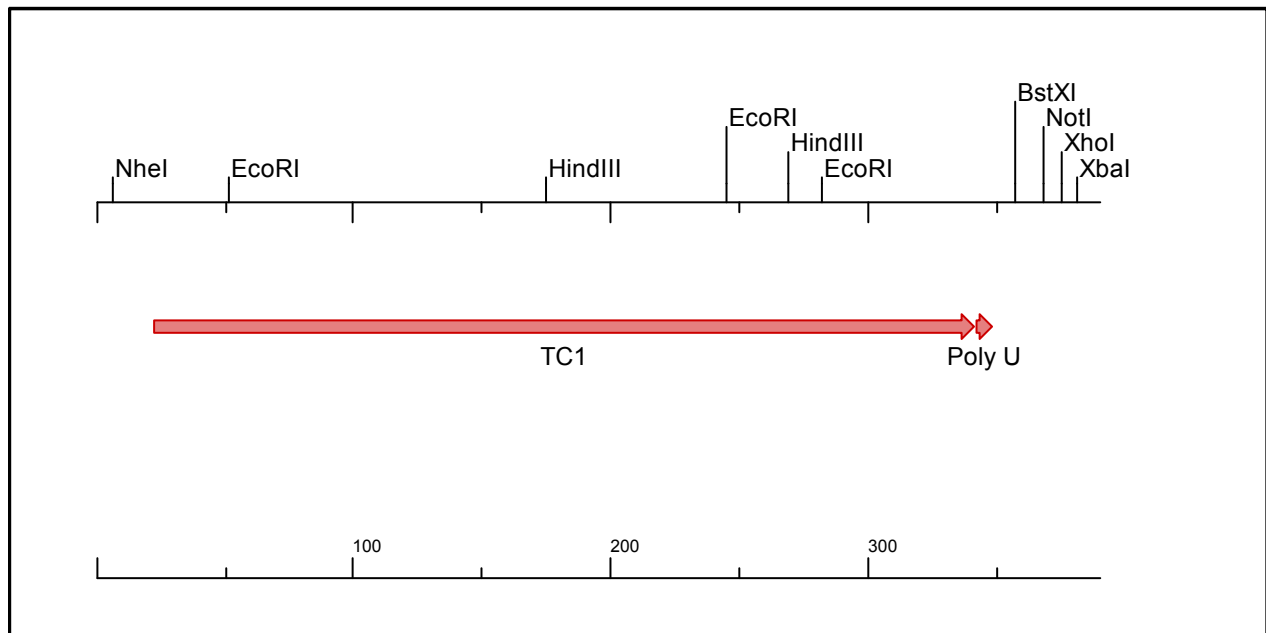
Start	End	Name
36	716	Fusion Protein
363	683	reverse- P50 C-term Domain
684	710	NLS

```

1  ggcaatggta ctgttggttaa agaagcttgc ccaccatgaa actgctgtct
51  tctatcgaac aagcatgcga tatttgccga cttaaaaaagc tcaagtgctc
101 caaagaaaaa ccgaagtgcg ccaagtgtct gaagaacaac tgggagtgtc
151 gctactctcc caaaaccaa aggtctccgc tgactagggc acatctgaca
201 gaagtggaat caaggctaga aagactggaa cagctatttc tactgatttt
251 tcctcgagaa gaccttgaca tgattttgaa aatggattct ttacaggata
301 taaaagcatt gttagcggaa gcggcggcga aagaagcggc ggcgaaagcg
351 gcggcgatcg atattgaacc gtattatctg tttccgaaac cggaaagcac
401 cgaactggat agcaaacgcc gcctgcaggt gtttgtgagc gcgccgaaaa
451 ccattaacat tgataaatat aaaccgacca aatttgtgat tgcgtttcag
501 cgccatgtgg ataccccgag ctttgatggc tttggcgaat ggggtgggcg
551 caacgaagaa gaagaatatt ttcgcattca gattgatgat aaacagggtg
601 aagattgcct gctgtatatt gaagaaggcg gcaccgtgtg cggcgcgacc
651 cgcgatatgc gcgtgattaa actgaacagc gcgggtaccc ccaagaagaa
701 gcgcaagggt tgatgaaatc tatccagcac agtggcggcc gctcgagtct
751 agaggg

```


Design 2



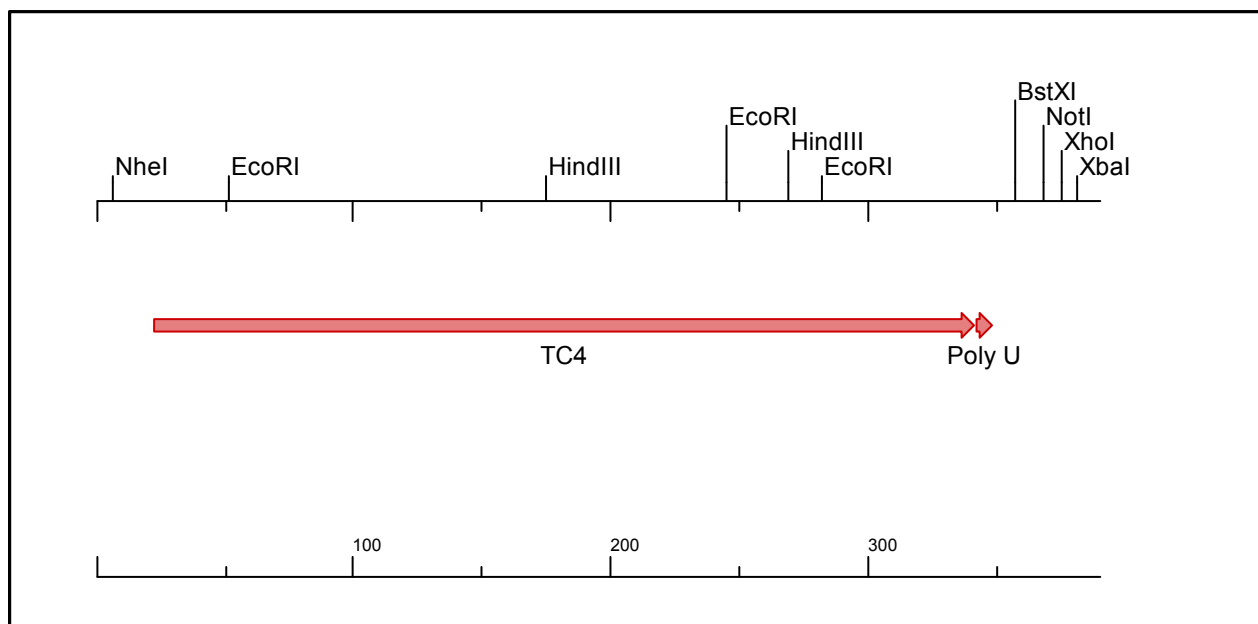
Molecule: pDH7-CMV-TC1, 390 bps DNA

Start	End	Name
23	341	TC1
342	348	Poly U

```

1  ttgacgggcta gcaaacaccg gtgaacgaaa ctctgggagc tgcgattggc
51  agaattccgt tagcaaggcc gcaggacttg catgcttatc ctgcggcgcg
101 ggcgcgtttc ccggtctggg cgcacttcgg tgacggtaca ggccgggtta
151 cgcgcccggc ttaagtgttt ctcgaaagctt acaagaagga cagcacgaat
201 aaaacctgcg taaatccgcc ccatttgtgt aagggtagtg ggtcgaattc
251 cgctcagagt tggcacttaa gcttgctaac ggaattcccc catatccaac
301 ttccaattta atctttcttt ttttaatttc acttatttgc gtttttttga
351 atctatccag cacagtggcg gccgctcgag tctagagggc

```



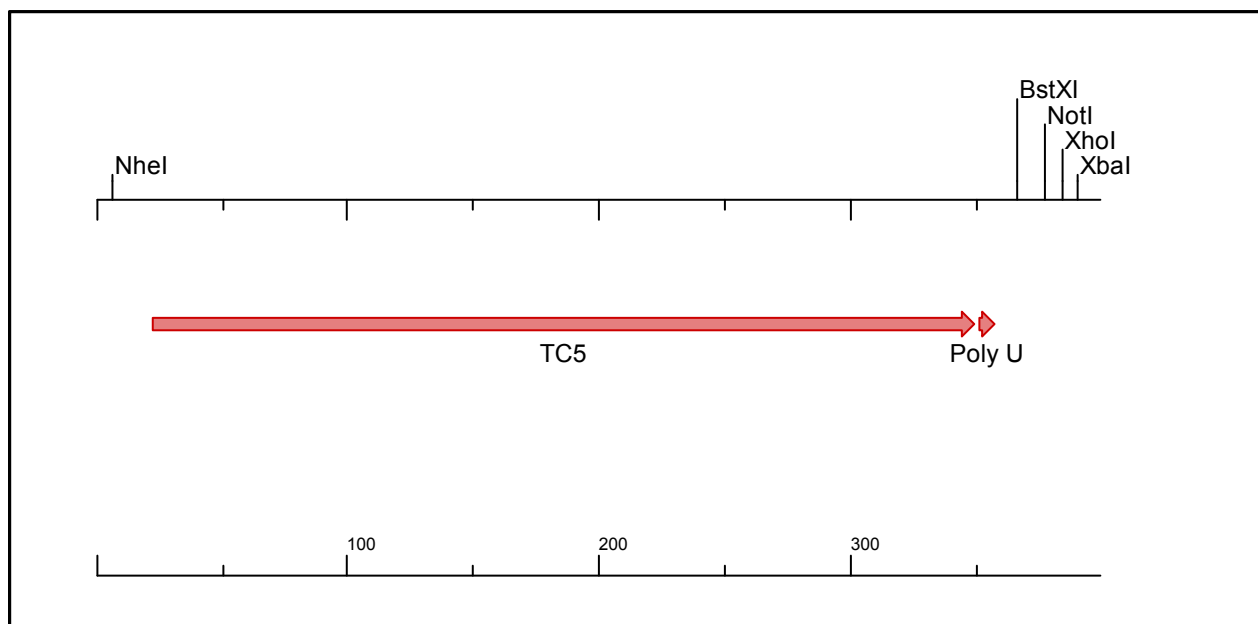
Molecule: pDH7-CMV-TC4, 390 bps DNA

Start	End	Name
23	341	TC4
342	348	Poly U

```

1  ttgacggcta gcaaacaccg gtgaacgaaa ctctgggagc tgcgattggc
51  agaattccgt tagcaaggcc gcaggacttg catgcttata ctgcggcgcg
101 ggcgcgtttc ccggtctggg cgcacttcgg tgacgggtaca ggccgggtta
151 cgcgcgccgc ttaagtgttt ctcgaagctt acaagaagga cagcacgaat
201 aaaacctacg taaaaccgcc ccatttgtgt cagggtagtg ggtcgaattc
251 cgctcagagt tggcacttaa gcttgctaac ggaattcccc catatccaac
301 ttccaattta atctttcttt ttttaatttc acttatttgc gtttttttga
351 atctatccag cacagtggcg gccgctcgag tctagagggc

```



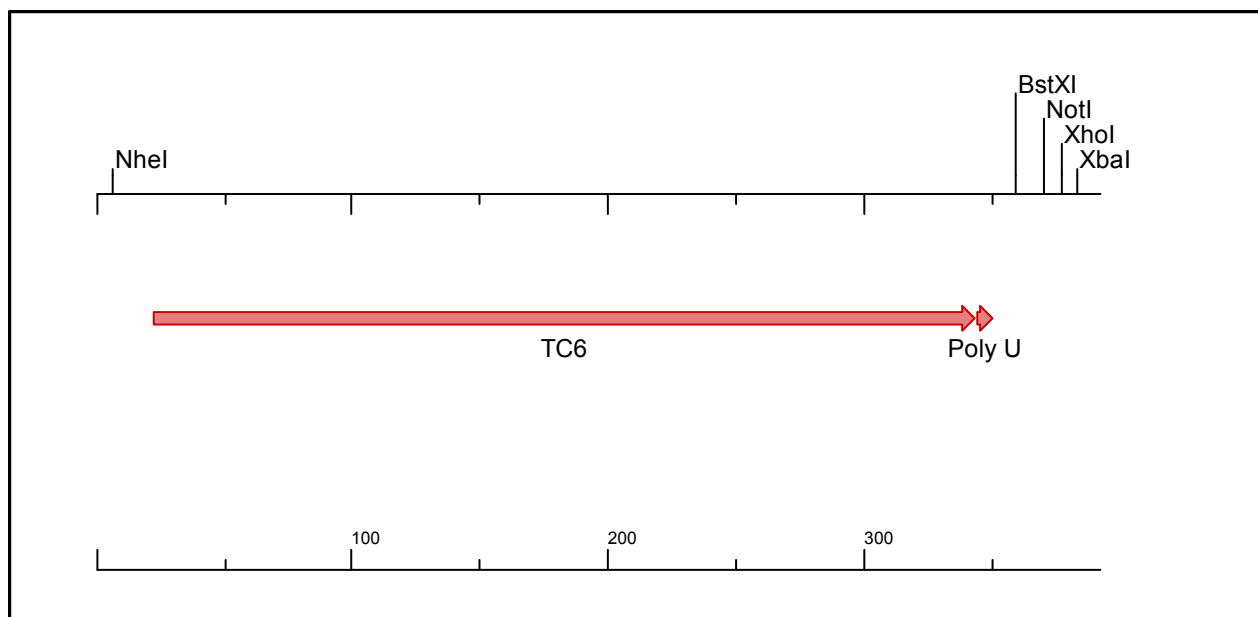
Molecule: pDH7-CMV-TC1, 390 bps DNA

Start	End	Name
23	341	TC1
342	348	Poly U

```

1  ttgacggcta gcaaacaccg gtgaacgaaa ctctgggagc tgcgattggc
51  agaattccgt tagcaaggcc gcaggacttg catgcttatc ctgcggcgcg
101 ggcgcgtttc ccgggagtat atgggcgcac ttcggtgacg gtacaggctc
151 ctgggttacg cgcccgctt aagtgtttct cgaagcttac aagaaggaca
201 gcacgaataa aacctgcgta aatccgcccc atttgtgtaa gggtagtggg
251 tcgaattccg ctcaagattg gcacttaagc ttgctaacgg aattcccca
301 tatccaaact ccaatttaat ctttcttttt taattttcac ttatttgcgt
351 tttttttgaa tctatccagc acagtggcgg ccgctcgagt ctagagggc

```



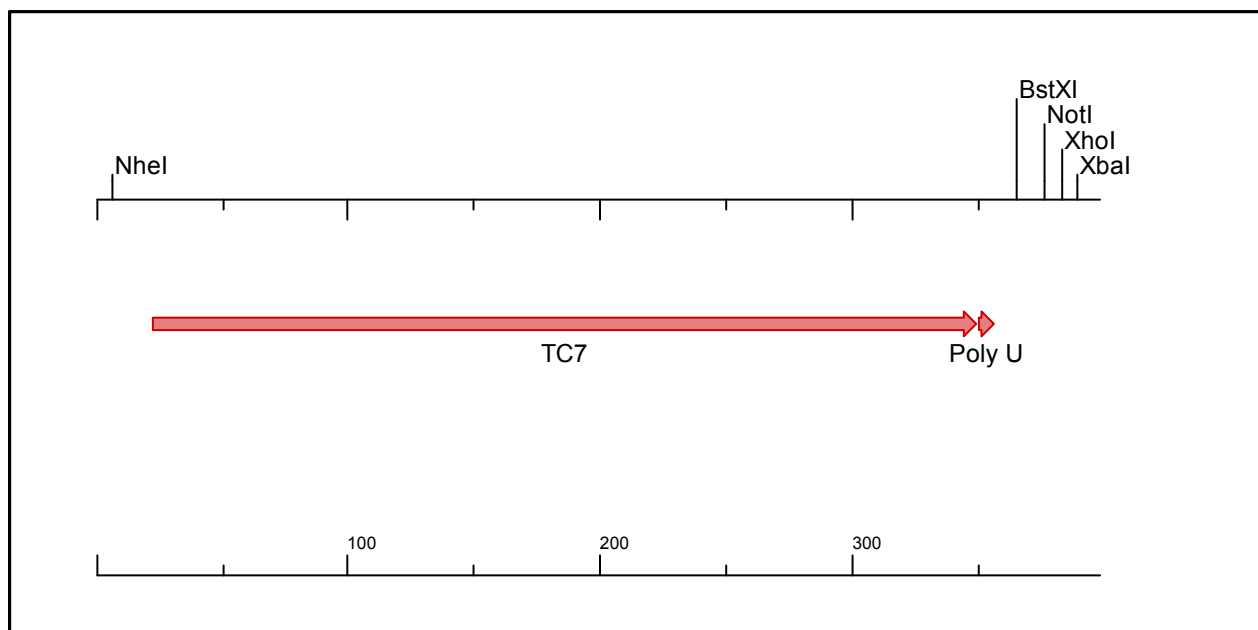
Molecule: pDH7.4-CMV-TC6, 392 bps DNA

Start	End	Name
23	343	TC6
344	350	Poly U

```

1  ttgacggcta gcaaacaccg gtgaacgaaa ctctgggagc tgcgattggc
51  agaattccgt tagcaaggcc gcaggacttg catgcttata ctgcggcgcg
101 ggcgcgtttc ccggtctggg cgcagcgcaa gctgacggta caggccgggt
151 tacgcgcccg ccttaagtgt ttctcgaagc ttacaagaag gacagcacga
201 ataaaacctg cgtaaatacg ccccatattgt gtaagggtag tgggtcgaat
251 tccgctcaga gttggcactt aagcttgcta acggaattcc cccatatcca
301 acttccaatt taatctttct tttttaattt tcacttattt gcgttttttt
351 gaatctatcc agcacagtgg cggccgctcg agtctagagg gc

```



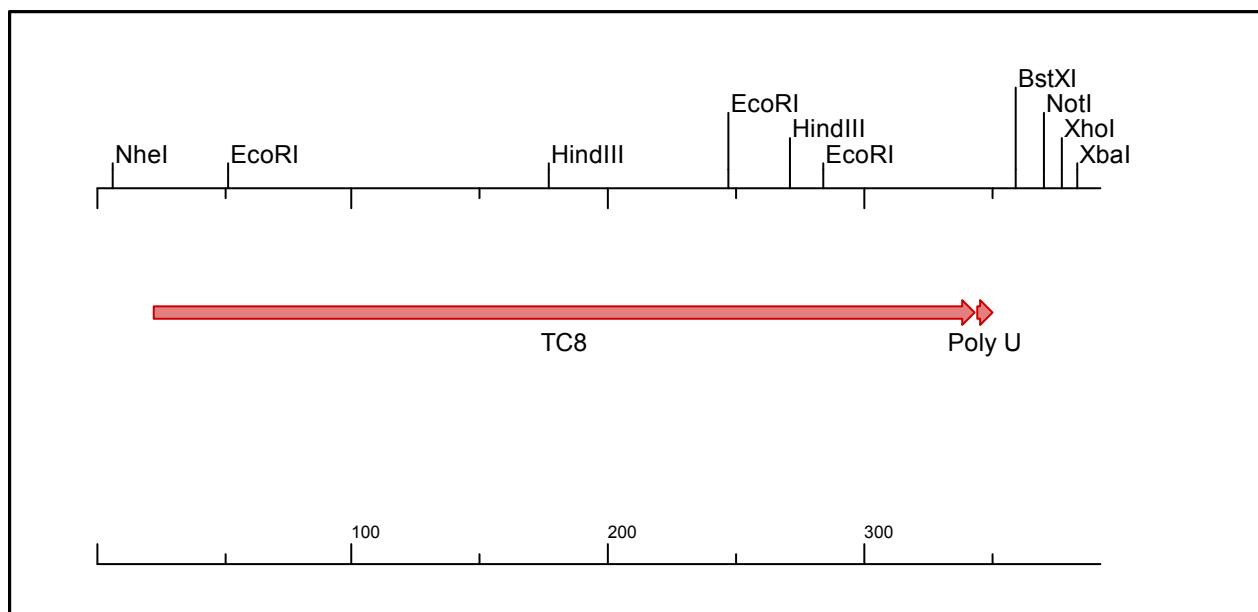
Molecule: pDH7.5-CMV-TC7, 398 bps DNA

Start	End	Name
23	349	TC7
350	356	Poly U

```

1  ttgacggcta gcaaacaccg gtgaacgaaa ctctgggagc tgcgattggc
51  agaattccgt tagcaaggcc gcaggacttg catgcttata ctgcggcgcg
101 ggcgcggttt ccgggagtat atgggcgcac ttcggtgacg gtacaggctc
151 ctgggttacg cgcccgccct aagtgtttct cgaagcttac aagaaggaca
201 gcacgaataa aacctacgta aaaccgcccc atttgtgtca gggtagtggg
251 tcgaattccg ctcagagttg gcacttaagc ttgctaacgg aattcccca
301 tatccaactt ccaatttaat ctttcttttt taattttcac ttatttgcgt
351 ttttttgaat ctatccagca cagtggcggc cgctcgagtc tagagggc

```



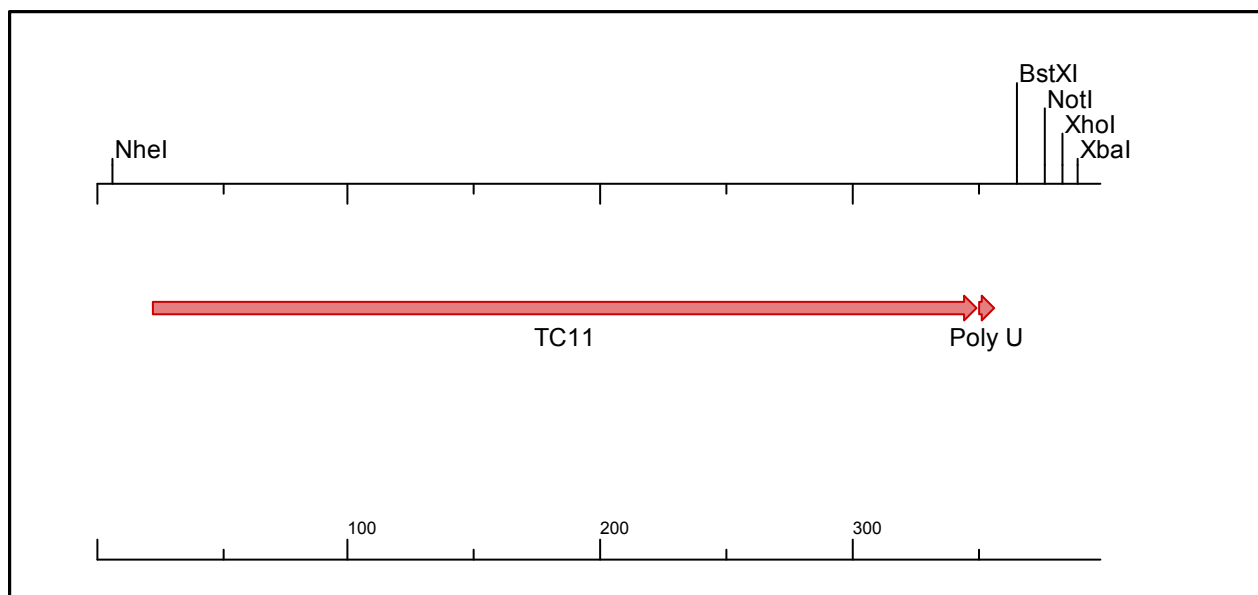
Molecule: pDH7.6-CMV-TC8, 392 bps DNA

Start	End	Name
23	343	TC8
344	350	Poly U

```

1  ttgacggcta gcaaacaccg gtgaacgaaa ctctgggagc tgcgattggc
51  agaattccgt tagcaaggcc gcaggacttg catgcttatc ctgcggcgcg
101 ggcgcgtttc ccggtctggg cgcagcgcaa gctgacggta caggccgggt
151 tacgcgcccg ccttaagtgt ttctcgaagc ttacaagaag gacagcacga
201 ataaaacctt cgtaaaaccg cccatttgt gtcagggtag tgggtcgaat
251 tccgctcaga gttggcactt aagcttgcta acggaattcc cccatatcca
301 acttccaatt taatctttct tttttaattt tcacttattt gcgttttttt
351 gaatctatcc agcacagtgg cggccgctcg agtctagagg gc

```



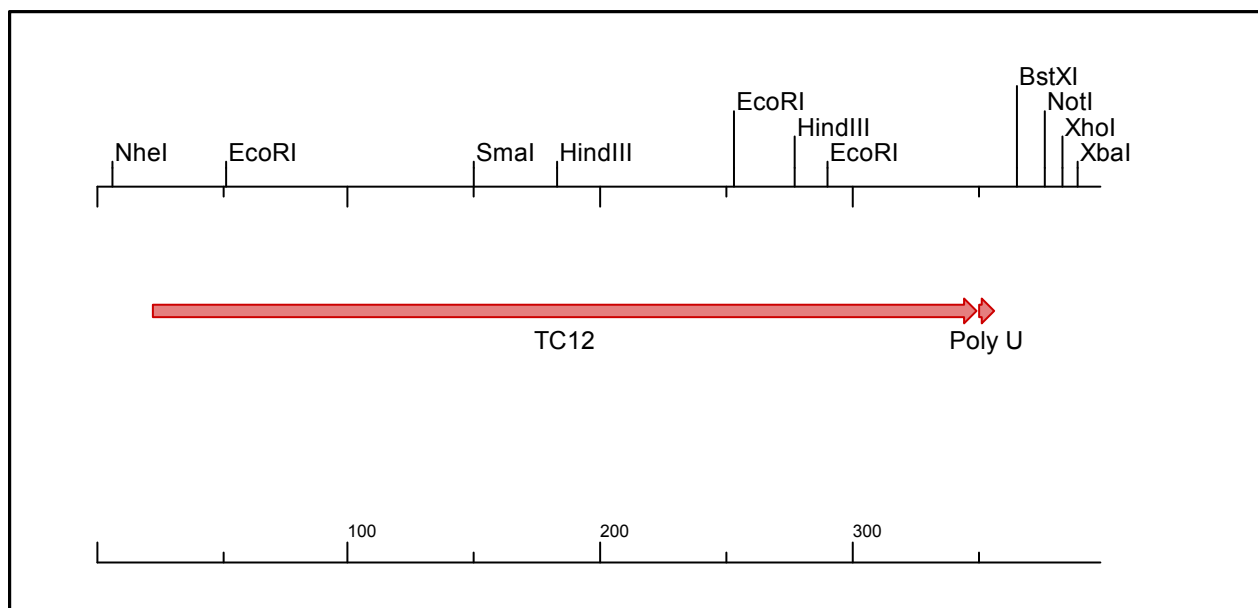
Molecule: pDH7.7-CMV-TC11, 398 bps DNA

Start	End	Name
23	349	TC11
350	356	Poly U

```

1  ttgacggcta gcaaacaccg gtgaacgaaa ctctgggagc tgcgattggc
51  agaattccgt tagcaaggcc gcaggacttg cagggagtat atgggcgcac
101 ttcgggtgacg gtacaggctc cttgcttata ctgcggcgcg ggcgcgtttc
151 ccgggttacg cgcccgccct aagtgtttct cgaagcttac aagaaggaca
201 gcacgaataa aacctgcgta aatccgcccc atttgtgtaa gggtagtggg
251 tcgaattccg ctcagagttg gcacttaagc ttgctaacgg aattcccca
301 tatccaactt ccaatttaat ctttcttttt taattttcac ttatttgcgt
351 ttttttgaat ctatccagca cagtggcggc cgctcgagtc tagagggc

```



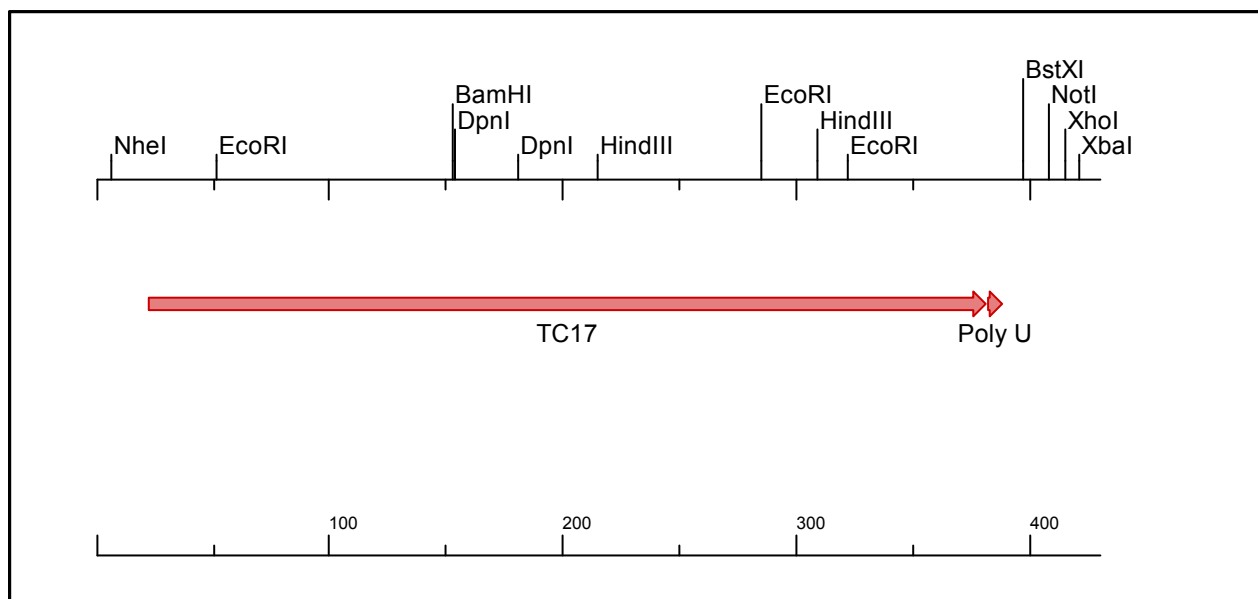
Molecule: pDH7.8-CMV-TC12, 398 bps DNA

Start	End	Name
23	349	TC12
350	356	Poly U

```

1  ttgacggcta gcaaacaccg gtgaacgaaa ctctgggagc tgcgattggc
51  agaattccgt tagcaaggcc gcaggacttg cagggagtat atgggcgcac
101 ttcggtgacg gtacaggctc cttgcttata ctgcggcgcg ggcgcgtttc
151 ccgggttacg cgcccgccct aagtgtttct cgaagcttac aagaaggaca
201 gcacgaataa aacctacgta aaaccgcccc atttgtgtca gggtagtggg
251 tcgaattccg ctcaagattg gcacttaagc ttgctaacgg aattcccca
301 tatccaactt ccaatttaat ctttcttttt taattttcac ttatttgcgt
351 ttttttgaat ctatccagca cagtggcggc cgctcgagtc tagagggc

```

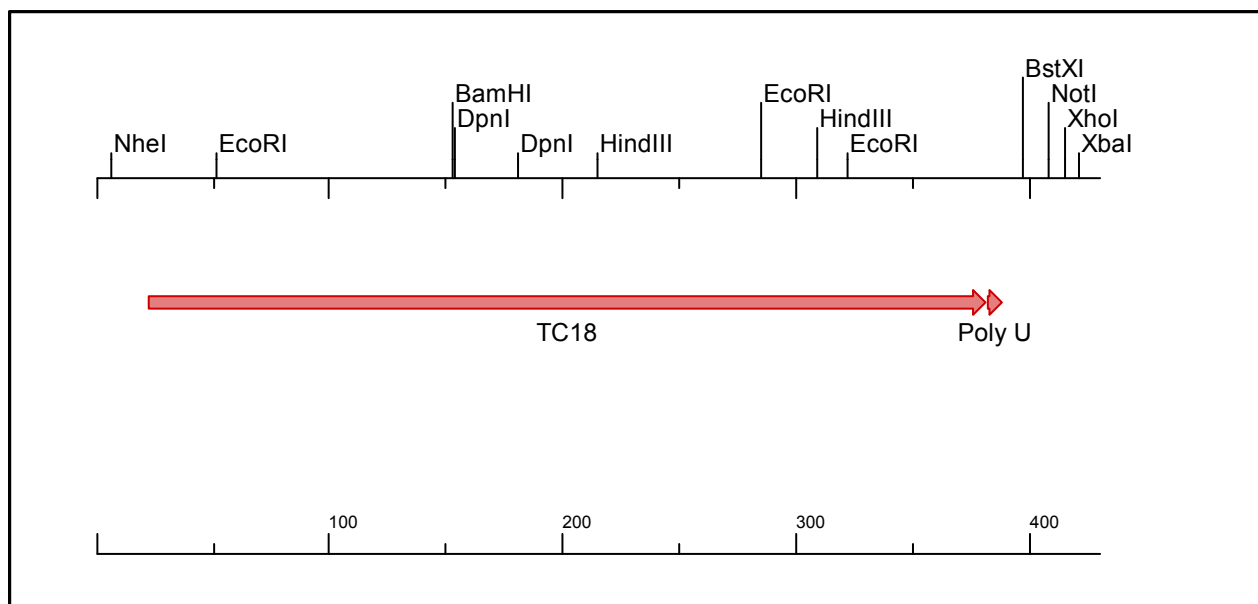
Molecule: pDH7.9-CMV-TC17, 430 bps DNA

Start	End	Name
23	381	TC17
382	388	Poly U

```

1  ttgacggcta gcaaacaccg gtgaacgaaa ctctgggagc tgcgattggc
51  agaattccgt tagcaaggcc gcaggacttg cagggagtat atgggcgcac
101 ttcggtgacg gtacaggctc cttgcttata ctgcggcgcg ggcgcgtttc
151 ccggatcctg aaactgtttt aagggttgcc gatcgggtta cgcgcccgcc
201 ttaagtgttt ctggaagctt acaagaagga cagcacgaat aaaacctgcg
251 taaatccgcc ccatttgtgt aagggttagtg ggtcgaattc cgctcagagt
301 tggcaattaa gcttgctaac ggaattcccc catatccaac ttccaattta
351 atctttcttt tttaattttc acttatttgc gtttttttga atctatccag
401 cacagtggcg gccgctcgag tctagagggc

```



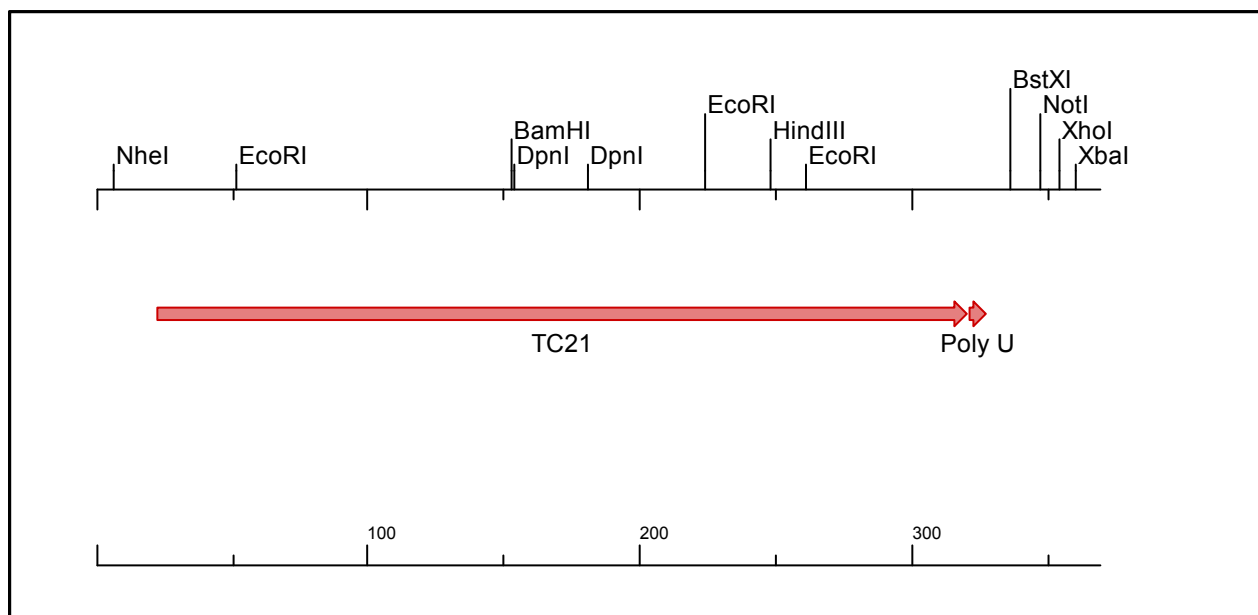
Molecule: pDH7.10-CMV-TC18, 430 bps DNA

Start	End	Name
23	381	TC18
382	388	Poly U

```

1  ttgacggcta gcaaacaccg gtgaacgaaa ctctgggagc tgcgattggc
51  agaattccgt tagcaaggcc gcaggacttg cagggagtat atgggcgcac
101  ttcggtgacg gtacaggctc cttgcttata ctgcggcgcg ggcgcgtttc
151  ccggatcctg aaactgtttt aaggttggcc gatcgggtta cgcgcccgcc
201  ttaagtgttt ctgaagctt acaagaagga cagcacgaat aaaacctacg
251  taaaaccgcc ccatttgtgt cagggtagtg ggtcgaattc cgctcagagt
301  tggcacttaa gcttgctaac ggaattcccc catatccaac ttccaattta
351  atctttcttt tttaattttc acttattttg gtttttttga atctatccag
401  cacagtggcg gccgctcgag tctagagggc

```



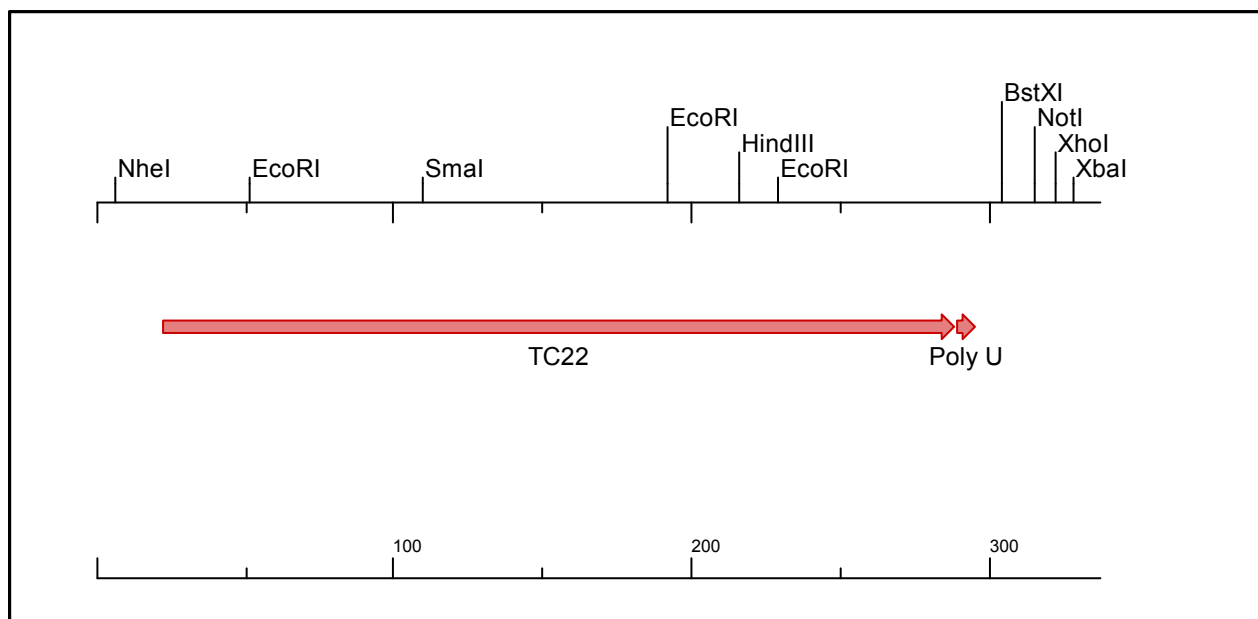
Molecule: pDH7.11-CMV-TC21, 369 bps DNA

Start	End	Name
23	320	TC21
321	327	Poly U

```

1  ttgacggcta gcaaacaccg gtgaacgaaa ctctgggagc tgcgattggc
51  agaattccgt tagcaaggcc gcaggacttg cagggagtat atgggcgcac
101 ttcggtgacg gtacaggctc cttgcttata ctgcggcgcg ggcgcgtttc
151 ccggatcctg aaactgtttt aaggttggcc gatcgggtta cgcgcccgcc
201 ttaagtgttt ctcgtagtgg gtcgaattcc gctcagagtt ggcacttaag
251 cttgctaacg gaattccccc atatccaact tccaatttaa tctttctttt
301 ttaattttca cttatttgcg tttttttgaa tctatccagc acagtggcgg
351 ccgctcgagt ctagagggc

```



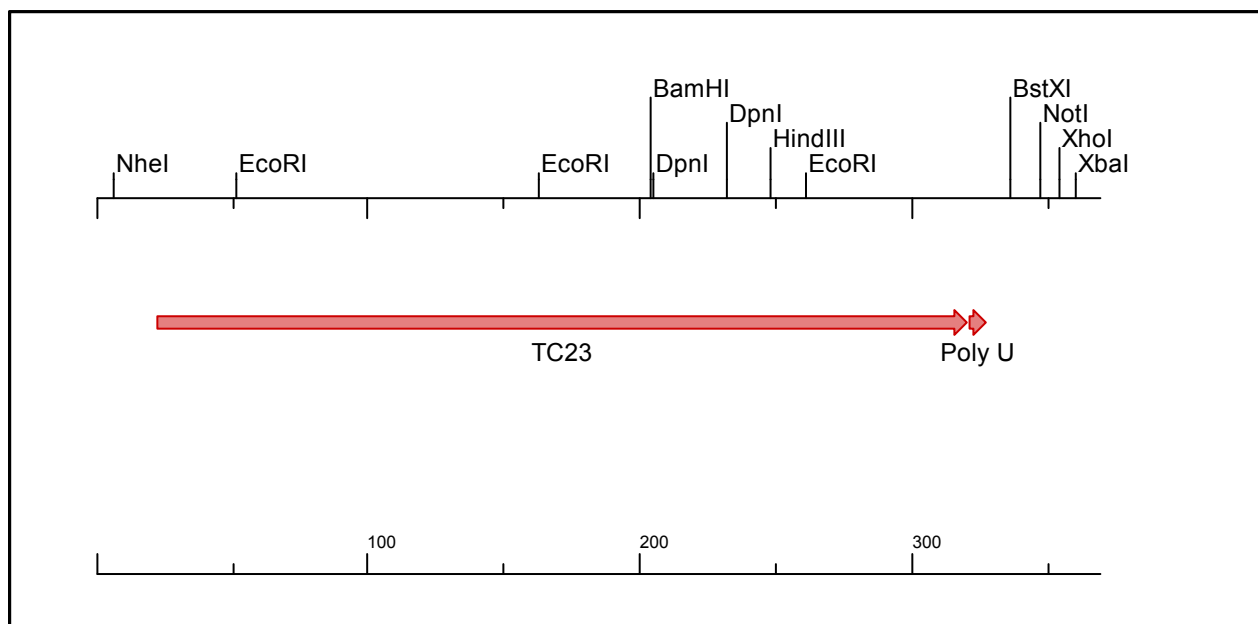
Molecule: pDH7.12-CMV-TC22, 337 bps DNA

Start	End	Name
23	288	TC22
289	295	Poly U

```

1  ttgacggcta gcaaacaccg gtgaacgaaa ctctgggagc tgcgattggc
51  agaattccgt tagcaaggcc gcaggacttg catgcttata ctgcggcgcg
101 ggcgcgtttc ccgggagtat atgggcgcac ttcggtgacg gtacaggctc
151 ctgggttaacg cgcccgccct aagtgtttct cgtagtgggt cgaattccgc
201 tcagagttgg cacttaagct tgctaacgga attcccccat atccaacttc
251 caatttaatc tttctttttt aattttcact tatttgcggt tttttgaatc
301 tatccagcac agtggcgggc gctcgagtct agagggc

```



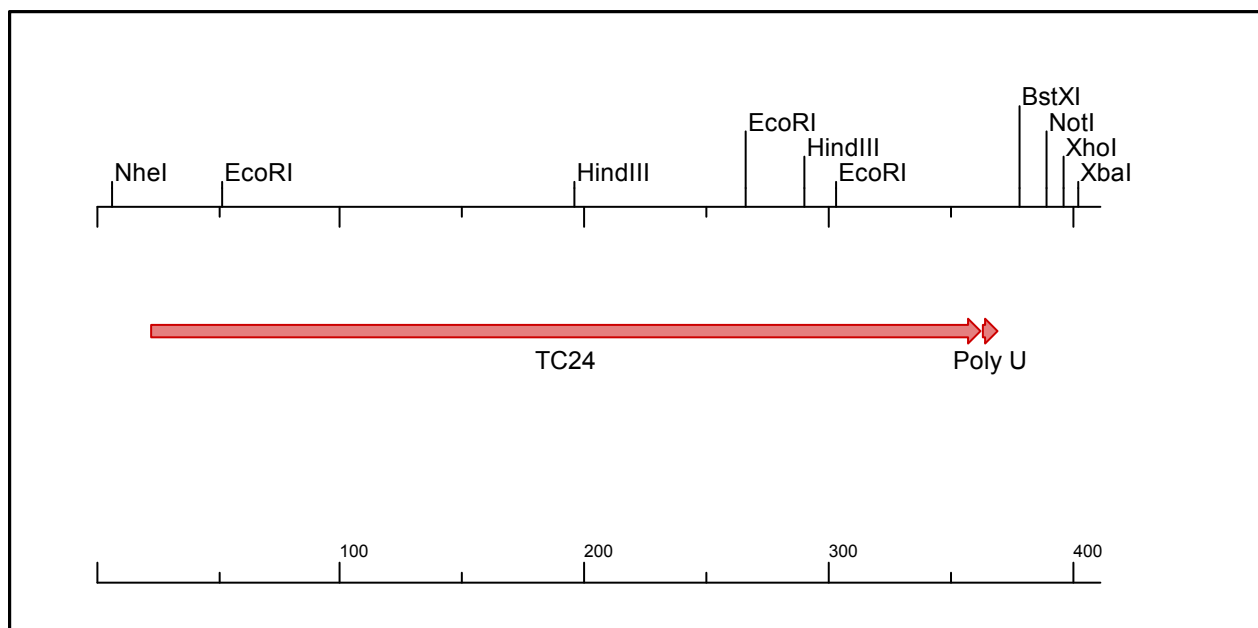
Molecule: pDH7.13-CMV-TC23, 369 bps DNA

Start	End	Name
23	320	TC23
321	327	Poly U

```

1  ttgacggcta gcaaacaccg gtgaacgaaa ctctgggagc tgcgattggc
51  agaattccgt tagcaaggcc gcaggacttg cagggagtat atgggcgcac
101 ttcgggtgacg gtacaggctc cttgcttata ctgcggcgcg ggcgcgtttc
151 ccgtagtggg tcgaattccg ctcagggtta cgcgcccgcc ttaagtgttt
201 ctcgatcct gaaactgttt taaggttggc cgatcgagtt ggcacttaag
251 cttgctaacg gaattcccc atatccaact tccaatttaa tctttctttt
301 ttaattttca cttatttgcg tttttttgaa tctatccagc acagtggcgg
351 ccgctcgagt ctagagggc

```



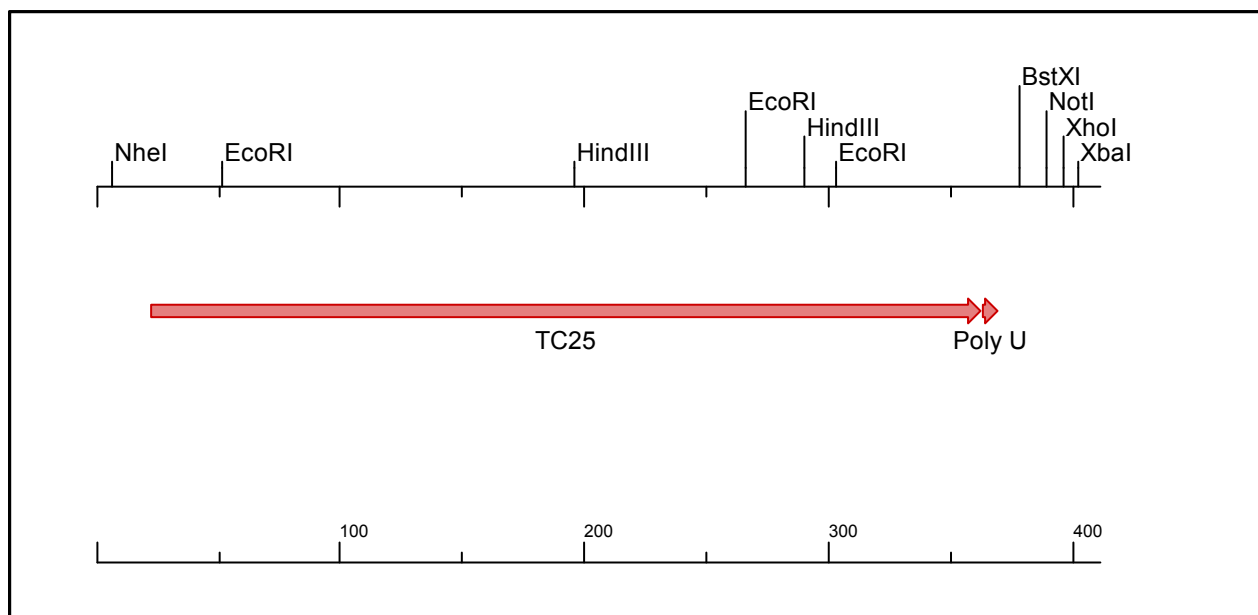
Molecule: pDH7-CMV-TC24, 411 bps DNA

Start	End	Name
23	362	TC24
363	369	Poly U

```

1  ttgacggcta gcaaacaccg gtgaacgaaa ctctgggagc tgcgattggc
51  agaattccgt tagcaaggcc gcaggacttg caaaaaatat ggaacgcttc
101 acgtgcttat cctgcggcgc gggcgcgttt cccggtctgg gcgcacttcg
151 gtgacggtagc aggccggggtt acgcgcccgc cttaagtgtt tctcgaagct
201 tacaagaagg acagcacgaa taaaacctgc gtaaatccgc cccatttggtg
251 taagggtagt gggtcgaatt ccgctcagag ttggcactta agcttgctaa
301 cggaattccc ccatatccaa cttccaattt aatctttctt ttttaatttt
351 cacttatttg cgtttttttg aatctatcca gcacagtggc ggccgctcga
401 gtctagaggg c

```



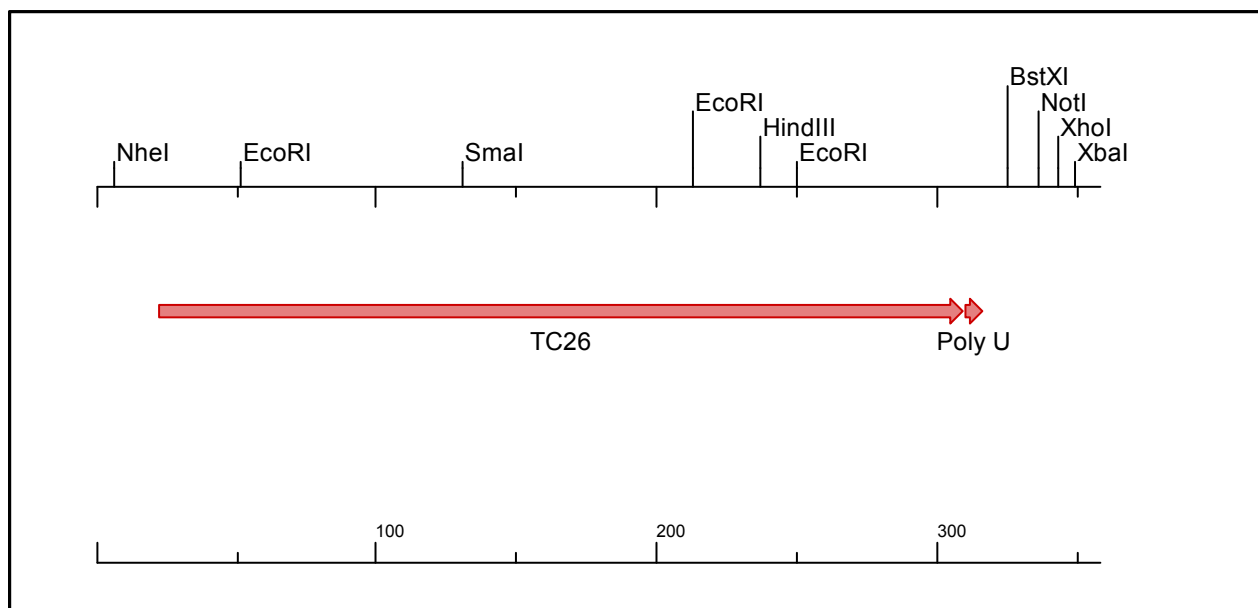
Molecule: pDH7-CMV-TC25, 411 bps DNA

Start	End	Name
23	362	TC25
363	369	Poly U

```

1  ttgacggcta gcaaacaccg gtgaacgaaa ctctgggagc tgcgattggc
51  agaattccgt tagcaaggcc gcaggacttg caaaaaatat ggaacgcttc
101 acgtgcttat cctgcggcgc gggcgcgttt cccggtcttg gcgcacttcg
151 gtgacggtac aggccgggtt acgcgcccgc cttaagtgtt tctcgaagct
201 tacaagaagg acagcacgaa taaaacctac gtaaaaaccgc cccatttgtg
251 tcagggtagt gggtcgaatt ccgctcagag ttggcactta agcttgctaa
301 cggaattccc ccatatccaa cttccaattt aatctttctt ttttaatttt
351 cacttatttg cgtttttttg aatctatcca gcacagtggc ggccgctcga
401 gtctagaggg c

```



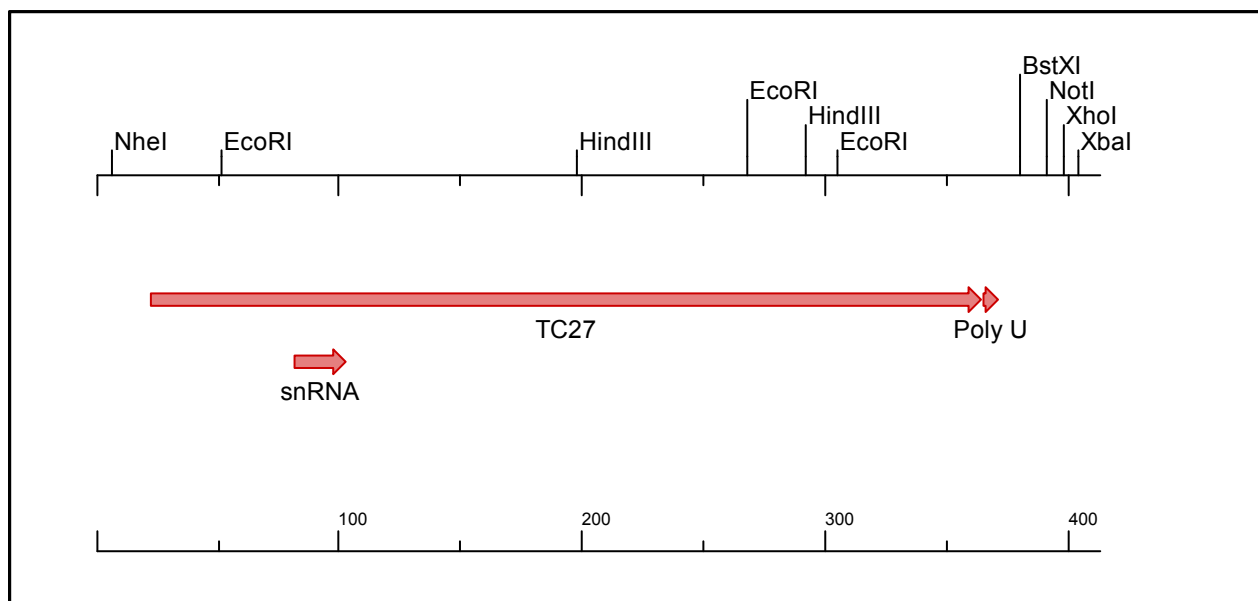
Molecule: pDH7.16-CMV-TC26, 358 bps DNA

Start	End	Name
23	309	TC26
310	316	Poly U

```

1  ttgacggcta gcaaacaccg gtgaacgaaa ctctgggagc tgcgattggc
51  agaattccgt tagcaaggcc gcaggacttg caaaaaatat ggaacgcttc
101 acgtgcttat cctgcggcgc gggcgcggtt cccgggagta tatgggcgca
151 cttcgggtgac ggtacaggct cctgggttac gcgcccgcct taagtgtttc
201 tcgtagtggg tcgaattccg ctcagagttg gcacttaagc ttgctaacgg
251 aattccccca tatccaactt ccaatttaat ctttcttttt taattttcac
301 ttatttgcgt ttttttgaat ctatccagca cagtggcggc cgctcgagtc
351 tagagggc

```

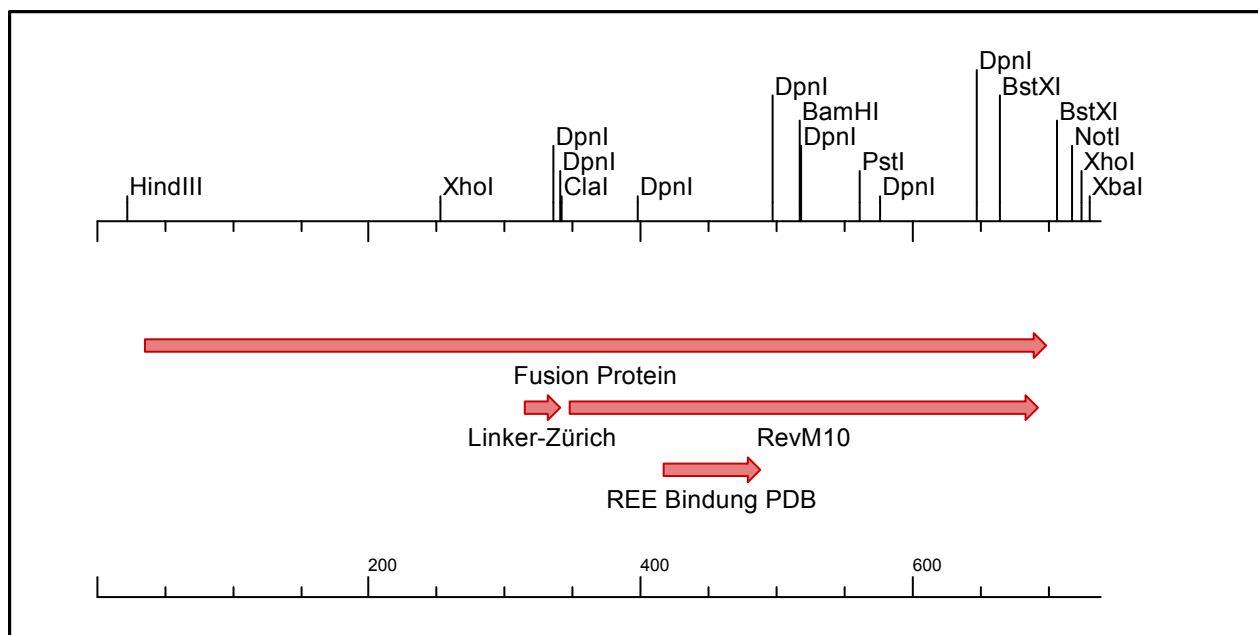
Molecule: pDH7.17-CMV-TC27, 413 bps DNA

Start	End	Name
23	364	TC27
82	103	snRNA
365	371	Poly U

```

1  ttgacgggcta gcaaacaccg gtgaacgaaa ctctgggagc tgcgattggc
51  agaattccgt tagcaaggcc gcaggacttg caaaaaatat ggaacgcttc
101 acgtgcttat cctgcggcgc gggcgcgttt cccggtcttg gcgcagcgca
151 agctgacggc acaggccggg ttacgcgccc gccttaagtg tttctcgaag
201 cttacaagaa ggacagcacg aataaaacct gcgtaaatcc gcccatttg
251 tgtaagggta gtgggtcgaa ttccgctcag agttggcact taagcttgct
301 aacggaattc ccccatatcc aacttccaat ttaatctttc ttttttaatt
351 ttcacttatt tgcgtttttt tgaatctatc cagcacagtg gcggccgctc
401 gagtctagag ggc

```



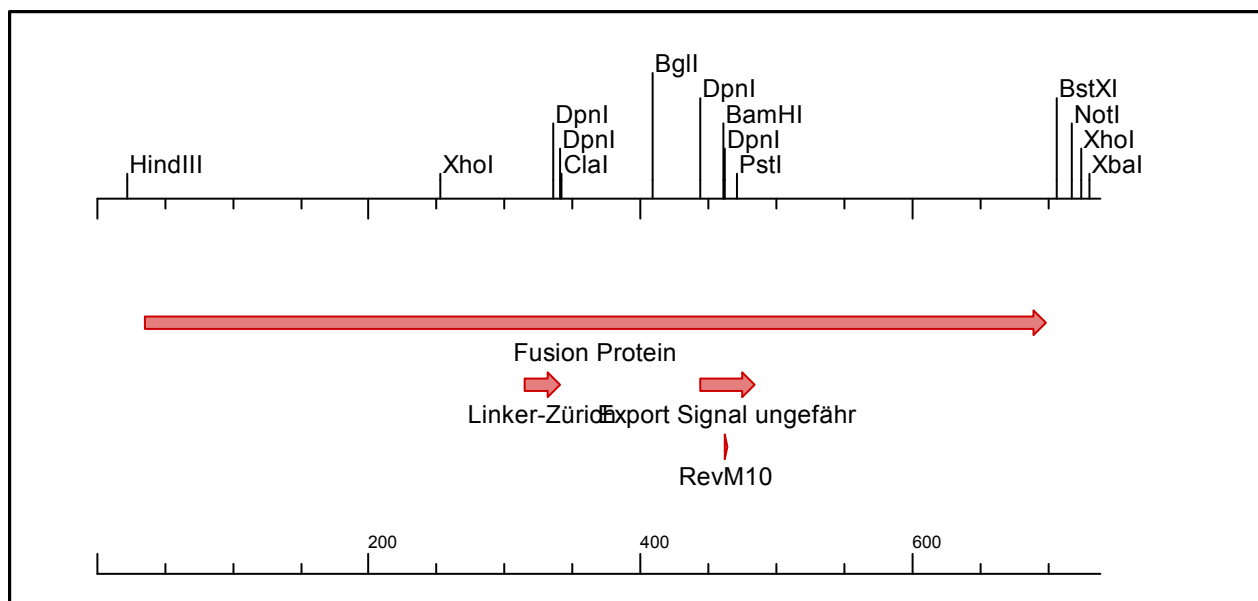
Molecule: pDH24-CMV-RevM10-Gal4BD ohne CMV ohne term, 738 bps DNA

Start	End	Name
36	698	Fusion Protein
315	341	Linker-Zürich
348	692	RevM10
417	488	REE Bindung PDB

```

1  ggcaatggta ctgttggttaa agaagcttgc ccaccatgaa actgctgtct
51  tctatcgaac aagcatgcga tatttgccga cttaaaaaagc tcaagtgtct
101 caaagaaaaa ccgaagtgcg ccaagtgtct gaagaacaac tgggagtgtc
151 gctactctcc caaaaccaa aggtctccgc tgactagggc acatctgaca
201 gaagtggaa caaggctaga aagactggaa cagctatttc tactgatttt
251 tcctcgagaa gaccttgaca tgattttgaa aatggattct ttacaggata
301 taaaagcatt gttaggcacc ccggcggcgg cgattgatcc gatcgatgcc
351 ggcaggagcg gcgacagcga cgaggacctg ctgaaggccg tgaggctgat
401 caagttcctg taccagagca accccccccc caaccgag ggcaccaggc
451 aggccaggag gaacaggagg aggaggtgga gggagaggca gaggcagatc
501 cacagcatca gcgagaggat cctgagcacc tacctgggca ggagcgccga
551 gccggtgccc ctgcagctgc cgccggatct gcggtgacc ctggactgca
601 acgaggactg cggcaccagc ggcaccagc gcgtgggcag cccccagatc
651 ctggtggaga gccccaccat cctggagagc ggcgccaagg agtgatgaaa
701 tctatccagc acagtggcgg ccgctcgagt ctagaggg

```



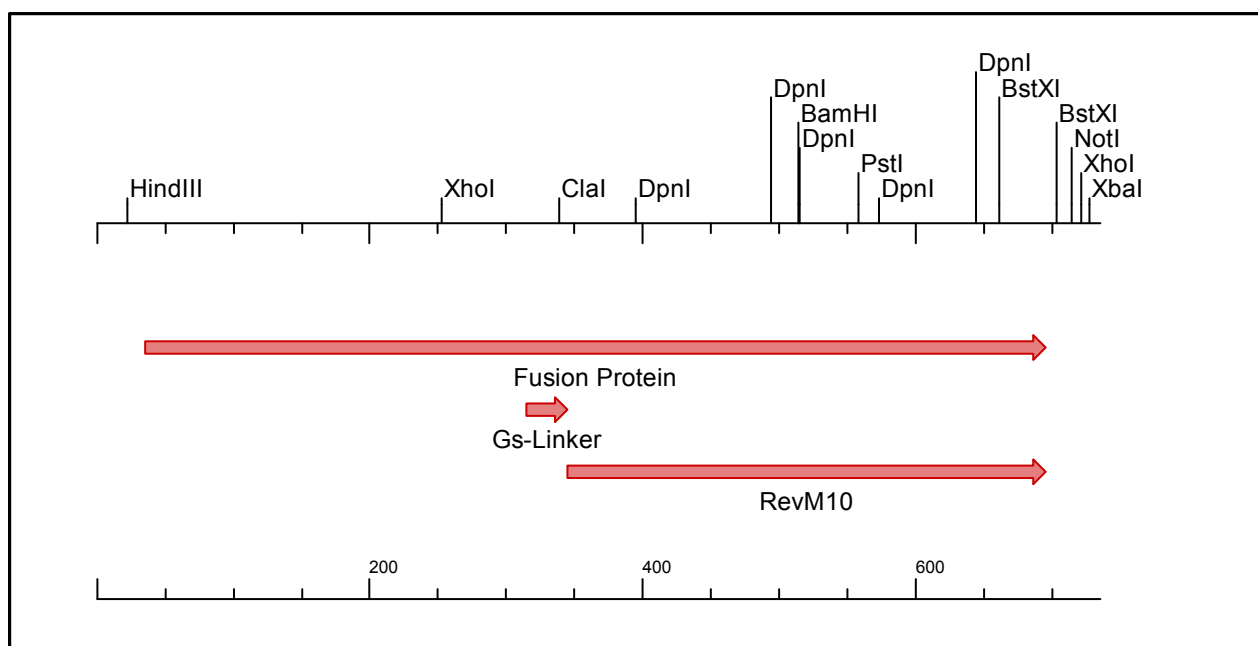
Molecule: pDH25-CMV-Gal4DBD-RevM10-C-term, 738 bps DNA

Start	End	Name
36	698	Fusion Protein
315	341	Linker-Zürich
444	484	Export Signal ungefähr
462	464	RevM10

```

1  ggcaatggta ctgttggttaa agaagcttgc ccaccatgaa actgctgtct
51  tctatcgaac aagcatgcga tatttgccga cttaaaaaagc tcaagtgctc
101  caaagaaaaa ccgaagtgcg ccaagtgtct gaagaacaac tgggagtgtc
151  gctactctcc caaaaccaa aggtctccgc tgactagggc acatctgaca
201  gaagtggaat caaggctaga aagactggaa cagctatttc tactgatttt
251  tcctcgagaa gaccttgaca tgattttgaa aatggattct ttacaggata
301  taaaagcatt gttaggcacc ccggcgggcg cgattgatcc gatcgatgaa
351  aaagcgggca gcgaactgat taccgccgagc gaagtgctga ttcagccgag
401  cggcgtgggc cagaccggca gcaccggctg cgatgaaaac tgcgatctga
451  ccctgcgcct ggatccgccc ctgcagctgc cggtgcccga agcgagccgc
501  ggctgtata ccagcctgat tcgcgaaagc attagccata ttcagcgcca
551  gcgcgaacgc tggcgccgcc gccgcaaccg ccgcgcgcag cgcaccggcg
601  aaccgaaccc gccgccgaac agccagtatc tgtttaaaat tctgcgcgtg
651  gcgaaactgc tggatgaaga tagcgatggc agccgcggcg cgtgatgaaa
701  tctatccagc acagtggcgg ccgctcgagt ctagaggg

```



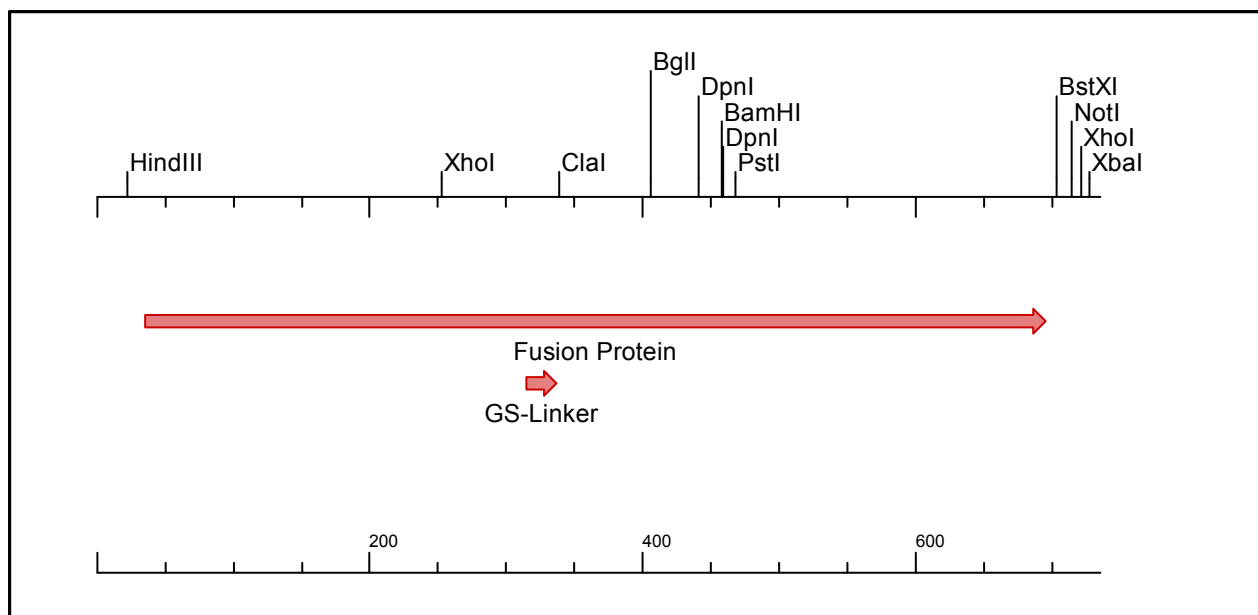
Molecule: pDH26-CMV-RevM10-Gal4BD, 735 bps DNA

Start	End	Name
36	695	Fusion Protein
315	345	Gs-Linker
345	695	RevM10

```

1  ggcaatggta ctggttgtaa agaagcttgc ccaccatgaa actgctgtct
51  tctatcgaac aagcatgcga tatttgccga cttaaaaagc tcaagtgtct
101 caaagaaaaa ccgaagtgcg ccaagtgtct gaagaacaac tgggagtgtc
151 gctactctcc caaaaccaa aggtctccgc tgactagggc acatctgaca
201 gaagtggaat caaggctaga aagactggaa cagctatttc tactgatttt
251 tcctcgagaa gaccttgaca tgattttgaa aatggattct ttacaggata
301 taaaagcatt gttaggctcc ggcggcggcg gctccggcat cgatgccggc
351 aggagcggcg acagcgacga ggacctgctg aaggccgtga ggctgatcaa
401 gttcctgtac cagagcaacc cccccccaa ccccgagggc accaggcagg
451 ccaggaggaa caggaggagg aggtggaggg agaggcagag gcagatccac
501 agcatcagcg agaggatcct gagcacctac ctgggcagga gcgccgagcc
551 ggtgcccctg cagctgccgc cggatctgcg gctgaccctg gactgcaacg
601 aggactgcgg caccagcggc acccagggcg tgggcagccc ccagatcctg
651 gtggagagcc ccaccatcct ggagagcggc gccaaaggagt gatgaaatct
701 atccagcaca gtggcggccg ctcgagtcta gagggg

```



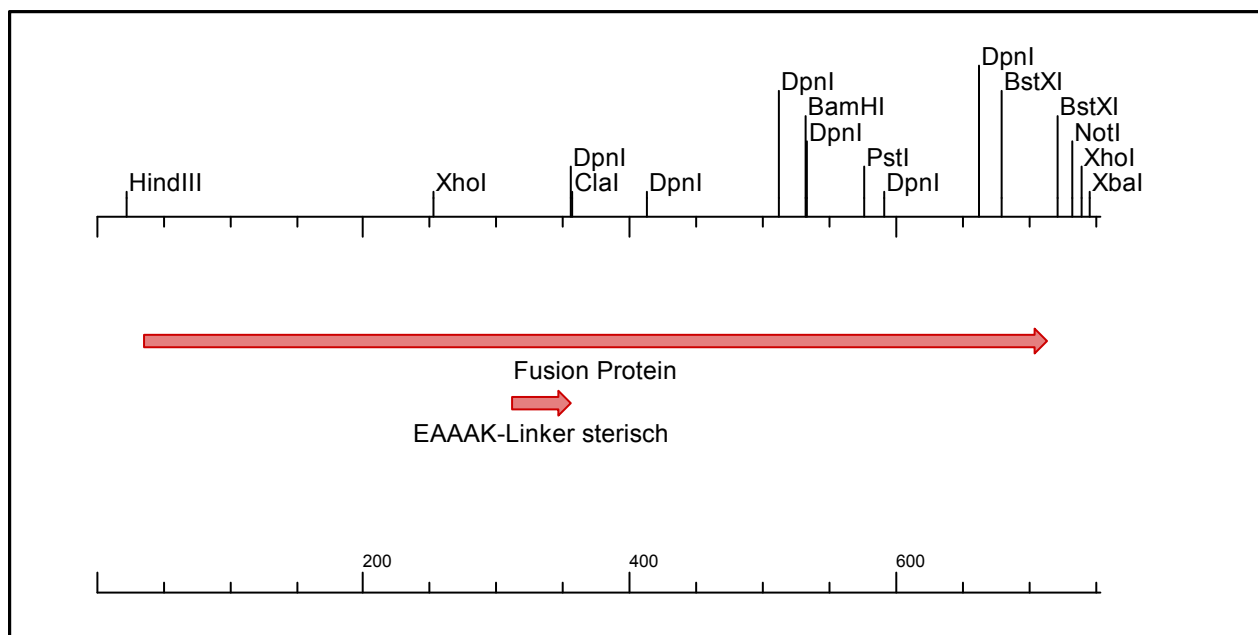
Molecule: pDH27-CMV-Gal4DBD-RevM10-C-term_GS_Linker, 735 bps DNA

Start	End	Name
36	695	Fusion Protein
315	337	GS-Linker

```

1  ggcaatggta ctgttggtaa agaagcttgc ccaccatgaa actgctgtct
51  tctatcgaa aagcatgcga tatttgccga cttaaaaagc tcaagtgtct
101 caaagaaaaa ccgaagtgcg ccaagtgtct gaagaacaac tgggagtgtc
151 gctactctcc caaaaccaa aggtctccgc tgactagggc acatctgaca
201 gaagtggaa caaggctaga aagactggaa cagctatttc tactgatttt
251 tcctcgagaa gaccttgaca tgattttgaa aatggattct ttacaggata
301 taaaagcatt gttaggctcc ggcggcggcg gctccggcat cgatgaaaaa
351 gcgggcagcg aactgattac cccgagcgaa gtgctgattc agccgagcgg
401 cgtgggcccag accggcagca ccggctgcga tgaaaactgc gatctgaccc
451 tgcgcctgga tccgccgctg cagctgccgg tgcccgaagc gagccgcggc
501 ctgtatacca gcctgattcg cgaaagcatt agccatattc agcgccagcg
551 cgaacgctgg cgccgcgcc gcaaccgccg cgcgcagcgc accggcgaac
601 cgaaccgcgc gccgaacagc cagtatctgt ttaaaattct gcgcgtggcg
651 aaactgctgg atgaagatag cgatggcagc cgcggcgcgt gatgaaatct
701 atccagcaca gtggcggccg ctcgagtcta gaggg

```



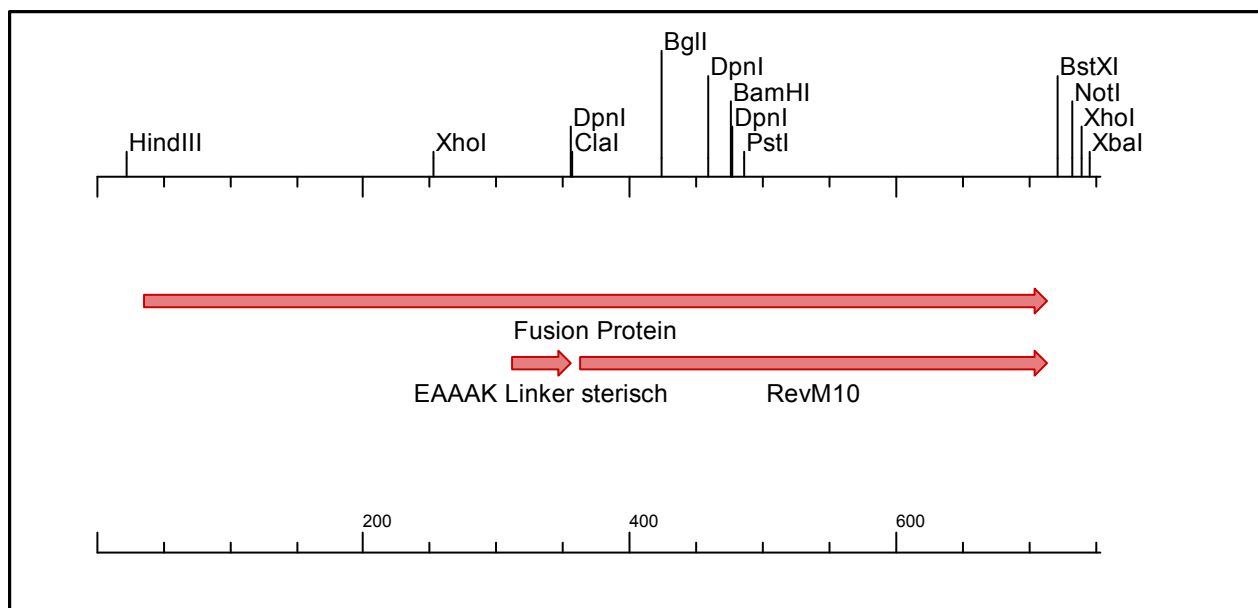
Molecule: pDH28-CMV-Gal4-revM10-Helix Linker, 753 bps DNA

Start	End	Name
36	713	Fusion Protein
312	356	EAAAK-Linker sterisch

```

1  ggcaatggta ctgttggtta agaagcttgc ccaccatgaa actgctgtct
51  tctatcgaa aagcatgcga tatttgccga cttaaaaagc tcaagtgtct
101 caaagaaaaa ccgaagtgcg ccaagtgtct gaagaacaac tgggagtgtc
151 gctactctcc caaaaccaa aggtctccgc tgactagggc acatctgaca
201 gaagtggaa caaggctaga aagactggaa cagctatttc tactgatttt
251 tcctcgagaa gaccttgaca tgattttgaa aatggattct ttacaggata
301 taaaagcatt gttagcggaa gcggcggcga aagaagcggc ggcgaaagcg
351 gcggcgatcg atgccggcag gagcggcgac agcgacgagg acctgctgaa
401 ggccgtgagg ctgatcaagt tcctgtacca gagcaacccc cccccaacc
451 ccgagggcac caggcaggcc aggaggaaca ggaggaggag gtggaggagg
501 aggcagaggc agatccacag catcagcgag aggatcctga gcacctacct
551 gggcaggagc gccgagccgg tgccccctgca gctgccgccg gatctgcggc
601 tgaccctgga ctgcaacgag gactgcggca ccagcggcac ccagggcgtg
651 ggcagcccc agatcctggg ggagagcccc accatcctgg agagcggcgc
701 caaggagtga tgaaatctat ccagcacagt ggcggccgct cgagtctaga
751 ggg

```



Molecule: pDH29-CMV-Gal4DBD-RevM10-C-term_Helix Linker, 753 bps DNA

Start	End	Name
36	713	Fusion Protein
312	356	EAAAK Linker sterisch
363	713	RevM10

```

1  ggcaatggta ctgttggttaa agaagcttgc ccaccatgaa actgctgtct
51  tctatcgaac aagcatgcga tatttgccga cttaaaaagc tcaagtgtct
101 caaagaaaaa ccgaagtgcg ccaagtgtct gaagaacaac tgggagtgtc
151 gctactctcc caaaaccaa aggtctccgc tgactagggc acatctgaca
201 gaagtggaat caaggctaga aagactggaa cagctatttc tactgatttt
251 tcctcgagaa gaccttgaca tgattttgaa aatggattct ttacaggata
301 taaaagcatt gttagcggaa gcggcggcga aagaagcggc ggcgaaagcg
351 gcggcgcgac atgaaaaagc gggcagcgaa ctgattaccc cgagcgaagt
401 gctgattcag ccgagcggcg tgggccagac cggcagcacc ggctgcgatg
451 aaaactgcga tctgacctg cgccctggatc cgccgctgca gctgccggtg
501 cccgaagcga gccgcggcct gtataccagc ctgattcgcg aaagcattag
551 ccatattcag cgccagcgcg aacgctggcg ccgccgccgc aaccgccgcg
601 cgcagcgcac cggcgaaccg aaccgcgcgc cgaacagcca gtatctgttt
651 aaaattctgc gcgtggcgaa actgctggat gaagatagcg atggcagccg
701 cggcgcgtga tgaaatctat ccagcacagt ggcggccgct cgagtctaga
751  ggg

```

VII. Abbreviations

aa	Amino acid
Amp	Ampicillin
Akt/PKB	Protein Kinase B
ARP2/3	Actin-Related Protein 2, Actin-Related Protein 3 complex
ATP	Adenosine triphosphate
Bp	Base pair
BSA	Bovine serum albumin
Ca ²⁺	Calcium ion
cAMP	Cyclic adenosine monophosphate
CHO	Chinese hamster ovary
CMV	Cytomegalovirus
DMEM	Dulbecco's modified Eagle medium
DMSO	Dimethyl sulfoxide
DNA	Deoxyribonucleic acid
dNTP	Deoxynucleotide triphosphate
EA	enzymatic activity
<i>E. coli</i>	<i>Escherichia coli</i>
EDTA	Ethylenediaminetetraacetic acid
ER	Endoplasmic reticulum
eGFP	enhanced green fluorescent protein
eYFP	enhanced yellow fluorescent protein
FCS	Fetal calf serum
fw	forward
GOI	Gene of interest
hEF1 α	human elongation factor α
HEK	Human embryonic kidney
HEPES	4-(2-hydroxyethyl)-1-piperazineethanesulfonic acid
HTH	Helix-turn-helix
HRP	Horseradish peroxidase
IP3	Inositol-1,4,5-trisphosphat
IP3R	Inositol-1,4,5-trisphosphat receptor
IKB	nuclear factor of kappa light polypeptide gene enhancer in B-cells inhibitor
KM	Kanamycin
Kcal	kilocalorie
LB	Lysogeny broth medium
MAPK	Mitogen-activated protein kinase
MCS	Multiple cloning site
miRNA	Micro RNA

MQ H ₂ O	Millipore water
NADPH	Nicotinamide adenine dinucleotide phosphate
NEB	New England Biolabs®
NF-KB	nuclear factor kappa-light-chain-enhancer of activated B cells
OD ₆₀₀	Optical density (600 nm)
o/n	Over night
PAGE	polyacrylamide gel electrophoresis
PBS	Phosphate buffered saline
PCR	Polymerase chain reaction
PEI	Polyethyleneimine
PEST	Peptide containing repeats of Proline, glutamate, serin, threonine
pNP	p-nitrophenol
pNPP	p-nitrophenyl phosphate
rev	reverse
RNA	Ribonucleic acid
RNAi	RNA interference
rpm	Rounds per minute
RT	Room temperature
SDS	Sodium dodecyl sulfate
SEAP	Human placental secreted alkaline phosphatase
ss	Secretion signal
SV40	Simian virus 40
TAE	Tris-acetate-EDTA
TEMED	Tetramethylethylenediamine
tGFP	turbo green fluorescent protein
Tm	Melting temperature
Tris	tris-(hydroxymethyl)-aminomethane
Tween-20	Polyoxyethylene (20) sorbitan monolaurate
U	Unit(s)
v/v	volume / volume

VIII. Appendix

Peer-Review publications and patents in the field of sensor-effector systems

Designer cells programming quorum-sensing interference with microbes.

Nature Communications volume 9, Article number: 1822 (2018)

Ferdinand Sedlmayer, **Dennis Hell**, Marius Müller, David Ausländer and Martin Fussenegger

The following publication and patent belong to the PhD thesis:

Self-adjusting cytokine neutralizer cells as a closed-loop delivery system of anti-inflammatory biologicals. ACS Synthetic Biology, 2018, 7 (11), pp 2518–2528

Dennis Hell

Sensor-Effektor Zellen zu der Verwendung in der Therapie. Patent 10 2018 211 201.

Dennis Hell

Affidavit

I hereby declare that my thesis entitled: „ **Development of self-adjusting cytokine neutralizer cells as a closed-loop delivery system of anti-inflammatory biologicals**” is the result of my own work. I did not receive any help or support from commercial consultants. All sources and / or materials applied are listed and specified in the thesis.

Furthermore I verify that the thesis has not been submitted as part of another examination process neither in identical nor in similar form.

Besides I declare that if I do not hold the copyright for figures and paragraphs, I obtained it from the rights holder and that paragraphs and figures have been marked according to law or for figures taken from the internet the hyperlink has been added accordingly.

Eidesstattliche Erklärung

Hiermit erkläre ich an Eides statt, die Dissertation: „**Entwicklung von selbstregulierenden Zytokin-Neutralisierer-Zellen als Closed-Loop Abgabesystem von anit-inflammatorischen Biologikals**“, eigenständig, d. h. insbesondere selbständig und ohne Hilfe eines kommerziellen Promotionsberaters, angefertigt und keine anderen, als die von mir angegebenen Quellen und Hilfsmittel verwendet zu haben. Ich erkläre außerdem, dass die Dissertation weder in gleicher noch in ähnlicher Form bereits in einem anderen Prüfungsverfahren vorgelegen hat.

Weiterhin erkläre ich, dass bei allen Abbildungen und Texten bei denen die Verwertungsrechte (Copyright) nicht bei mir liegen, diese von den Rechtsinhabern eingeholt wurden und die Textstellen bzw. Abbildungen entsprechend den rechtlichen Vorgaben gekennzeichnet sind sowie bei Abbildungen, die dem Internet entnommen wurden, der entsprechende Hypertextlink angegeben wurde.

Author:

Hell

Dennis

Last name

First name

, den

Die vorliegende Arbeit wurde in der Zeit vom 01. Mai. 2015 bis 05. September 2017 an der Universitätsklinikums Würzburg in der Abteilung Tissue Engineering und Regenerative Medizin experimentell angefertigt

Acknowledgements – Danksagung

Während meines Forschungsaufenthalts in Würzburg und bei anschließenden Veröffentlichungen, wurde ich leider mit zahlreichen unerfreulichen Situationen konfrontiert. Ich sah meine Arbeit aufgrund nicht-wissenschaftlicher und finanzieller Probleme, durch die immer wieder das Vorankommen des Projekts langwierigen Verzögerungen unterlag, zeitweilen gefährdet. Die einzige Möglichkeit, die Arbeit zu einem erfolgreichen Ende führen zu können, sah ich durch einen Wechsel der Betreuungsperson. Zu meinem großen Glück, erklärte sich Prof. Dr. Harald Wajant bereit, diese Position für meine Arbeit einzunehmen. Er konnte mir den Geist und die Grundhaltung der Wissenschaft wieder näher bringen, indem er mir zeigte, dass es ihm um die Sache selbst, um die Betreuung eines Doktoranden ging.

An dieser Stelle möchte ich mich bei ihm für die zahlreichen, Hinweise, Hilfestellungen, fachlichen Diskussionen und für den stetigen Antrieb, den ich hierbei erfuhr, herzlichst bedanken. Er hat mich auf dem Gebiet der therapeutischen Proteine und der NF- κ B Signalisierung, bis hin zur schriftlichen Ausarbeitung unterstützt und mich auf meinem Weg zur Promotion begleitet.

Bedanken möchte ich mich zudem bei Steffan und Carolin Krzimirski für die zahlreichen interessanten Gespräche und für die entstandene Freundschaft.

Zusätzlich möchte ich mich bei Christoph Rücker bedanken. Unvergesslich wird mir unser gemeinsamer Klettertag im Donautal und unser Einsatz in der Route „Weg der Jugend“ bleiben. Isabell Lang möchte ich für die Unterstützung bei den GPL Analysen danken.

Ein weiteres großes und von Herzen kommendes Dankeschön gilt außerdem meiner Familie, die mir während der Promotion, immer unterstützend zur Seite stand und mir den Rücken frei hielt. Ohne euch würde die vorliegende Arbeit nicht existieren. Danke auch an meine Freundin, die mir hin und wieder half meine innere Ruhe und Ausgeglichenheit zurückzugewinnen.

